Effects of Nutrients, Photoinhibition & Photoacclimation on Photosystem II Function of Freshwater Phytoplankton Communities

by

Joel Harrison

A thesis
presented to the University of Waterloo
in fulfillment of the
thesis requirement for the degree of
Doctor of Philosophy
in
Biology

Waterloo, Ontario, Canada, 2011

Author’s Declaration

I hereby declare that I am the sole author of this thesis. This is a true copy of the thesis, including any required final revisions, as accepted by my examiners.

I understand that my thesis may be made electronically available to the public.

Abstract

Electron flow through Photosystem II (PSII) is essential to all life on Earth. The efficiency of this process in freshwater phytoplankton can be depressed by nutrient limitation, ultraviolet radiation (UVR), and excessive photosynthetically active radiation (PAR). The effects of nutrients and radiation on PSII function of natural communities were assessed using changes in the variable fluorescence of PSII (PSII VF), as determined by a pulse amplitude modulation (PAM) fluorometer. The net susceptibility to photoinhibition of PSII depends upon the sensitivity of the assemblage to photodamage and the efficiency of recovery. Damage and recovery rates were quantified by fitting changes in F_V:F_M during experimental spectral exposures to the model of Kok (1956). Phytoplankton from deep chlorophyll maxima were found to exhibit much higher photosynthetic impairment under UVR exposure than epilimnetic communities in two lakes, due to differences in both damage and recovery rates. In six temperate lakes of the Dorset-Haliburton region, the susceptibility to UVR-induced photoinhibition of PSII was found to be a function of the water transparency (dissolved organic carbon content) of the systems from which the plankton were isolated, with no obvious taxonomic pattern to the responses. Nutrient (nitrogen & phosphorus) supplementation of communities from the Dorset Lakes and from Lake Ontario did not have strong effects on PSII VF, and did not alter the response of Lake Ontario phytoplankton to spectral irradiance. Diurnal changes in F_V:F_M of Lake Ontario phytoplankton were modeled and average values for the upper half of the water column showed reasonable agreement with observed data; however it is suggested that the addition of a model to simulate vertical mixing could improve the depth-specific accuracy of the predictions. It is concluded that the light history (photoacclimation status) of phytoplankton is the major determinant of the sensitivity of PSII to UVR, and that the nutrient status and taxonomic composition of phytoplankton communities have a comparatively minor influence.

Acknowledgements

I would like to thank my supervisor, Professor Ralph Smith, for his encouragement, guidance and dedication to this work, and, in the early stages, for helping me make the difficult transition from teacher's college to academic research. I also owe a debt of gratitude to Professor Bill Taylor, who never seemed to tire of me popping into his office unannounced, with yet another question. Sincere thanks to the members of my thesis committee: Professors Bruce Greenberg and Mark Servos and Dr. Michael Arts. Work on Lake Ontario benefited greatly from the nearby proximity of the Frenchman's Bay Marina and I thank its members for displaying incredible patience with the (initially) unseaworthy crew of the Lady Jane. Work on the Dorset Lakes would not have been possible without use of the Dorset Environmental Science Centre facilities and the kind assistance of its staff, in particular, Ron Ingram and Dr. Andrew Paterson. I am also grateful to Bill for accommodating me in his laboratory at the DESC and for allowing me to crash at his cottage in Baysville. All of the research described in this thesis was supported by an NSERC Discovery Grant, and my bills were paid in part by Ontario Graduate Scholarships. Many technicians helped with both laboratory and field work over the course of this project, and I would especially like to thank Lee Pinnell, Farrah Chan, Richard Elgood, Adam Houben, and Vicky Jackson for their assistance. Lee Pinnell must be acknowledged a second time for his skills on the basketball court. My experience at the University of Waterloo was greatly enriched by the company of Tedy Ozersky, Patrick McCamphill, David Isherwood, Taylor Dawson, Greg Silsbe, Sairah Malkin, Katie Thomas, Erin Jones, Jennifer Hood, Amanda Poste, and Ryan Scott, with all of whom I shared the occasional edifying scientific discussion and innumerable pitchers of beer at the Grad House. Finally, thanks to my siblings Myles, Byron, and Bethany, my father, Dr. Lloyd Harrison, and to Jill, for all of their love and support.

Dedication

For my mother, Phyllis Ruth Harrison (1952–2002), whose love and laughter I miss dearly.

Table of Contents

List of Figures

List of Tables

List of Symbols & Abbreviations

ϕ_f: quantum yield of fluorescence

ϕ_p: quantum yield of photochemistry

$\varepsilon_{k(\lambda)}$: biological effectiveness coefficient for photodamage by wavelength, λ

θ_a: zenith angle of incident light in air

θ_w: angle to the downward vertical of a transmitted beam in water

AP: alkaline phosphatase

ATP: adenosine tri-phosphate

BWF: biological weighting function

C: carbon

CDOM: chromophoric dissolved organic matter

CFC: chlorofluorocarbon

Chl *a*: chlorophyll *a*

CO_2: carbon dioxide

CPD: cyclobutane pyrimidine dimer

DCM: deep chlorophyll maxima

DIPI, IPI: daily *in situ* photoinhibition, *in situ* photoinhibition

DNA: deoxyribonucleic acid

DOC: dissolved organic carbon

$\bar{E}_\lambda$%: mean epilimnetic irradiance, as percent subsurface for wavelength, λ

ELA: Experimental Lakes Area

ERC: exposure response curve

E_S: estimate of irradiance history of water sample

F_O, F_V, F_M: minimum, variable, and maximum fluorescence of Photosystem II

FA: fatty acid

FRRF: fast repetition rate fluorometry

G: increase in F_V:F_M (modeled)

IC: induction curve

k: rate constant for photodamage

KD_λ: vertical attenuation coefficient for wavelength, λ

LHC: light harvesting complex

L: decrease in F_V:F_M (modeled)

MAAs: mycosporine-like amino acids

N: nitrogen

NADPH: nicotinamide adenine dinucleotide phosphate

NPQ: non-photochemical quenching

Nu+, **Nu-**: nitrogen- and phosphorus-supplemented, non-supplemented water samples

NWRI: National Water Research Institute

P: phosphorus

PAM: pulse amplitude modulation

PAR: photosynthetically active radiation (400–700 nm)

PFD: photon flux density

PN: particulate nitrogen

POC: particulate organic carbon

PP: particulate phosphorus

PSI, PSII: Photosystem I, Photosystem II

PQ: plastoquinol

PTOX: plastoquinol terminal oxidase

RC: reaction centre

rETR: relative electron transport rate

r: rate constant for recovery from photodamage

RF: reflectance

ROS: reactive oxygen species

RLC: rapid light curve

SRP, TDP, TP: soluble reactive phosphorus, total dissolved phosphorus, total phosphorus

TSR: total solar radiation (UVR+PAR+infrared)

UVA: ultraviolet-A (320–400 nm)

UVB: ultraviolet-B (280–320 nm)

UVC: ultraviolet-C (10–280 nm)

UVR: ultraviolet radiation (10–400 nm)

VF: variable fluorescence

Z_{mix}: mixing (epilimnion) depth

Chapter 1: General Introduction

1.1 Phytoplankton

The term *plankton* refers to all of the free-floating organisms in the water column of an aquatic environment, and derives from the Greek word *πλαγκτός* or 'planktos', which means 'drifting' (OED). Distinct from the suspended animals, or zooplankton, *phytoplankton* are all of the plant-like (*i.e.*, photosynthetic) organisms suspended in a body of fresh or saline water. This extremely broad category encompasses life forms both prokaryotic (cyanobacteria) and eukaryotic (algae), and includes many thousands of species, which span five orders of magnitude in size, from the smallest unicells (~0.2 µm) to the largest colonies (~20,000 µm). Phytoplankton are extraordinarily diverse not only with respect to size, but also with respect to morphology and behaviour. Many species are roughly spherical in shape, but other taxa, or parts of them, have been likened to stars (*Asterionella* colonies), barrels (centric diatoms), necklaces (*Anabaena*), tear drops (*Cryptomonas*), vases (*Dinobryon*), horns (*Ceratium*), bristles (*Mallomonas*), and so forth, while still others are so strangely shaped as to defy analogy altogether. Despite being planktonic, many phytoplankton possess flagella, and therefore the capacity for autonomous locomotion; some cyanobacteria can control their buoyancy using gas vacuoles; other species are planktonic in the strictest sense of the word, and are completely at the mercy of the physical forces which characterize all aquatic environments to some extent. It is clear that the functional group called 'phytoplankton' includes a rather diverse array of life forms, but these prokaryotic and eukaryotic planktonic microorganisms are unified by their dependence on the process of photosynthesis to support their growth and metabolic requirements.

1.1.1 Phytoplankton photosynthesis

Life as we know it on this planet could not have evolved without two important consequences of the photosynthesis that took place in Earth's early oceans: an oxygen-rich atmosphere, and the stratospheric ozone layer. The former allowed aerobic organisms to develop on land, and the latter

served to protect them from harmful solar radiation. Presently, despite constituting a mere 0.2% of primary producer biomass, marine phytoplankton are responsible for approximately half of net primary productivity globally (Field *et al.* 1998), and the oceanic 'biological pump' represents an important sink for the increasingly-abundant greenhouse gas carbon dioxide (CO_2) (Falkowski & Raven 2007). In lakes, as in marine environments, phytoplankton function as the base of the food-web, making energy from the sun, carbon from the atmosphere, and inorganic nutrients available to higher trophic levels, as well as to heterotrophic bacteria. They therefore represent an important link between the abiotic and the biotic, and as such play a critical role in the ecology of most aquatic ecosystems.

1.1.2 Photosynthetic electron flow, Photosystem II and its fluorescence

The process of oxygenic photosynthesis can be summarized as

$$6\,CO_2 + 6\,H_2O \rightarrow 6\,O_2 + C_6H_{12}O_6 \qquad (1.1)$$

Despite the apparent simplicity of Equation 1.1, photosynthesis is a complex process involving a wide variety of cellular components and biochemical reactions, many of which are still imperfectly understood. Accordingly, I will focus this section only on the aspects of photosynthesis relevant to the topic of this thesis, which is how solar radiation affects phytoplankton at Photosystem II (PSII). This entails an explanation of the 'light reactions' of photosynthesis, which take place in the thylakoid lumen, but not the 'dark reactions' which take place in the stroma of the chloroplast, and are responsible for the fixation of CO_2 into organic compounds by chemical reduction (*i.e.*, the Calvin-Benson-Bassham cycle).

The light-dependent reactions of photosynthesis—which produce O_2, chemical energy (ATP), and reductant (NADPH)—are accomplished by the combined action of two protein-pigment complexes known as PSII and Photosystem I (PSI) which are embedded in the thylakoid membrane of the chloroplast. When the energy of a photon is absorbed by pigment molecules associated with a

PSII light-harvesting complex (LHC), it is subsequently channelled to a PSII reaction centre (RC) and used to drive a series of charge separations (redox reactions) that ultimately extract electrons from water (producing oxygen gas) and channel them through the plastoquinone (PQ) pool, cytochrome b_6f complex, PSI, and thereafter to the $NADP^+$ molecule that will be used to fix inorganic carbon (see Falkowski & Raven 2007). Various other cofactors (*e.g.* plastocyanin and ferredoxin) are also involved, and the overall process is known as linear photosynthetic electron flow. Alternative pathways such as the Mehler reaction (water-water cycle), cyclic flow around PSI, and the plastoquinol terminal oxidase mechanism (PTOX; McDonald *et al.* 2011) can uncouple photosynthetic electron flow from the production of NADPH.

PSII exists as a dimer in the thylakoid membrane, and each monomer contains 20 protein subunits, 35 chlorophylls, 2 phaeophytins, 11 β-carotenes, >20 lipids, 2 plastoquinones, 2 haem irons, 1 non-haem iron, 4 manganese atoms, 3 or 4 calcium atoms, 3 Cl^- ions, 1 bicarbonate ion, >15 detergents, and >1, 300 water molecules, resulting in a total molecular mass of 350 kDa (Umena *et al.* 2011). Each monomer of the PSII RC dimer is composed of the D1 and D2 proteins,[1] in association with cytochrome b_{559}, CP43 and CP47 (Falkowsi & Raven 2007). During photosynthesis, the D1 protein is repeatedly degraded, re-synthesized and re-inserted into the thylakoid membrane as part of a rapid cycle (Aro *et al.* 1993) that is an inherent consequence of PSII photochemistry (Anderson *et al.* 1997). When the rate of D1 damage exceeds that of repair, such as during exposure to UVR or very high PAR, net D1 damage accumulates, resulting in photoinhibition of PSII (Bouchard *et al.* 2006).

In this thesis, changes in chlorophyll *a* fluorescence are used to infer the proportion of functional PSII RCs, and hence, to measure photoinhibition. The quantum yield for fluorescence (ϕ_f)

[1] "When these proteins are radioactively labeled with ^{35}S they appear as broad, *diffuse* bands on an autoradiogram following polyacrylamide gel electrophoresis and fluorography; hence, the names D1 and D2" (p.224 of Falkowski & Raven 2007).

is a function of the rates of the 3 processes by which energy from an absorbed photon may be dissipated

$$\phi_f = \frac{k_f}{k_f + k_d + k_p} \quad (1.2)$$

where k_f, k_d, and k_p are the rate constants for fluorescence, heat, and photochemistry, respectively (Falkowski & Raven 2007). When thermal dissipation is absent (*i.e.,* $k_d = 0$), such as after a sufficient period of darkness (>30 min), and all PSII RCs can accept an electron (*i.e.,* are in an oxidised, or "open" state), ϕ_f is at a minimum (F_o). However, when all PSII RCs are unable to perform a charge separation (*i.e.*, are "closed"; $k_p = 0$), such as after an intense exposure to light (or "saturation pulse"), ϕ_f rises to a maximum (F_M). The variable fluorescence of PSII ($F_V = F_M - F_O$), is the difference between the fluorescence yields when all RCs are open and when all RCs are closed, and is proportional to the total number of functional RCs (Anderson *et al.* 1997). The maximum quantum yield of PSII photochemistry (ϕ_p) is therefore related to changes in fluorescence by

$$\phi_p = \frac{k_p}{k_f + k_p + k_d} = \frac{F_M - F_0}{F_M} = \frac{F_V}{F_M} \quad (1.3)$$

as stated in Falkowski & Raven (2007). Changes in F_V:F_M can therefore be used to quantify photoinactivation and repair of PSII (Anderson *et al.* 1997; Campbell & Tyystjärvi 2011). Depressed PSII VF can also reflect nutrient stress in phytoplankton (Sylvan *et al.* 2007; Rattan 2009; but see Parkhill *et al.* 2001) and this topic is discussed fully in Chapter 4. All F_V:F_M data reported in this thesis were obtained using a pulse amplitude modulation (PAM) fluorometer (Schreiber *et al.* 1986). Specific details relating to the PAM methodology are provided in the data chapters that follow.

1.1.3 Ultraviolet radiation

Ultraviolet radiation (UVR) is radiation of wavelength 10–400 nm, conventionally subdivided into the UVC (10–280 nm), UVB (280–320 nm) and UVA (320–400 nm) wavebands. Due to absorbance

by ozone and other atmospheric constituents, very little solar irradiance of wavelength <300 nm reaches the surface of the earth, so that UVC is ecologically irrelevant, and natural UVBR can be more accurately defined as irradiance of wavelength 300–320 nm. Beyond the UVR waveband is the longer-wavelength irradiance (400–700 nm) that energizes photosynthesis, referred to as photosynthetically active radiation (PAR).

1.1.4 Historical and projected trends in surface incident UVR

The link between chlorofluorocarbon (CFC) use and the destruction of stratospheric ozone was recognized in the 1970s (Molina & Rowland 1974), and by the mid-1980s it had been established that Antarctic ozone levels were steadily decreasing, and had been for over a decade (Farman *et al*. 1985). Based on measurements recorded in Toronto during 1989–1993, it was later discovered that ozone depletion was increasing surface incident UVBR at temperate latitudes as well as polar (Kerr & McElroy 1993). In a rare instance of political responsiveness to a looming environmental crisis, governments worldwide agreed to ban the production of ozone-destroying substances (CFCs and related compounds); this international commitment was formalized by the ratification of the Montreal Protocol in 1987, following the Vienna Convention of 1985. Due to these measures, stratospheric ozone is no longer decreasing; however recovery to pre-1980 levels is not expected until ~2050 at mid-latitudes, with slower recovery expected over polar regions (McKenzie *et al*. 2011). The stratospheric cooling that accompanies global warming (of the troposphere) may slow recovery of the ozone layer at high latitudes by increasing polar stratospheric cloud formation (McKenzie *et al*. 2011). Future levels of UVBR reaching the earth at all latitudes are subject to some uncertainty, because factors such as cloud cover (Liley 2009), air pollutants (Alpert & Kishcha 2008) and other aerosols (*e.g.*, volcanic ash; Ohvril *et al*. 2009) are also influential, and likely to change over the next century in response to global warming and human population growth.

1.1.5 Plankton UVR exposure in lakes

Plankton UVR exposure in aquatic environments is a function not only of the incident photon flux density (PFD) of irradiance, but also of the spectral transparency of the water column and the vertical position of the organisms in the body of water, each of which are in turn a function of several controlling factors. The spectral transparency of the water column in lakes depends on absorption of light by water itself, absorption by dissolved substances, and both absorption and scattering by particulate substances.[2] Contrary to popular conception, pure water is not clear, but rather a pale shade of blue, because it absorbs red light (600–700 nm) more strongly than green or blue (Kirk 1983). This absorption by the H_2O molecule is an important determinant of light penetration in the marine environment, where absorption by dissolved and particulate substances is relatively low, but much less important in lakes, where these substances are typically found in much higher concentrations (Kirk 1983).

Lakes vary greatly in water transparency: in some, 1% of the surface PFD of UVR can be found at depths greater than 10 m, but in others UVR penetrates to only a few centimeters (Morris *et al*. 1995). Although scattering and absorption by particles (*e.g*., phytoplankton) can contribute appreciably to light attenuation in some lakes (Laurion *et al*. 2000; Smith *et al*. 2004), the concentration of chromophoric dissolved organic matter (CDOM), as inferred from the concentration of its bulk surrogate, dissolved organic carbon (DOC), is the best predictor of UVR transparency across freshwater ecosystems (Morris *et al*. 1995). CDOM is responsible for the 'tea colour' apparent in many temperate lakes, and is chiefly composed of humic and fulvic acids (the term 'humic' is often

[2]These terms are somewhat arbitrary. Typically, 'dissolved' refers to substances that can pass through a glass-fibre filter (nominal pore size = 0.8 µm), and 'particulate' refers to substances that cannot. Other filter types are sometimes used, so that dissolved may refer to substances < 0.2 µm (such as in parts of this thesis) or other values between 0.1 and 1 µm. Since very few organisms or inorganic particles are of this size, the differences among methodologies are thought to be of low importance, and no universal cut-off size to delineate the dissolved from particulate has yet been established in limnology.

used to describe water of a brownish colour). Absorption by CDOM is inversely and exponentially related to the wavelength of the irradiance being absorbed, so that the most damaging UVBR is attenuated much more rapidly with depth than UVAR, which penetrates much less deeply than PAR (Kirk 1983). There is evidence that global climate change is altering concentrations of DOC, and therefore CDOM, in lakes (Schindler *et al.* 1996; Jennings *et al.* 2010) and this could have drastic effects on the UVR transparency of freshwater ecosystems.

1.1.6 Ecological and physiological effects of UVR on phytoplankton in lakes

UVR affects myriad aspects of phytoplankton eco-physiology, including photosynthesis, biochemical composition, and the taxonomic makeup of natural communities. Effects on photosynthesis are perhaps the best-studied, due to the inherent light-dependence of this process. Losses of daily primary production in lakes due to UVR reported in the literature range from appreciable (26%) to negligible (2.5%), and studies of marine phytoplankton suggest that UVAR can actually enhance primary production under conditions of fast water-column mixing in certain geographical areas (Helbling *et al.* 2003; Gao *et al.* 2007*b*). These variable findings may reflect variation related to physiological acclimation and/or adaptation at the community level, as the sensitivity of phytoplankton to photosynthetic impairment by UVR appears to vary systematically among lakes according to latitude and elevation, and/or according to cell size distributions or water clarity (Villafañe *et al.* 1999; Helbling *et al.* 2001; Villafañe *et al.* 2003; Sobrino *et al.* 2005; Helbling *et al.* 2006).

UVR can also alter the biochemical composition of phytoplankton, and this can have indirect effects on higher trophic levels. For instance, zooplankton (daphnids) fed UVR-irradiated algae have been found to be smaller, undergo increased mortality, and be less fecund than controls (De Lange & Van Donk 1997; Scott *et al.* 1999). UVR can reduce algal lipid content (Arts & Rai 1997; De Lange & Van Donk 1997) by inhibiting biosynthesis or inducing lipid peroxidation (Hessen *et al.* 1997).

The effects of UVR on fatty acid (FA) quality are not well understood: while early studies reported UVR-induced decreases in microalgal polyunsaturated FAs (Goes *et al.* 1994; Wang & Chai 1994) more recent work has shown either negligible effects, or increased polyunsaturated FAs under UVR stress (Tank *et al.* 2003; Liang *et al.* 2006; Leu *et al* 2006, 2007), sometimes concurrent with decreased monounsaturated FAs (Leu *et al.* 2007) or saturated FAs (Liang *et al.* 2006). There is ample evidence that UVR decreases algal C:P ratios (Watkins *et al.* 2001; Xenopoulos *et al*. 2002; Tank *et al. 2003;* Leu *et al.* 2006, 2007) but the effects on C:N ratios appear to be relatively minor, possibly due to comparable inhibition of C and N uptake (Mousseau *et al.* 2000; Leu *et al.* 2007).

The nutritional status of phytoplankton can influence UVR sensitivity, and UVR can inhibit the uptake and assimilation of inorganic nutrients. Decreased cellular N content under UVR-stress has been observed (Leu *et al.* 2006) and may reflect UVBR-induced damage to N incorporation mechanisms and/or increases in membrane permeability (Sobrino *et al.* 2004). Hiriart *et al.* (2002) found N-deficiency to increase susceptibility to UVR-induced photoinhibition in Lake Erie phytoplankton. However, Shelly *et al.* (2002) found repair capacity stimulated under UVBR exposure, while several studies have found no correlation between UVR-sensitivity and nutrient status of freshwater phytoplankton (Furgal & Smith 1997; Hiriart-Baer & Smith 2004). Allen and Smith (2002) found UVR to inhibit P uptake by phytoplankton in natural samples, but Shelly *et al.* (2005) observed little consistent effect of UVR on P uptake by the marine chlorophyte *Dunaliella tertiolecta* during a starvation experiment. This latter observation would support the suggestion (Xenopoulos *et al.* 2002) that P acquisition has evolved to be a relatively UVR-resistant process, because P is needed for recovery and protective mechanisms. Heraud *et al.* (2005) found increased UVR-sensitivity of *D. tertiolecta* under P starvation due to compromised repair capacity, suggesting that algal P status can potentially modulate the UVR sensitivity of phytoplankton, and UVR and P

co-regulation of primary production has been documented in two boreal lakes (Xenopoulos *et al.* 2002).

Larger cells are thought to be more robust to UVR-induced damage because of their smaller surface area to volume ratio, *i.e.*, longer path-length to the nucleus, which makes them more resistant to cyclobutane pyrimidine dimer (CPD) accumulation and other forms of damage due to molecular self-shading (Garcia-Pichel 1994). Furthermore, it has been proposed that cells need to be a minimum of ~1 µm in order to effectively utilize mycosporine-like amino acids (MAAs) for UVR photoprotection, and that this photoprotective strategy becomes potentially cost-effective for cells >10 µm (Garcia-Pichel 1994). A number of studies have indeed found higher sensitivity in smaller cells (Van Donk *et al.* 2001; Hiriart *et al.* 2002; Xenopoulos & Frost 2003; Andreasson & Wängberg 2006) but others differ (Laurion & Vincent 1998; Ferreyra *et al.* 2006), and it may be that smaller cells are more vulnerable to DNA damage but more resistant to photosystem damage (Villafañe *et al.* 2003).

Microalgal sensitivity to UVR appears to vary appreciably among freshwater phytoplankton taxa. Several studies suggest high tolerance in cyanobacteria (Kaczmarska *et al.* 2000; Jiang & Qiu 2005) and chlorophytes (Cabrera *et al.* 1997; Watkins *et al.* 2001; Villafañe *et al.* 2004), whereas the diatom (Watkins *et al.* 2001; Villafañe *et al.* 2004), chrysophyte (Xenopoulos & Frost 2003), and cryptophyte (Kaczmarska *et al.* 2000) groups appear to contain more sensitive species. However, there is undoubtedly inter-specific, and even intra-specific, variation in UVR sensitivity within phyla (Leu *et al.* 2007; Wulff *et al.* 2007). While further physiological research is needed, differences in susceptibility to UVR likely reflect variation in photo-protective pigmentation (MAAs, scytonemin), repair mechanisms and cellular morphology (unicells *vs.* colonies) among taxa (Banaszak 2003). There is evidence from the Experimental Lakes Area (ELA) that UVR may act as a structuring agent for phytoplankton community composition among lakes (Xenopoulos *et al.* 2009), but more research

is needed to distinguish the role of UVR from its environmental covariates (*e.g.* temperature) in a more robust fashion, so that these results can be generalized to other freshwater ecosystems with greater confidence. For further details concerning eco-physiological effects of UVR on freshwater phytoplankton see Harrison & Smith (2009).

1.2 Thesis objectives in outline

The general objective of my doctoral research was to investigate how solar radiation affects PSII function of natural phytoplankton communities in temperate lakes, and to elucidate the factors controlling the susceptibility to photoinhibition. To fulfill this general objective, four specific objectives were pursued:

1) Determination of how PSII function of phytoplankton communities from different strata, and therefore different irradiance conditions, of the same lakes respond to UVR and PAR.

2) A comparison of how irradiance affects PSII function of phytoplankton communities from different lakes of varying spectral transparency (DOC concentration) and trophic status (nutrient content).

3) An investigation of the individual and interactive effects of nutrient limitation and photoinhibition on PSII function of phytoplankton in Lake Ontario.

4) The prediction of diurnal and among-date variation of *in situ* PSII efficiency of Lake Ontario phytoplankton, in a depth-specific manner, using a spectrally-resolved kinetic model for photoinhibition.

Harrison & Smith (2011*a*, 2011*b*) are based on chapters 2 and 3, respectively.

Chapter 2: Deep chlorophyll maxima and UVR acclimation by epilimnetic phytoplankton

2.1 SUMMARY

It is well established that ultraviolet radiation (UVR) has many harmful effects on phytoplankton, but the factors controlling algal sensitivity to UVR are not fully understood. I exposed phytoplankton communities from the epilimnia and deep chlorophyll maxima (DCM) of two Canadian lakes to 14 irradiance treatments of various spectral quality and monitored changes in the maximum quantum efficiency of Photosystem II photochemistry (F_V:F_M) using a PAM fluorometer. Phytoplankton from DCM did not show marked differences from epilimnetic communities in taxonomy or nutrient status, but exhibited substantially higher photosynthetic impairment under UVR exposure. These results suggest that epilimnetic phytoplankton acclimate to *in situ* light conditions in a spectrally-specific manner, and that UVA radiation is a stronger stressor than UVBR or PAR in the mixed layers of the study lakes. Model estimates of damage and recovery rate constants revealed that the phytoplankton of the two lakes relied upon different strategies of UVR-acclimation, in one lake minimizing susceptibility to photodamage and in the other maximizing recovery efficiency.

2.2 INTRODUCTION

Ultraviolet radiation (UVR; 280–400 nm) has deleterious effects on the photosynthetic capacity, biochemical composition, and nutrient uptake ability of phytoplankton (Harrison & Smith 2009) with potential consequences for species interactions in aquatic ecosystems (Sommaruga 2003). Although UVBR (280–320 nm) is more destructive on a per photon basis (Cullen *et al.* 1992), UVA radiation (UVAR; 320–400 nm) can have a greater net effect on integrated water column productivity (*e.g.*, Hiriart-Baer & Smith 2004). Because the absorbance spectrum of chromophoric dissolved organic matter increases exponentially with decreasing wavelength, UVBR is rapidly attenuated in the water

column while UVAR penetrates to greater depths, and may characterize the entire mixed layer of small, clear lakes (Morris *et al*. 1995). In a recent review, Harrison & Smith (2009) noted that 11 studies of UVR's effect on daily areal potential primary production reported UVAR to exert the dominant negative effect *in situ*. However, there is laboratory-based evidence for high UVAR-resistance of phytoplankton (Nilawati *et al*. 1997) and several field studies suggest UVAR can indirectly enhance and/or drive photosynthesis in marine phytoplankton (Helbling *et al*. 2003; Gao *et al*. 2007*b*).

It is well established that phytoplankton make physiological changes, such as adjusting intracellular chlorophyll *a* (Chl *a*) or Photosystem II (PSII) reaction centre (RC) content, in response to changes in irradiance climate (Falkowski & Raven 2007). Beyond being simply high- or low-light acclimated, prior UVR exposure can play a major role in modulating UVR sensitivity of phytoplankton (Guan & Gao 2008; Sobrino *et al*. 2008). Acclimation to UVR can be accomplished *via* the accumulation of intracellular sunscreens such as mycosporine-like amino acids (MAAs; Banaszak 2003), accumulation of carotenoids that quench reactive oxygen species (Banaszak 2003), or increased efficiency of photorepair (Guan & Gao 2008). Algal MAA production is photo-inducible by UVR, particularly UVBR (Hannach & Sigleo 1998; Klisch & Häder 2002), although PAR can also be effective (Korbee *et al*. 2005). The photoinducibility of MAAs may vary taxonomically (Hannach & Sigleo 1998), but these compounds are probably widespread in natural phytoplankton, especially those of high UVR exposure systems (Laurion *et al*. 2002).

Deep chlorophyll maxima (DCM) are subsurface peaks in Chl *a* found in the marine environment (Cullen 1982) as well as large (Fahnenstiel & Scavia 1987; Barbiero & Tuchman 2001) and small lakes (Fee 1976; Pick *et al*. 1984*a*). There are a number of factors thought to be responsible for DCM formation, including low-light acclimation (low C:Chl *a*), passive sedimentation of cells, differential grazing pressure between strata, and increased access to inorganic

nutrients (Camacho 2006), and the relative importance of these factors can vary spatially (Fennel & Boss 2003) and temporally (Fahnenstiel & Scavia 1987). Whatever their causal origin(s), DCM located within the photic zone but below the maximum depth to which UVR penetrates provide an opportunity to characterize the UVR stress responses of natural communities having minimal prior exposure. Comparisons against the UVR responses of co-occurring epilimnetic communities can then provide evidence on the extent and mechanisms of adjustment to UVR exposure by communities in the same geochemical and climatic milieu (*i.e.*, the same lake). While not perfectly controlled as measures of physiological processes (taxonomic composition, for example, can vary between DCM and epilimnion), such comparisons offer a means of inferring the importance and nature of spectral acclimation and/or selective adaptation in nature without the artificiality of laboratory or mesocosm experiments.

To my knowledge, the only investigation of DCM UVR sensitivity to date was conducted in alpine lakes by Saros *et al*. (2005). These researchers conducted 7-day *in situ* bag incubations, and found no effect of UVR on biovolume of DCM phytoplankton at ambient nutrient conditions, but with nitrogen (N) and phosphorus (P) supplementation observed reduced growth due to UVR relative to PAR-only exposed samples (10- vs 20-fold increases in total biovolume, respectively). These authors concluded that nutrient availability rather than UVR was responsible for DCM formation in their study lakes. No comparison was made with epilimnetic phytoplankton in this study. However, phytoplankton from the base of the mixed layer have been found to exhibit low tolerance to UVR relative to those from the near-surface in two boreal lakes that frequently undergo diurnal micro-stratification (Xenopoulos & Schindler 2003), suggesting that the mechanisms responsible for UVR tolerance can be induced, and relaxed, on relatively short timescales in natural phytoplankton communities.

Variable fluorescence techniques, such as pulse amplitude modulation (PAM) fluorometry (Schreiber *et al*. 1986*b*), allow rapid and non-invasive assessment of phytoplankton photosynthetic health (Falkowski & Raven 2007). The variable fluorescence of Chl *a* (F_V) is the difference between the maximal fluorescence of PSII (F_M) when all RCs are closed, and the minimum fluorescence (F_O) found when all PSII RCs are capable of performing photochemistry (*i.e.*, $F_V = F_M - F_O$). In the dark-adapted state, F_V:F_M represents the maximum quantum efficiency of PSII photochemistry and is a sensitive indicator of the photoinhibition of photosynthesis (Krause & Weis 1991; Long *et al*. 1994).

If spectral irradiance history is a major determinant of phytoplankton UVR sensitivity in nature, it would be expected that (1) epilimnetic communities should exhibit higher resistance to UVR-induced photoinhibition than those from DCM and (2) that the difference in sensitivity should be greatest in the UVA spectral region. To test these hypotheses, I characterized the *in situ* spectral radiation environment of epilimnetic and DCM phytoplankton of two lakes, and used F_V:F_M to determine damage and recovery kinetics under experimental spectral exposures.

2.3 METHODS

2.3.1 Lake Sampling & Profiling

Blue Chalk and Plastic Lakes (Table 2.1) are located in the Muskoka-Haliburton area of Ontario, Canada, and are regularly monitored by the Dorset Environmental Science Centre (Ontario Ministry of Environment). Blue Chalk Lake was sampled on 5 and 8 September and Plastic Lake on 6 and 9 September 2009. Metalimnia were sampled 3 days after epilimnia. Whole-water samples were taken 3 h after sunrise using a Niskin bottle and screened through a 200-µm mesh (Nitex) to remove larger zooplankton grazers before being poured into opaque plastic carboys previously rinsed with lake water. Epilimnetic samples comprised equal parts water from 0.5 m, 1 m, and 2 m depths;

metalimnetic samples were from 9 m, 10 m, and 11 m. Carboys were stored in coolers for the 3.5 h between water sampling and the start of laboratory experiments.

Profiles of temperature and algal spectral fluorescence were taken immediately prior to water sampling with a FluoroProbe (bbe Moldaenke, GmbH). Radiometric profiling was done 4.5 h after sunrise on 6 and 7 September for down-welling irradiance using a freshly-calibrated BIC-2104 radiometer (Biospherical Instruments Inc.; 305 nm, 320 nm, 340 nm & broadband PAR) and a Satlantic OCI-200 radiometer (Satlantic Inc.; 380 nm & 399 nm).

2.3.2 Water Chemistry and Pigments

For dissolved organic carbon (DOC) determination, 40 mL of water were filtered through 47 mm GF/F filters and stored in amber glass vials at room temperature in the dark until analysis using a Dohrman DC-190 High-Temperature TOC Analyzer (Rosemount Analytical Inc., Santa Clara, California, USA). Samples were acidified using 20% phosphoric acid and sparged to remove dissolved inorganic C prior to analysis. Both filters and vials were pre-combusted (4 h at 450°C).

Particulate N (PN) and organic C (POC) were determined by filtering 100–200 mL of sample water onto ashed (4 h at 450°C) 25 mm GF/F filters which were stored frozen (-20°C) in plastic Petri dishes until return to the University of Waterloo. The filters were then dried in a dessicator, acid-fumed (10% HCl for 24 h) and analysed (980°C combustion, 700°C reduction) with a CE-440 Elemental Analyzer (Exter Analytical, Inc., North Chelmsford, Massachusetts, USA).

Table 2.1. Physical properties of Blue Chalk and Plastic Lakes.

Lake	Location	Lake area (ha)	Lake volume (m^3 x 10^5)	Mean depth (m)	Max depth (m)	Shoreline length (km)
Blue Chalk	45°12'N 78°57'W	52	45	8.5	23.0	5.7
Plastic	45°11'N 78°49'W	32	25	7.9	16.3	3.1

Samples for soluble reactive phosphorus (SRP) and total dissolved phosphorus (TDP) were filtered at low vacuum pressure (100 mm Hg) through 0.2-µm pore-size polycarbonate filters and these filtrates, along with a whole water sample for total phosphorus (TP) determination, were stored frozen (-20°C) in 60-mL polyethylene bottles until time of analysis. In all cases P concentration was determined spectrophotometrically by the ammonium molybdate method (Stainton *et al.* 1977). Samples for TDP and TP analyses were first digested with potassium persulphate in an autoclave (30 min at 120°C). Particulate P (PP) was estimated as the difference between the total and dissolved fractions.

Chl *a* concentration was determined by filtering 300–500 mL of sample water onto 47 mm GF/F filters which were kept frozen (-20°C) in the dark in glass scintillation vials until the time of analysis. Pigment was then extracted into 90% acetone (18–24 h) in the dark at -20°C and the extract analysed with a Turner Designs fluorometer (Sunnyvale, CA, USA) before and after acidification to correct for phaeophytin pigment (Parsons & Strickland 1963).

For determination of phytoplankton absorption spectra, 500 mL were filtered and stored until analysis as described above for Chl *a* determination. Pigments were extracted into absolute methanol in the dark at -20°C for 24 h, clarified by filtration, and analysed for absorbance between 200–800 nm in a Carey 100 UV-Visible Scanning Spectrophotometer (Varian Instruments, California, USA).

2.3.3 Laboratory Experiments

A specialized UVR incubation apparatus was employed to assess the effects of UVR on phytoplankton photosynthetic performance (Figure 2.1). This 'incUVator' was used to generate powerful exposures of various spectral quality by way of a xenon arc lamp (1 kW; Oriel Instruments) and 7 optical cut-off filters (Schott and Hoya Optics) with nominal 50% transmission at 305 nm, 320 nm, 340 nm, 360 nm, 385 nm, 400 nm and 420 nm. The light of half the treatments also passed through neutral density filters (perforated nickel plates) approximately halving the total photon flux

density (PFD), and yielding 2 possible intensities, which, combined with the optical filters, yielded a total of 14 distinct irradiance treatments that approximate the spectral balance of natural sunlight (Figure 2.2). Water was circulated throughout the base of the incubation unit to keep samples at ± 1°C of ambient epilimnetic temperature (20.3°C). Samples from both strata were incubated at the same temperature so that effects on enzymatic processes would not obscure any variation in UVR response due to irradiance history. How this temperature increase may have affected the DCM samples is considered later in this chapter.

Prior to starting the damage phase of the experiment, 2 L of lake water in a culture flask were placed in a cooler equipped with a fluorescent light bulb for 1 h to facilitate the repair of any photodamage incurred during the 3 h of solar exposure prior to the time of sampling. The scalar irradiance at the top of the flask was about 55 μmol m^{-2} s^{-1} of PAR. From this flask 100-mL subsamples were then distributed among 14 Pyrex 400-mL beakers which were placed in the incUVator. Incubations ran for 120 minutes during which time the UVR treatments were sampled 11 times and the PAR-only treatments 4 times, as less effect was anticipated in the absence of UVR.

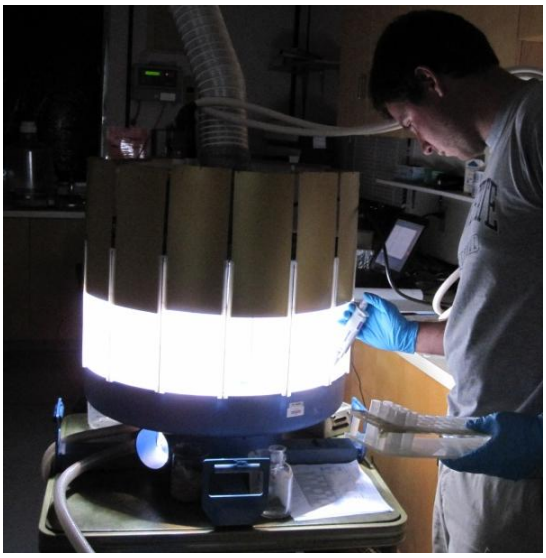

Figure 2.1. Summer technician Lee Pinnell withdraws a sample from the UVR incubator, or 'incUVator', which generated the spectral exposures used for all experimental work.

The PAR output of the bulb was monitored during the experiment with a LI-COR photometer. At each sampling time a 4-mL aliquot was withdrawn and stored in a dark incubator at *in situ* temperature for 30 min to allow the relaxation of non-photochemical quenching. Dark-adapted samples were then poured into a quartz vial (WALZ) and F_V:F_M was determined by a Water-PAM via application of a saturation pulse sufficient to temporarily close all PSII RCs (3650 μmol m^{-2} s^{-1} red light for 0.8 s). The sample signal was corrected with that of 0.2 μm-filtered water (100 mm Hg) to correct for dissolved fluorescence.

To assess the kinetics of light-dependent recovery from UVR damage, 3 beakers (>300 nm, >325 nm, and >410 nm treatments) were transferred to the illuminated cooler wherein scalar

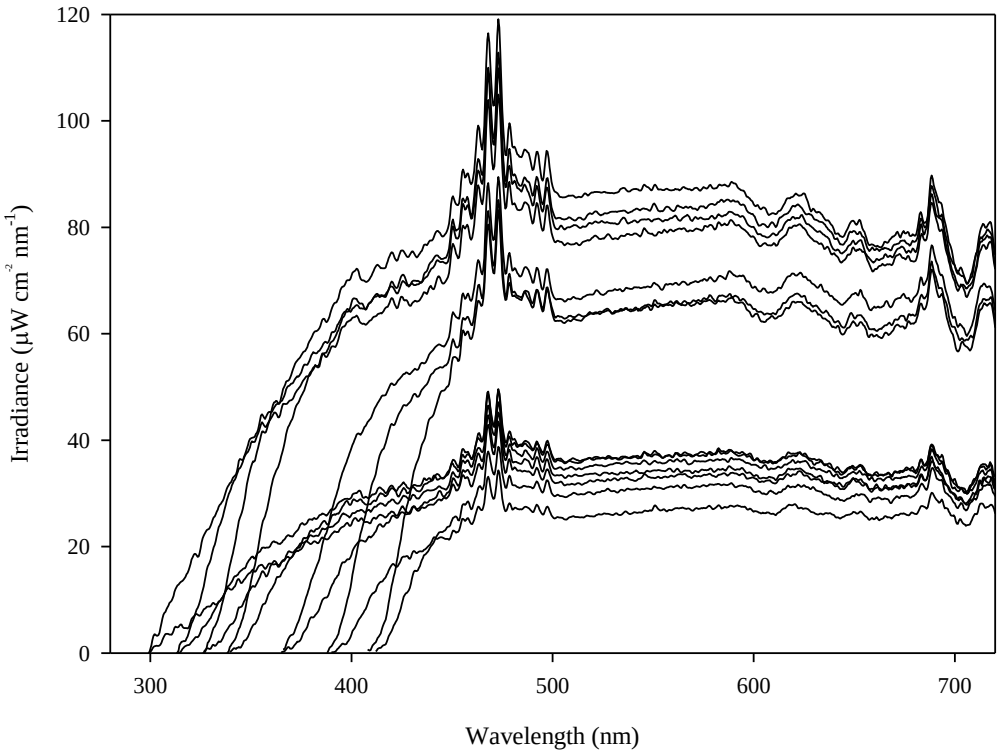

Figure 2.2. Spectral irradiance treatments used for damage phase of experiments.

irradiance at the sample level was approximately 15 μmol m^{-2} s^{-1} of PAR. Every 30 min for 150 min 4-mL aliquots were removed to assess the recovery of F_V:F_M. The air temperature in the cooler was monitored continuously and never changed more than 1.2°C during the 2.5-h experiments. Additional samples (>315 nm, >340 nm, and >390 nm treatments) were placed in a dark incubator at *in situ* temperature and analysed according to the same schedule in order to assess the relative contributions of dark and light repair to the recovery of F_V:F_M.

2.3.4 Estimation of Damage and Recovery Rate Constants

Nonlinear regression analysis was used to fit the decrease in F_V:F_M over time under UVR exposure to an equation of the form

$$P / P_i = r / (k + r) + k / (k + r) \cdot e^{-t \cdot (k + r)} \quad (2.1)$$

in which t is time, P_i is F_V:F_M prior to light exposure, P is F_V:F_M at time t, and k and r are rate constants related to damage and recovery processes, respectively (Heraud & Beardall 2000). To obtain a second set of r values representative of recovery potential in the absence of UVR, data obtained under the low-PAR of the recovery experiments were fitted to the equation:

$$P = P_d + d \cdot (1 - e^{-r \cdot t}) \quad (2.2)$$

in which P_d equals F_V:F_M after the conclusion of the damage phase and $d = P_i - P_d$, *i.e.*, the loss of F_V:F_M under UVR exposure during the damage phase.

2.3.5 Statistical Analysis

All statistical analyses were performed using SYSTAT Version 10 (SPSS, 2000).

2.4 RESULTS

2.4.1 Nutrients, Vertical Structure and Light Climate

Blue Chalk and Plastic Lakes had similar ambient water chemistry (Table 2.2) and were thermally stratified at the time of sampling with mixing depths of 6.5 and 6.0 m, respectively (Figure 2.3).

Table 2.2. Stratum-specific water chemistry of Blue Chalk and Plastic Lakes.

	Epilimnia			**Metalimnia**		
	Blue Chalk	Plastic	**Average**	Blue Chalk	Plastic	**Average**
Chl *a* (µg L^{-1})	1.49	1.29	**1.39**	7.33	4.71	**6.02**
POC (µg L^{-1})	265	266	**265.5**	453	629	**541**
PP (µg L^{-1})	2.52	2.17	**2.35**	4.51	3.88	**4.20**
PN (µg L^{-1})	34.7	34.3	**34.5**	66.3	72.3	**69.3**
TP (µg L^{-1})	5.42	3.05	**4.24**	6.12	5.03	**5.58**
TDP (µg L^{-1})	2.90	0.88	**1.89**	1.61	1.15	**1.38**
C:Chl *a* (mass)	178	206	**192**	61.8	134	**97.9**
C:N (atoms)	8.94	9.04	**8.99**	7.96	10.1	**9.03**
C:P (atoms)	272	316	**294**	259	418	**339**
DOC (mg L^{-1})	2.2	1.8	**2.0**	1.4	2.1	**1.8**

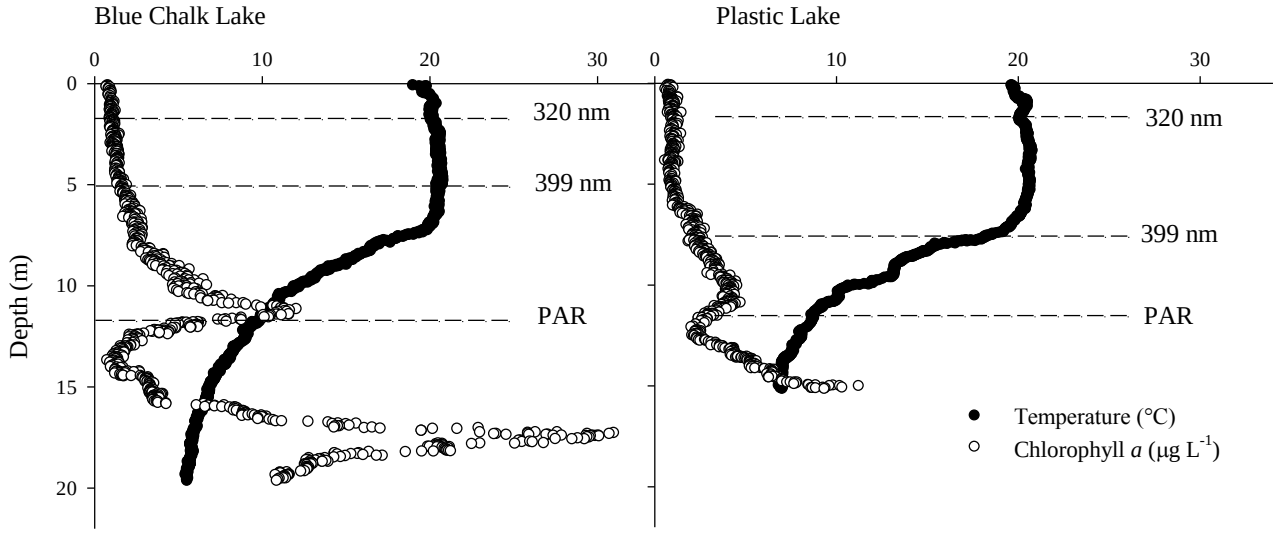

Figure 2.3. Vertical profiles of Blue Chalk and Plastic Lakes, showing fluorescence-based estimates of Chl *a* (µg L^{-1}), temperature (°C) and 1% surface irradiance depths (dashed lines).

Metalimnetic concentrations of TP, PP and PN were all higher than epilimnetic concentrations in both lakes. Differences in sestonic C:N and C:P between strata within lakes were generally small, with epilimnetic ratios higher than metalimnetic in Blue Chalk, but lower in Plastic Lake. The metalimnia of both lakes had substantially higher Chl *a* and POC content, as well as lower C:Chl *a*. Based on fluorescence data, it can be inferred that the peaks in algal biomass I sampled were centred at about 11 m depth in both lakes (Figure 2.3). Larger fluorescence peaks were detected in the hypolimnia but were not sampled. I suspect that these peaks represent photosynthetic (purple or green) bacterial biomass. These taxa are known to thrive under very low PAR, require anoxic conditions (Pfennig 1989) – which were present in the hypolimnia of the study lakes in September 2009 (Andrew Paterson, Pers. Comm.) – and are known to occur below DCM (Camacho 2006).

Consistent with the low Chl *a* and DOC concentrations of their epilimnia, the water columns of both lakes were highly UVR-transparent (Table 2.3). The 1% irradiance depth for 320 nm (UVBR) was greater than 1.5 m in each lake, and the 1% depth for 399 nm was found at 85% of the mixing depth in Blue Chalk and extended beyond the base of the epilimnion in Plastic Lake. The DCM in both lakes lay directly above the photic (1% PAR) depths, but below the depths of any significant UVR penetration (Figure 2.3).

Table 2.3. Vertical attenuation coefficients and corresponding 1% surface irradiance depths in Blue Chalk and Plastic Lakes.

		305 nm	320 nm	340 nm	380 nm	399 nm	PAR
Blue Chalk	KD (m^{-1})	3.5	2.7	2.0	1.1	0.9	0.4
	1% depth (m)	1.3	1.7	2.4	4.2	5.1	12
Plastic	KD (m^{-1})	3.8	2.8	2.1	0.8	0.6	0.4
	1% depth (m)	1.2	1.6	2.2	5.6	7.5	12

2.4.2 Community Composition

FluoroProbe fluorescence profiles indicated that the communities of both lakes were dominated by the 'diatom' (fucoxanthin/peridinin) group that additionally comprises chrysophytes and dinoflagellates. Microscopic examination confirmed this, and revealed that while many of the same species were common to the strata of both lakes, there were some differences in the dominant taxa. The epilimnion of Blue Chalk Lake showed high abundances of the diatom *Tabellaria* and the dinoflagellate *Ceratium*, as well as unicellular chrysophytes. These taxa were also present in the metalimnion but the biovolume there was dominated by colonies of the chrysophyte genus *Synura*. Plastic Lake had a more diverse community than Blue Chalk, with the diatom *Asterionella formosa* and the colonial chrysophyte *Uroglena* making large contributions to the biovolume of the epilimnion, and *Asterionella*, *Synura*, and naked dinoflagellates being common in the metalimnion. The microplankters *Staurastrum* and *Dinobryon* were found in all samples examined, as were the nanoplankters *Merismopedia minima*, *Chromulina nebulosa*, *Chroococcus minutus* and *Monosiga* sp., among others.

2.4.3 UVR Incubations (Damage)

Values of F_V:F_M were generally high (0.608 ± 0.026, mean ± SD), even prior to the 1 h of low-PAR recovery time allotted prior to beginning the UVR incubations, after which they increased to approximately the accepted optimal value of 0.65 (Falkowski & Raven 2007; 0.649 ± 0.013). Epilimnetic mean F_V:F_M was about 94% of metalimnetic prior to low-PAR recovery, but increased to about 97% afterward, suggesting that the difference in F_V:F_M between strata was due to slightly more accumulated photodamage in the epilimnetic community, relative to the metalimnetic, prior to sampling.

During 120 min of UVR incubation F_V:F_M decreased in response to all spectral treatments. Metalimnetic samples experienced greater losses of F_V:F_M than epilimnetic samples under all

irradiance treatments and the magnitude of the difference in response varied spectrally (Figure 2.4). Samples from both strata showed similarly mild responses to PAR-only (>410 nm) exposure and severe responses to full-spectrum irradiance (>300 nm), but phytoplankton from the epilimnia exhibited much higher UVAR (>325 nm) resistance than those of metalimnetic origin (Figure 2.5).

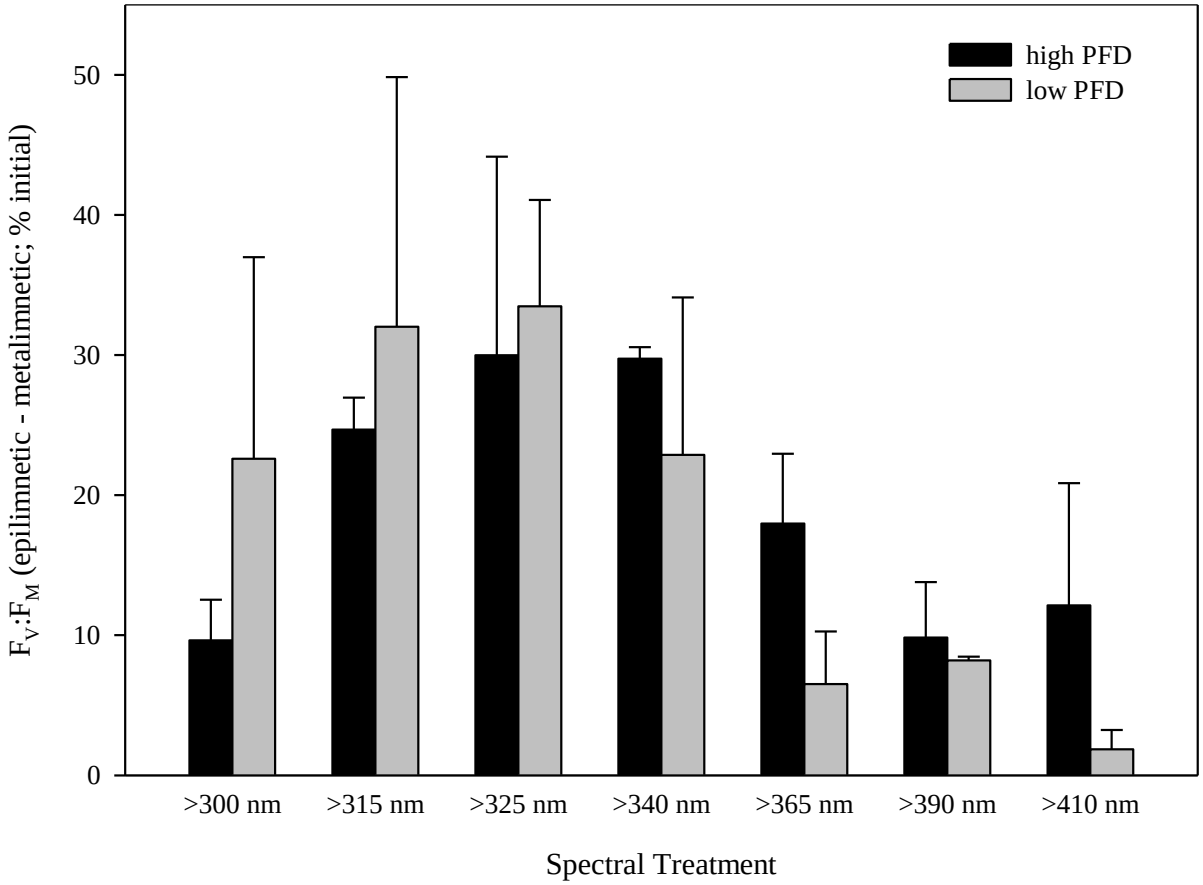

Figure 2.4. Mean difference in F_V:F_M (epilimnetic - metalimnetic) after 120 minutes spectral exposure, expressed as a percentage of pre-exposure F_V:F_M for Blue Chalk and Plastic Lakes. Error bars represent +/- 1 SD.

2.4.4 PAR Incubations (Recovery)

Epilimnetic samples recovered more completely from the photodamage incurred during the damage experiments than those from the metalimnia, with the greatest rate of recovery generally occurring during the first 30 min (Figure 2.5). The absolute increase in $F_V:F_M$ after 30 min was higher for epilimnetic samples than metalimnetic samples for both >300 nm and >325 nm exposure treatments (Figure 2.5). The time course of recovery of $F_V:F_M$ was well-described by Equation 2.2 (mean R^2 = 0.90). Recovery rate constants calculated from low-PAR incubations were significantly different from those calculated based on the UVR-exposure incubations (based on non-overlap of 95% confidence intervals) for only two of the treatments (>300 nm for the Plastic Lake metalimnion and >325 nm in the epilimnion of Blue Chalk Lake), but were slightly higher in general. Although obtained using different exposure treatments (>315, >340 and >390 nm *vs*. >300, >325 and >410 nm) rates of dark recovery (r = 0.0003–0.0052 min^{-1}) were approximately an order of magnitude lower than rates of recovery under low PAR (r = 0.0041–0.0478 min^{-1}).

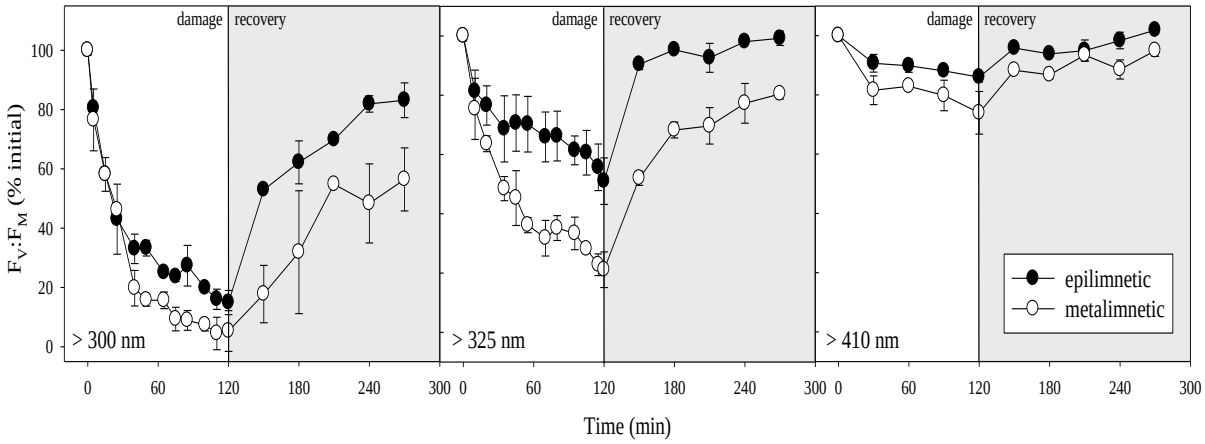

Figure 2.5. Mean effect of >300 nm, >325 nm, and >410 nm high PFD exposures on $F_V:F_M$ and subsequent recovery under dim PAR (shaded area) for both lakes. Error bars represent +/- 1 SD.

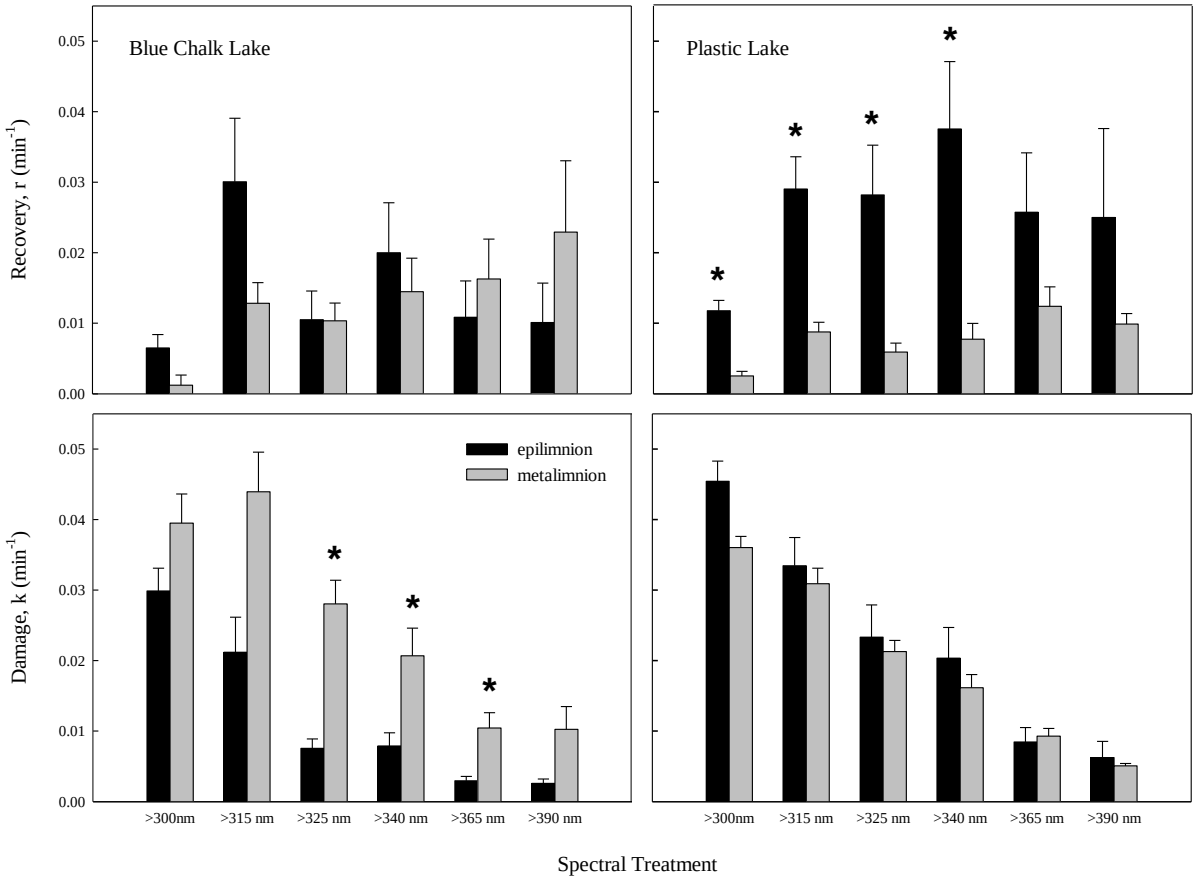

Figure 2.6. Damage (k) and recovery (r) rates estimated under various spectral UVR exposures (high PFD) for both strata of Blue Chalk and Plastic Lakes. Asterisks represent significant differences between strata based on non-overlap of 95% confidence intervals. Error bars represent +/- asymptotic standard errors from nonlinear regressions.

2.4.5 Damage and Recovery Kinetics

Damage phase F_V:F_M data fit Equation 2.1 well overall (mean R^2 = 0.89) with better fit for high PFD treatments (mean R^2 = 0.93) than low (mean R^2 = 0.84). Patterns among spectral treatments and strata were similar for both PFDs. Metalimnetic samples showed higher values of k than epilimnetic samples under all spectral treatments in Blue Chalk Lake (Figure 2.6). The difference in k between strata was small in Plastic Lake, although values of r were consistently much higher in the epilimnion than metalimnion (Figure 2.6). There was no discernable spectral pattern or difference between strata in r for Blue Chalk Lake.

2.4.6 UVR-Absorbing Compounds

Although distinct peaks that could correspond to MAAs or other UVR-absorbing pigments were not generally distinguishable, absorption normalized to Chl *a* content in the UV was found to be greater for epilimnetic seston samples, with the magnitude of the disparity between strata increasing with decreasing wavelength (Figure 2.7).

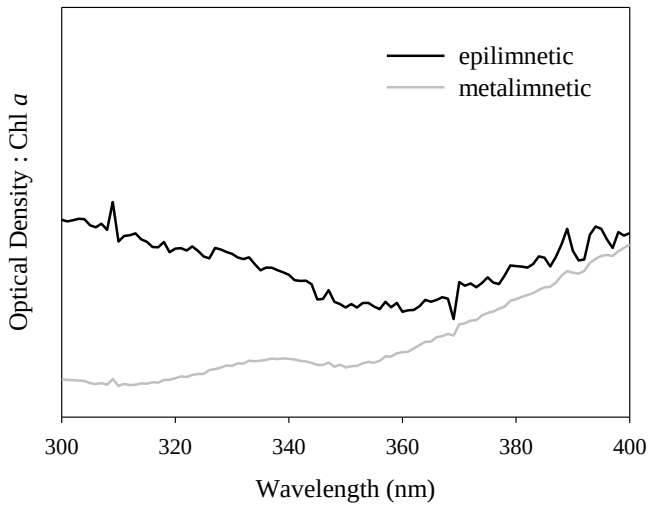

Figure 2.7. Average UVR absorption spectra of phytoplankton from the 2 strata of Blue Chalk and Plastic Lakes normalized to Chl *a* content.

2.5 DISCUSSION

Despite sharing many taxa and not differing drastically in N or P status, I found DCM phytoplankton to be more susceptible to UVR-induced photoinhibition than epilimnetic phytoplankton, with a large disparity in response to UVAR. The UVR tolerance of the epilimnetic phytoplankton was achieved by minimizing damage in Blue Chalk Lake, and by maximizing recovery efficiency in Plastic Lake.

2.5.1 Nature of the deep communities

Elevated metalimnetic *in situ* fluorescence signals corresponded with higher extracted Chl *a* (about fourfold) but also POC (about twofold) compared to the average for the epilimnia, suggesting much higher metalimnetic phytoplankton biomass and not merely shade-acclimated assemblages. However the lower metalimnetic C:Chl *a* values show that the algae were indeed acclimated to low light, as expected.

A deep maximum of phytoplankton biomass is often formed by a small number of taxa or single taxon (see Camacho 2006), and based on the spectral fluorescence profiles I suspected this to be the case in the study lakes. However, microscopic examination revealed that DCM taxonomic diversity was comparable to that of the mixed layers and in both lakes contained a mixture of dinoflagellates, diatoms and both unicellular and colonial chrysophytes.

Seston C:N and C:P ratios (Table 2.1) were similar among strata, and suggested only moderate N limitation, but extreme P limitation of the phytoplankton in both strata of both lakes (Healey & Hendzel 1980). The low DP (Table 2.1) and SRP (< 1 μg L^{-1}, data not shown) were also consistent with P limitation. While it was not the purpose of this study to investigate the mechanism(s) responsible for DCM formation, the results indicated that nutrients supplied from the hypolimnia did not support better nutrient conditions in the metalimnia and were probably not a key mechanism for DCM maintenance in the study lakes.

2.5.2 UVR sensitivity of the deep phytoplankton maxima

The metalimnetic communities examined showed higher susceptibility to UVR-induced photoinhibition under all spectral treatments employed, with a pronounced difference in response to short-wavelength UVAR. Because of its effects on enzymatic processes, such as D1 protein synthesis, low temperature can increase UVR sensitivity of phytoplankton by inhibiting recovery (Neale *et al*. 1998*b*), in particular, increasing sensitivity of F_V:F_M to UVAR (see Appendix C). To remove this known direct effect of temperature on UVR response, DCM phytoplankton were incubated at the mean epilimnetic temperature (20.3°C) during the UVR exposure experiments rather than metalimnetic temperature (~10°C). It is possible that the approximately 10°C higher epilimnetic temperature prior to UVR exposure stressed the DCM phytoplankton and contributed to their higher photosynthetic impairment, but the available data do not support this hypothesis. The air temperature during the initial low-PAR recovery period was about 21°C, so the sample was slowly warmed during the 1 h prior to the damage phase of the experiment. Experimental measurements of the effect of similar temperature increases on low temperature (winter) phytoplankton communities from Lake Erie showed no effects on F_V:F_M and positive effects on other fluorescence metrics (*e.g.*, electron transport rates; R.E.H. Smith & J.W. Harrison, unpub. data). The small differences in loss of F_V:F_M between epilimnetic and DCM samples under low-PFD and no UVR (>410 nm exposure) in the current study further suggest that the change in temperature had no appreciable negative effect on the ability of metalimnetic samples to protect F_V:F_M under illumination.

Taxonomic composition, cell size and nutrient status have all been proposed in the literature as potential determinants of phytoplankton UVR sensitivity (Harrison & Smith 2009). However, the taxonomic composition, as assessed by *in situ* spectral fluorescence and microscopic examination, did not appear to explain the high UVR sensitivity of the DCM, although it could help explain the differences in epilimnetic damage and recovery rates, as I later discuss. Considering both lakes

together, the genus *Synura* contributed a much larger fraction of the metalimnetic than epilimnetic phytoplankton biomass, but it is unlikely that this explains the high sensitivity of the DCM. Colonial forms are thought to be more UVR-tolerant than unicells (*e.g.*, Van Donk *et al*. 2001), and another colonial chrysophyte, *Uroglena*, comprised a large portion of the epilimnetic biovolume in Blue Chalk Lake. Given the abundance of colonies (*Synura*, *Asterionella*) as well as large, naked dinoflagellates in the metalimnia, a smaller average cell size across the nano- to microplankton size range, which has been related to increased rates of photodamage (Key *et al.* 2010), is also an unlikely explanation for my results. Picocyanobacteria are usually the dominant autotrophic picoplankton in lakes (Sterner *et al*. 2000), can be important members of deep phytoplankton layers (*e.g.* Wilhelm *et al.* 2006) and can exhibit high sensitivity to photodamage (Key *et al.* 2010). However, Plastic Lake is too acidic (pH < 6.0; Keller *et al*. 2008) to contain picocyanobacteria (Stockner *et al*. 2000), and *in situ* fluorometery did not show the large phycoerythrin or phycocyanin signals in either lake that would be expected if such organisms were an important part of the DCM, so it appears unlikely that the presence of UVR-sensitive metalimnetic picophytoplankton underlie these results. I therefore conclude that differences in cell size between strata are an unlikely explanation for the observed differences in UVR sensitivity. A definitive answer would demand further work, such as UVR exposure experiments performed on size-fractionated (<2 µm, 2–20 µm, >20 µm) phytoplankton assemblages from epilimnetic and DCM communities.

All four of the phytoplankton communities were moderately N-limited and extremely P-limited based on the criteria of Healey & Hendzel (1980), but metalimnetic C:N and C:P ratios were somewhat higher than epilimnetic in Plastic Lake. N and P deficiency have been shown to increase sensitivity to UVR (Hiriart *et al*. 2002; Heraud *et al*. 2005), probably by inhibiting recovery processes (Harrison & Smith 2009), so it is possible that nutrient stress contributed to the low recovery rates exhibited by the metalimnetic community of Plastic Lake. However, despite having higher C:P and

C:N, the recovery rates of the Plastic Lake epilimnetic community were higher than those found in either stratum of Blue Chalk (Figure 2.6). Stoichiometric ratios are widely accepted indicators of algal nutrient status but do suffer interference from non-algal seston and uncertainty due to the complexity of controls on algal nutrient demand ratios (*e.g.* Sterner *et al.* 2008). It is possible that additional indicators of nutrient status, such as alkaline phosphatase assays, could have more clearly revealed inter-stratum differences in algal nutrient status related to UVR response. Nitrogen and phosphorus deficiency have been reported to depress phytoplankton quantum yields (*e.g.* Sylvan *et al.* 2007) but the initial values (*i.e.*, before experimental damage) in this study were high and similar between strata. While differences in nutrient status cannot be ruled out, the data do not provide strong evidence of consistent differences between strata that would explain the observed differences in UVR response.

Given the available evidence for the study lakes, physiological change in response to the prevailing light climate appears likely to account for much of the observed differences. I was unable to find distinct peaks in particulate UVR absorption that could correspond to specific MAAs, but the greater light absorption in the UV range by the epilimnetic phytoplankton could suggest photoprotective pigmentation (*e.g.* Gao *et al*. 2007*b*). Quenching of reactive oxygen species and efficient repair of PSII RCs are additional likely mechanisms that could explain the UVR-tolerance of the phytoplankton from the mixed layer (Roy 2000), and while I did not assay for the former, the latter will be discussed shortly.

The DCM were found to be acclimated to low light, as reflected by their low C:Chl *a* content (Falkowski & Raven 2007), and this could explain the high rates of photodamage incurred by the phytoplankton from the metalimnion of Blue Chalk Lake, that showed much higher values of k than in the epilimnion. Under low light conditions, a large ratio of PSII antennae pigment to PSII RCs is desirable because photon capture limits PSII photochemistry and not electron flow to PSI (Falkowski

& Raven 2007). During exposure to the high PFD spectra, such a high Chl *a* to PSII RC ratio would lead to prolonged reduction (closure) of PSII RCs and consequent D1 protein damage that causes photoinhibition and is expressed as a decrease in F_V:F_M (Long *et al*. 1994). This could explain the generally higher sensitivity to all the spectral treatments but not the variation in the magnitude of response to the different spectral exposures. Furthermore, under the low PFD treatments, there was almost no difference in response to PAR, but a marked difference in UVR-induced photoinhibition after 2 h of exposure. The DCM were therefore not merely low-PAR acclimated, but were particularly impaired by UVR, suggesting they lacked the requisite mechanisms for efficient photosynthesis under UVR stress, such as rapid D1 repair and/or reaction oxygen species quenching (Roy 2000). The argument for UVR-acclimation as the key factor differentiating phytoplankton from the different strata is strengthened by the comparative spectra of *in situ* irradiance *vs* phytoplankton response. The largest difference in phytoplankton response was in the UVA, corresponding to the "window" of maximum difference of *in situ* spectral exposure between the rapidly-attenuated UVBR and the deeply-penetrating PAR.

My results are consistent with those of Xenopoulos & Schindler (2003) who found phytoplankton from the base of the mixed layer to be more impacted by UVR than subsurface samples. Although their experimental design lacked the spectral resolution employed here, they also found UVAR to exert a strong effect relative to UVBR. Saros *et al*. (2005) found that DCM phytoplankton biovolume was unaffected by exposure to UVR at ambient nutrient conditions, but had a dramatic effect (~50% reduction) under N and P supplementation. How photoacclimation, or a lack thereof, contributed to this finding is difficult to discern, as no comparison was made to the epilimnetic community.

2.5.3 Physiological basis of algal UVR sensitivity (k & r)

Based on comparisons of k and r between strata and lakes, the epilimnetic phytoplankton communities in the two lakes used different acclimation strategies for UVR-resistance and achieved a similar outcome (functionality after lengthy exposure). Epilimnetic phytoplankton in Blue Chalk were able to minimize UVR-induced damage (low k) while those in Plastic Lake showed efficient recovery (high r). The reason for the use of different acclimation strategies is not clear. It has been proposed that larger cells are more resistant to UVR due to molecular self-shading (Garcia-Pichel 1994) and that small cells compensate for higher vulnerability to photodamage with more efficient repair processes (Six *et al*. 2009; Key *et al*. 2010). The phytoplankton community composition in part supports this hypothesis: I observed that large unicells of the genus *Ceratium* (>200 µm) comprised a large portion of Blue Chalk Lake's epilimnetic biomass, whereas colonies of *Uroglena* (individual cells ~10 µm) represented much of the epilimnetic biomass in Plastic Lake.

The somewhat higher values of r obtained under low-PAR (*i.e.*, in the recovery treatments) relative to those obtained under UVR-exposure (the damage phase of the experiments) may reflect UVR-induced inhibition of recovery processes during the damage experiments, possibly via UVBR effects on the DNA transcription (Strid *et al*. 1994) necessary for *de novo* synthesis of the D1 protein of PSII RCs. However, recovery rates under "benign" PAR can vary depending on the irradiance provided (*e.g.*, Gao *et al*. 2007*a*) so other mechanisms could be at play. Nonetheless, the comparable magnitude of recovery rates observed here during both damage and recovery experiments provides some assurance that the estimates are robust and the differences between lakes and strata meaningful.

My results are the first to show that phytoplankton from DCM exhibit demonstrably higher sensitivity to UVR-induced photoinhibition than epilimnetic communities of the same lakes and that spectral differences in UVR sensitivity between strata likely reflect differences in average spectral irradiance exposure *in situ*. Given the relatively high UVAR sensitivity of the deep communities, my

data suggest that UVAR is the major photoinhibitory stressor in the mixed layer and the waveband to which epilimnetic phytoplankton communities must acclimate, whether via minimization of damage or increased recovery efficiency. While various factors such as nutrient status and community composition may indeed act to modulate UVR sensitivity, my results suggest that light history can play a major role in determining how UVR affects phytoplankton photosynthesis. If temperate lakes are to undergo major changes in transparency due to climate change, whether towards a clearer (Schindler *et al*. 1996) or browner (Jennings *et al*. 2010) state, more research is necessary to clarify the mechanisms employed by phytoplankton to resist UVR stress, as well as the associated metabolic costs and implications for carbon cycling and phytoplankton composition in aquatic ecosystems.

Chapter 3: The spectral sensitivity of phytoplankton communities to UVR-induced photoinhibition differs among clear and humic temperate lakes

3.1 SUMMARY

I determined the spectral sensitivity of phytoplankton communities to photoinhibition in six temperate lakes spanning a transparency gradient due to variation in dissolved organic carbon (DOC) content. Changes in variable fluorescence (F_V:F_M) were monitored during experimental irradiance exposures and used to estimate spectral weighting functions for damage by ultraviolet radiation (UVR) and recovery rates. DOC explained a high proportion of the variation in UVR sensitivity, with clear-water phytoplankton communities showing greater resistance to UVR-induced photoinhibition than those of browner waters. These differences were greater when assessed in September, after clear-sky conditions, than in July, after several days of overcast skies, especially in the long-wavelength UVA spectral region. Surprisingly, the most UVR-sensitive phytoplankton communities were dominated by filamentous cyanobacteria, a putatively UVR-resistant taxon, whereas small unicellular eukaryotes were common in the most UVR-tolerant assemblages. Model estimates of *in situ* photoinhibition after 2 h exposure to an incident solar spectrum were only slightly higher in the clear lakes than browner ones, despite appreciably higher UVR exposure in the former. Phytoplankton in clear lakes can maintain values of F_V:F_M comparable to communities protected from UVR by high concentrations of DOC.

3.2 INTRODUCTION

Ultraviolet radiation (UVR; 280–400 nm) negatively affects phytoplankton photosynthesis (Cullen *et al*. 1992), growth (Litchman & Neale 2005) and other metabolic processes such as nutrient uptake

(Sobrino *et al*. 2004), by damaging important cellular components such as the D1 protein of Photosystem II (PSII) reaction centres (Bouchard *et al*. 2006), deoxyribonucleic acids (DNA; Sinha & Häder 2002), and cellular membranes (Murphy 1983). Changes in UVR exposure therefore have important consequences for planktonic primary production and food-web interactions in freshwater ecosystems (Harrison & Smith 2009). Lakes range widely in UVR transparency, largely due to variation in dissolved organic carbon (DOC) content (Morris *et al*. 1995), but more specifically, due to the light-absorbing fraction of DOC: chromophoric dissolved organic matter (CDOM). Because absorption of irradiance by CDOM is inversely and exponentially proportional to wavelength, the most energetic, and damaging, UVB radiation (UVBR; 280–320 nm) penetrates to only a fraction of the depth to which longer-wavelength UVA radiation (UVAR; 320–400 nm) reaches (Morris *et al*. 1995). Climate change is expected to alter the DOC content of lakes, and there exists evidence for both a clarifying (Schindler *et al*. 1996; Yan *et al*. 1996) and browning influence (reviewed by Jennings *et al*. 2010). The actual effects will likely vary geographically, according to how regional climate variables such as precipitation, irradiance, and temperature are affected (Zhang *et al*. 2010). Based on long-term monitoring (Schindler *et al*. 1996), spatial surveys (Williamson *et al*. 1996), and paleolimnological data (Pienitz & Vincent 2000), it has been proposed that climate-related changes in DOC may have far greater influence on plankton UVR exposure than changes in stratospheric ozone concentrations.

A growing body of evidence suggests that changes in UVR exposure can alter phytoplankton community composition in lakes, as has been observed in temperate (Kaczmarska *et al*. 2000), boreal (Xenopoulos *et al*. 2009), and alpine regions (Williamson *et al*. 2010). However, such work is typically done using artificial enclosures, which may not faithfully represent natural conditions (Carpenter 1996), or by correlating phytoplankton taxonomy with UVR exposure in nature, which can be problematic due to confounding environmental covariates (*e.g*., temperature; Xenopoulos *et al*.

2009). Careful examination of how communities respond to UVR stress could help inform the interpretation of apparent correlations between community structure and function and levels of UVR exposure. If UVR can structure community composition among lakes, the phytoplankton of more UVR-transparent habitats would be expected to exhibit greater resilience to UVR than phytoplankton from more colored lakes. Indeed, there is evidence that phytoplankton from clear lakes are more resistant to UVAR-induced photoinhibition (Moeller 1994) and UVBR-induced DNA damage (Villafañe *et al*. 2004) than those of less transparent systems. However, this evidence to date derives from relatively lengthy and harsh near-surface exposures, and contradictory findings also exist (Milot-Roy & Vincent 1994; Neale *et al*. 2001*b*).

The effects of UVR on phytoplankton depend upon the duration, photon flux density (PFD) and spectral quality of irradiance exposure, the susceptibility of the organisms to damage, and their ability to recover (Harrison & Smith 2009). The spectral composition of *in situ* irradiance varies among lakes according to the quantity and quality (optical density) of DOC and with depth in a given lake (Kirk 1983) while the biological effects of UVR are highly wavelength-dependent (Cullen *et al*. 1992). Phytoplankton are transported at varying rates through these vertical gradients of irradiance and spectral quality by mixing processes (Neale *et al*. 2003). Partly because the outcome of exposure depends on both damage and recovery processes, effects are typically non-linear with exposure time and irradiance (Neale *et al*. 2003; Hiriart-Baer & Smith 2005). Fixed-length exposures under arbitrary exposure regimes (Moeller 1994; Villafañe *et al*. 2004) will not necessarily give a measure of susceptibility or spectral response that represents that of the natural community (Neale *et al*. 2003; Hernando *et al*. 2006). Accurate description of the UVR response of a given phytoplankton taxon or assemblage, and a basis for predicting responses under altered exposure regimes, therefore requires both a biological weighting function (BWF), to quantify the biological effectiveness of the irradiance

based upon its spectral composition, and an exposure response curve (ERC) which describes the kinetics of the response (Cullen & Neale 1997).

The variable fluorescence (F_V) of PSII is the difference between the maximum (F_M) and minimum (F_O) levels of PSII fluorescence ($F_V = F_M - F_O$), and the ratio F_V:F_M represents the maximum quantum fluorescence yield of PSII. If irradiance is saturating and processes downstream from PSII are limiting photosynthesis, decreases in F_V:F_M are not accompanied by a proportionate reduction in the rate of carbon fixation (Behrenfeld *et al*. 1998). F_V:F_M is, however, a reliable indicator of net PSII reaction centre inactivation (Anderson *et al*. 1997), and I use it in this study to quantify the photoinhibition of PSII photochemistry in phytoplankton. The kinetics of UVR-induced photoinhibition (decreases in F_V:F_M) in algal cultures (Heraud & Beardall 2000) and some natural communities (Neale *et al*. 2001*a*; Harrison & Smith 2011*a*) are well described by the model of Kok (1956). The Kok model makes the rates of both damage (PSII inactivation) and recovery (of PSII function) explicit and to date appears to provide an acceptable basis for definition of the ERC for F_V:F_M.

This research was undertaken to determine: 1) whether a spectrally-resolved Kok model can describe the UVR responses of phytoplankton communities from six temperate lakes of varying UVR-transparency, 2) whether differences in phytoplankton spectral sensitivity and recovery efficiency among lakes are consistent with acclimation or adaptation to UVR, 3) the relative importance of variations in sensitivity to damage *vs*. recovery efficiency among communities from different lakes, and 4) what parts of the UV spectrum phytoplankton communities adapt or acclimate to, and whether this relates to *in situ* exposure history.

UVR effects on phytoplankton are generally thought to result from cellular absorption of UV photons and consequent damage to important components such as the D1 protein of PSII (Bouchard *et al*. 2006) or DNA (Sinha & Häder 2002). However, harmful reactive oxygen species (ROS), such

as peroxide, produced by the interaction of UVR with DOC compounds (Scully *et al*. 1996) may represent a significant extracellular stressor to phytoplankton in high DOC lakes (Kaczmarska *et al*. 2000). I therefore used reciprocal transfer experiments to test: 5) whether extracellular UVR photoproduct generation contributed to the apparent UVR sensitivity of phytoplankton from humic lakes.

3.3 METHODS

3.3.1 Field sampling and profiling

The study lakes (Blue Chalk, Brandy, Chub, Dickie, Fawn, and Plastic) are located in the Dorset-Haliburton region of Ontario, Canada and are regularly monitored by the Ontario Ministry of the Environment (Zhang *et al*. 2010). Each lake was profiled and sampled once during 24–29 July and once during 02–07 September 2009. Whole-water samples were collected 3 h after sunrise from depths of 0.5 m, 1 m, and 2 m using a Niskin bottle and combined to obtain an integrated epilimnetic sample from each lake. This sample was screened through a 200-μm mesh and stored in an opaque plastic carboy in a cooler until laboratory experiments began (3.5 h). Vertical profiles of spectral fluorescence and temperature were taken immediately prior to water sampling using a FluoroProbe (bbe Moldaenke) and epilimnion depths (Z_{mix}) were calculated from temperature data at 0.5-m resolution using the 1°C change-per-meter criterion. Algal fluorescence was calculated as the difference between the total fluorescence measured *in situ* and the fluorescence emitted by lake water passed through a 0.2-μm pore-size polycarbonate filter. Radiometric profiling was conducted 4.5 h after sunrise with BIC-2104 (305 nm, 320 nm, 340 nm and broadband photosynthetically active radiation (PAR); Biospherical Instruments) and Satlantic OCI-200 (380 nm, 399 nm; Satlantic) radiometers. Linear regression analysis of the natural logarithm of irradiance vs. depth was used to determine vertical attenuation coefficient (KD_λ) values for irradiance at 305 nm, 320 nm, 340 nm,

380 nm, 399 nm, and PAR. Coefficients for each wavelength from 299–399 nm for each lake were subsequently estimated by interpolation

$$KD_\lambda = e^{-a\,\lambda+b} \tag{3.1}$$

where a and b are coefficients from linear regression of the ln-transformed measured KD_λ values *vs.* wavelength (*i.e.*, λ = 305 nm, 320 nm, 340 nm, 380 nm, 399 nm; average R^2 = 0.99). Using the equation of Sterner (1990), the mean epilimnetic irradiance, as percent subsurface, was calculated as

$$\bar{E}_\lambda\% = \frac{100\,(1-e^{-KD_\lambda\,Z_{mix}})}{KD_\lambda\,Z_{mix}} \tag{3.2}$$

When not in use for profiling, the BIC radiometer was used to measure surface incident irradiance in the study area. Temperature sensors (StowAway TidbiT, Onset Computer) were moored at the sampling site in Fawn Lake at depths of 0.25 m, 0.5 m, 1 m, 1.5 m, 2 m, and 3 m from 01 August to 04 September to monitor diurnal variation in water column vertical temperature structure.

3.3.2 Water chemistry

Samples were analyzed for a suite of water chemistry parameters using the methods described in Chapter 2. Briefly, DOC (< 0.7 μm) was analyzed using a Dohrman DC-190 High-Temperature TOC Analyzer (Rosemount Analytical). Phosphorus (P) concentrations were determined spectrophotometrically by the ammonium molybdate method, including soluble reactive P (SRP), total dissolved P (TDP), and total P (TP). Particulate nitrogen (PN) and carbon (PC) were determined using a CE-440 Elemental Analyzer (Exeter Analytical) and particulate P (PP) as the difference between TP and TDP. Chlorophyll *a* (Chl *a*) was determined using a Turner Designs fluorometer with acidification to correct for phaeophytin pigment.

3.3.3 Phytoplankton taxonomy

Cells from Lugol's-preserved water samples (15–50 mL) were settled into counting chambers (>24 h) and viewed under inverted microscope (Axiovert 35, Carl Zeiss Canada) to identify the dominant biovolume contributors at genus level.

3.3.4 Laboratory experiments

UVR exposure experiments were conducted as in Chapter 2; only essentials details are provided herein. I generated 14 spectral exposure treatments using optical cut-off filters (>300 nm, >315 nm, >325 nm, >340 nm, >365 nm, >390 nm, and >410 nm) and neutral density filters (high and low PFDs) in combination with a xenon arc lamp. Prior to commencement of UVR incubations, lake water was exposed to low PAR (~55 μmol m^{-2} s^{-1}) for 1 h to facilitate the repair of PSII photodamage (Greer *et al*. 1986; Heraud & Beardall 2000) that may have occurred *in situ* during the 3 h between sunrise and sample collection. Water samples (100 mL) were then incubated in Pyrex beakers at *in situ* temperature for 120 min under the various spectra, during which time F_V:F_M was assessed at regular intervals. At each sampling time a 4-mL aliquot was withdrawn and dark adapted (30 min) prior to assessment of F_V:F_M via a saturation light pulse (3650 μmol m^{-2} s^{-1}) from a Water-PAM fluorometer (Heinz Walz GmbH). Dissolved fluorescence was corrected for with filtered water (< 0.2 μm).

To test the hypothesis that phytoplankton in humic waters would be more susceptible to oxidative stress from extracellular UVR photoproducts generated during the experiments than those of clear waters, reciprocal transfer experiments were conducted with Plastic and Fawn Lake phytoplankton on 15 and 26 July and 24 August 2010. Cells from each lake were isolated by successive filtration through 20-μm, 2-μm, and 0.2-μm pore-size polycarbonate filters. By agitating the filters, the cells from Fawn Lake were then re-suspended in the Plastic Lake filtrate and *vice versa.* Cells from each lake were also isolated and re-suspended in the water from which they were

isolated. UVR exposure experiments were then conducted as described above, except that each treatment was sampled only once, after 1 h of exposure. For each spectral treatment a three-way ANOVA (balanced design, no interactions) was performed with cell origin (Plastic *vs*. Fawn Lake phytoplankton), water type (humic *vs*. clear), and date as factors, followed by a Holm-Sidak test for pair-wise multiple comparisons to determine significant ($p < 0.05$) differences among dates. Assumptions of normality and homoscedasticity were tested and met in all cases.

3.3.5 Modeling of UVR response

Biological weighting functions (BWFs) were calculated according to Cullen & Neale (1997). Nonlinear regression analysis was used to fit the decrease in F_V:F_M over time under UVR exposure to an equation (*i.e.*, ERC) of the form

$$\frac{P}{P_i} = \frac{r}{r+k} + \frac{k}{r+k} e^{-(r+k)t} \tag{3.3}$$

where P is F_V:F_M at time t, P_i is F_V:F_M prior to UVR exposure, r is the rate constant related to recovery, t is time and k the rate constant related to damage, after Kok (1956). Mean irradiance in each sample beaker was calculated at 1-nm resolution using Eqs. 3.1 and 3.2. Principal components analysis (PCA) was conducted on the irradiance data (299–399 nm) normalized to PAR (E_N) for each sample, so that

$$k = E_{PAR}\left(m_0 + \sum_{j=1}^{z} m_j c_{i,j}\right) \tag{3.4}$$

where E_{PAR} is the mean PAR spectrum, m_0 is the coefficient of influence for the mean spectrum plus PAR, z is the number of component scores included in the analysis (determined by an F test), m_j is the coefficient of influence for each PC included in the analysis, and $c_{i,j}$ are the component scores from the PCA. The biological effectiveness coefficients ($\varepsilon_{k(\lambda)}$ in $[J\ m^{-2}]^{-1}$) for photodamage by wavelengths 299–399 nm were then calculated as

$$\varepsilon_{k(\lambda)} = \frac{\sum_{j=1}^{z} m_j w_{j(\lambda)}}{SD[E_{N(\lambda)}]} \tag{3.5}$$

where w_j are component weights.

For each study lake, the BWF-ERC model was applied to estimate percent F_V:F_M at depths of 1, 2.5, 5, 10, 20, 30, 40, 50, 75, and 100% of Z_{mix}, in addition to values of % mean epilimnetic F_V:F_M, after 2 h exposure to a clear-sky, mid-day (29 August 2010) incident solar spectrum (Figure 3.1), in the absence of vertical mixing and assuming 2% surface reflectance (Kirk 1983).

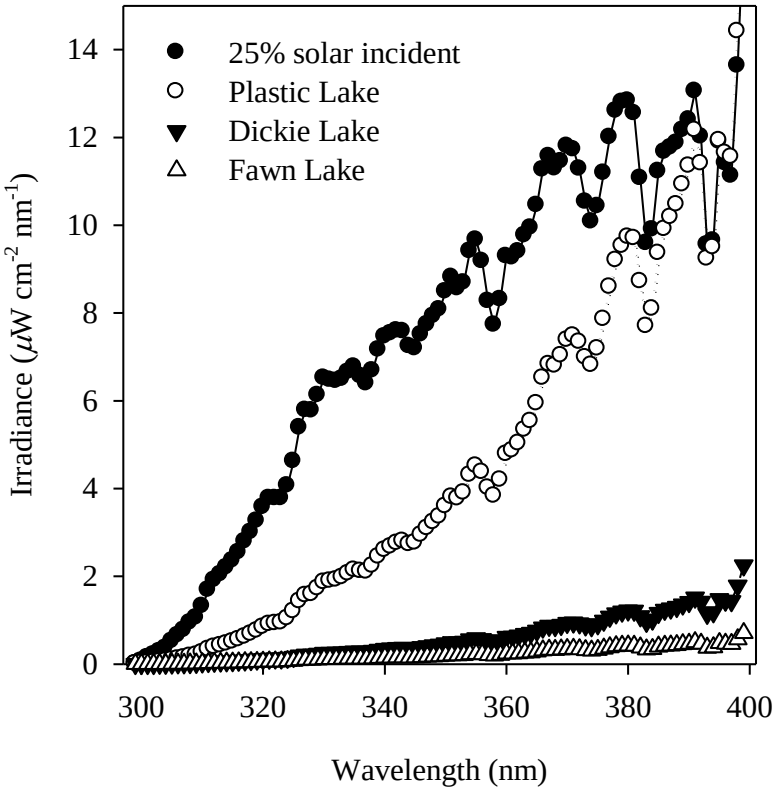

Figure 3.1. Mean epilimnetic UVR in 3 of the study lakes, representative of low (Plastic), medium (Dickie) and high (Fawn) DOC content, estimated by applying interpolated attenuation coefficients (averages from July and September) to a representative solar incident spectrum (clear sky, mid-day 29 August 2010) recorded near the study site at the University of Waterloo (43°29’25 N; 80°32’48 W). The incident solar spectrum has been scaled to 25% for ease of comparison.

3.3.6 Statistical analysis

In addition to the analyses previously described, a separate Pearson partial correlation analysis was conducted on the water chemistry and attenuation coefficient data from each sampling period, and simple linear regressions were performed with measures of UVR response (recovery rates, ε_K values for various wavebands) as dependent variables and water chemistry and transparency data as independent variables. ANOVA was conducted using SigmaPlot 11 (Systat Software). All other analyses were performed using SYSTAT 10 (Systat Software). Statistical relationships were considered to be significant if $p < 0.05$.

3.4 RESULTS

Table 3.1. Mixing depths and 1% irradiance depths of study lakes in July and September 2009.

		Z_{mix} (m)	1% irradiance depth (m)					
			305 nm	320 nm	340 nm	380 nm	399 nm	PAR
Jul	Brandy	3.0	0.05	0.07	0.10	0.22	0.30	2.01
	Fawn	3.0	0.06	0.09	0.12	0.33	0.43	2.41
	Chub	2.5	0.12	0.15	0.19	0.42	0.60	3.07
	Dickie	3.5	0.17	0.19	0.24	0.46	0.77	3.93
	Plastic	5.5	1.10	1.56	2.19	6.17	6.77	13.11
	Blue Chalk	5.0	1.31	1.84	2.62	6.27	7.94	12.43
Sep	Brandy	3.5	0.06	0.07	0.09	0.19	0.26	2.01
	Fawn	4.5	0.07	0.08	0.10	0.18	0.22	1.91
	Chub	4.0	0.10	0.12	0.16	0.33	0.43	2.98
	Dickie	4.5	0.14	0.17	0.22	0.53	0.68	3.72
	Plastic	6.0	1.22	1.63	2.27	5.54	7.37	12.96
	Blue Chalk	6.5	1.33	1.71	2.36	4.26	5.01	11.86

3.4.1 DOC and epilimnetic irradiance

The study lakes spanned a DOC gradient and contained 1.7–12.1 and 1.8–11.6 mg L^{-1} DOC during the July and September sampling periods, respectively. Vertical attenuation coefficients for UVR and

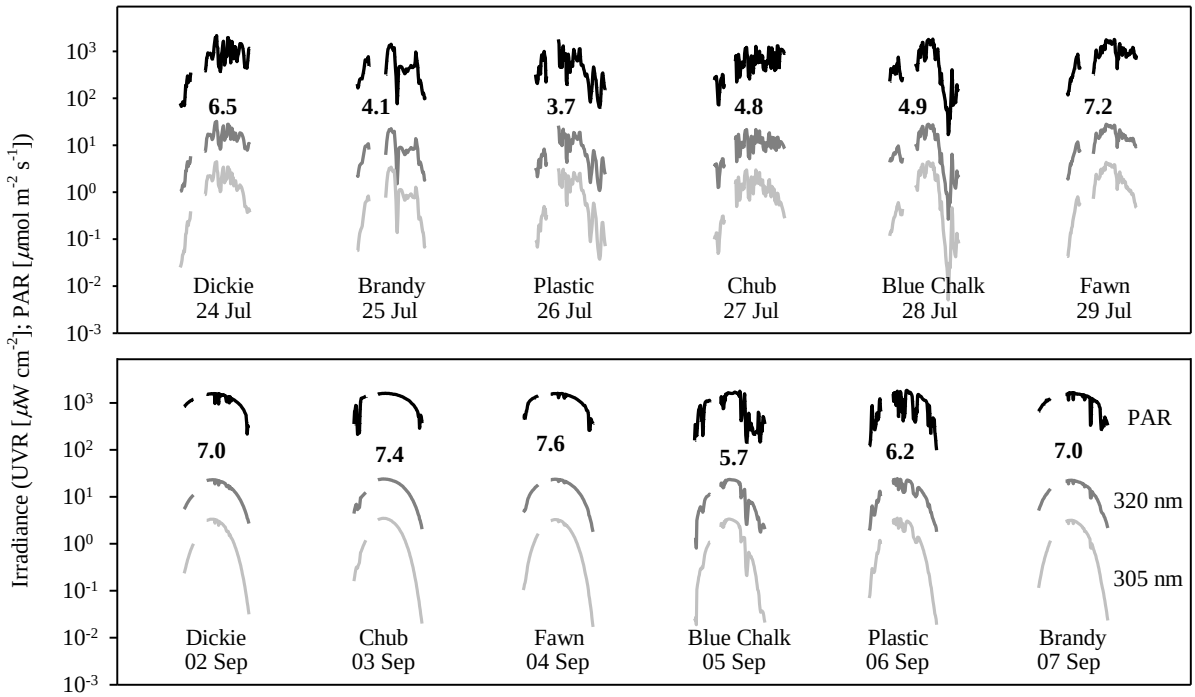

Figure 3.2. Surface incident irradiance at 305 nm (light-grey line), 320 nm (dark-grey line), and PAR (black line) during July (08:40–09:55 h, 12:15–17:30 h) and September (09:20–10:25 h, 12:35–18:00 h) of 2009, showing which lake was sampled and profiled on each date. Gaps in data correspond to times when the radiometer was used for water column profiling. Bold numbers show UVAR at 340 nm (kJ m^{-2}) integrated over the consistently monitored photoperiod (6.5 h) during each month.

PAR varied drastically among lakes, with larger differences between lakes at shorter wavelengths, resulting in a wide range of 1% irradiance depths in the UVR and for broadband PAR (Table 3.1). However, inter-system differences in mean epilimnetic UVR were found to be greatest in the long-UVA when interpolated attenuation coefficients were applied to a representative incident solar spectrum (Figure 3.1). Variation in DOC explained 91–99% (mean R^2 = 0.96) of the variability in UVR penetration among systems (n = 6) at the wavelengths examined (305 nm, 320 nm, 340 nm, 380 nm, and 399 nm). KD_{PAR} was slightly better correlated with Chl *a* than DOC in July (r = 0.92 *vs.* 0.90), but not in September (r = 0.90 *vs*. 0.98). July surface incident PAR and UVR (340 nm) were only 61% and 76% of the levels in September due to the cloudy conditions that prevailed in July (Figure 3.2). However, averaged across lakes, mean epilimnetic PAR was 22% and 340-nm irradiance only 1% higher in September, due to increases in Z_{mix} (Table 3.1). Temperature loggers moored in Fawn Lake between 29 July and 04 September revealed considerable temporal variation in thermal structure; *i.e.*, near-surface ephemeral thermocline formation in the top 0.5 m of the water column on some days (Figure 3.3), the implications of which I consider in the Discussion.

3.4.2 Water chemistry

DOC was highly correlated with trophic status among the study lakes (Table 3.2). The DOC-TP and DOC-Chl *a* relationships were stronger in July (r = 0.99, 0.99) than September (r = 0.90, 0.86). The two clear lakes (Blue Chalk and Plastic) had the highest C:Chl *a* ratios in both months, but DOC did not significantly ($p > 0.05$) explain variation in C:Chl *a* in July or September, as seston C:Chl *a* varied little among the remaining four humic lakes. Particulate C:N was generally low, at times showing evidence of moderate N limitation (C:N > 8.3) whereas in both sampling periods all lakes were P-limited; the majority exhibited extreme P limitation (C:P > 258). Seston C:P and C:N were not significantly ($p > 0.05$) correlated with DOC concentration.

Table 3.2. Water chemistry and phytoplankton composition for all study lakes in 2009, and mean values of DOC and Chl *a* for 15 July, 26 July, and 24 August 2010 in Fawn and Plastic Lakes, with standard deviations in parentheses; nd = not determined. Dominant phytoplankton taxa listed are genera, with corresponding divisions shown in parentheses; Ba = Bacillariophyta, Ch = Chrysophyta, Cr = Cryptophyta, Cy = Cyanophyta and Py = Pyrrophyta.

		DOC ($mg\ L^{-1}$)	Chl *a* ($\mu g\ L^{-1}$)	C:N (atoms)	C:P (atoms)	TP ($\mu g\ L^{-1}$)	SRP ($\mu g\ L^{-1}$)	Dominant phytoplankton
Jul	Brandy	12.1	9.2	7.4	375	21.3	3.4	*Aphanizomenon* (Cy)
2009	Fawn	8.0	5.6	8.4	188	16.2	2.6	*Anabaena* (Cy), naked dinoflagellates (Py)
	Chub	5.1	3.5	8.1	155	9.6	0.8	*Tabellaria* (Ba), *Synura* (Ch)
	Dickie	4.8	3.9	9.1	295	7.9	0.8	*Dinobryon* (Ch)
	Plastic	2.4	1.0	9.0	963	3.4	0.7	*Merismopedia* (Cy) & other nanoplankton (Ch and Cr)
	Blue Chalk	1.7	1.2	8.5	635	3.6	1.3	mixed nanoplankton (Ch and Cr)
Sep	Brandy	11.6	16.6	7.6	439	24.2	2.6	*Aphanizomenon* (Cy), *Anabaena* (Cy)
2009	Fawn	9.9	18.4	8.3	324	22.3	1.9	*Anabaena* (Cy)
	Chub	7.5	3.3	7.0	254	7.2	1.5	*Asterionella* & *Tabellaria* (Ba), *Cryptomonas* (Cr)
	Dickie	6.4	3.6	6.2	226	8.1	0.6	*Synura* (Ch)
	Plastic	1.8	1.3	9.0	316	3.1	0.1	*Uroglena* (Ch), *Asterionella* (Ba)
	Blue Chalk	2.2	1.5	8.9	272	5.4	0.5	small flagellates, *Tabellaria* (Ba), *Ceratium* (Py)
2010	Fawn	9.6 (0.3)	9.6 (1.2)	nd	nd	nd	nd	nd
(avg)	Plastic	2.4 (0.2)	1.5 (0.2)	nd	nd	nd	nd	nd

3.4.3 Phytoplankton community composition

FluoroProbe *in situ* fluorescence data showed Blue Chalk, Plastic, Dickie and Chub Lakes to be dominated by chromophytes (diatoms, dinoflagellates and chrysophytes) which generally agreed with my estimates of the dominant biovolume contributors based on microscopic examination (Table 3.2). Fluorescence data suggested approximately equal representation by the chromophyte, chlorophyte, cryptophyte and cyanobacterial groups in Brandy and Fawn Lakes; however, microscopic

examination revealed that these lakes were dominated by filamentous cyanobacteria, with the additional presence of naked dinoflagellates in Fawn Lake in July.

3.4.4 Phytoplankton UVR sensitivity

Initial values of F_V:F_M (prior to experimental exposure) were generally high (0.583 ± 0.048; mean ± SD) and improved after 1 h of exposure to low PAR (0.620 ± 0.040). In all cases, F_V:F_M decreased over time under all spectral exposures (Figure 3.4). Among lakes and dates, similarly drastic decreases in F_V:F_M were observed under UVBR exposure (>300 nm) and small decreases under PAR-only (>410 nm), but the most humic lakes, Brandy and Fawn, showed very high sensitivity to UVAR (>325 nm), while the communities from clear Blue Chalk and Plastic Lakes showed relatively low sensitivity, especially in September. Phytoplankton from the intermediately-humic Chub and Dickie Lakes exhibited an intermediate UVAR response (Figure 3.4).

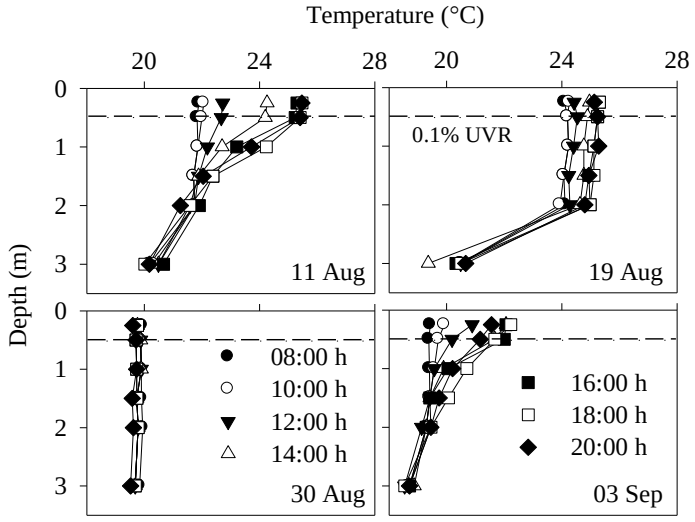

Figure 3.3. Diurnal variation of thermal structure in Fawn Lake for 4 dates in 2009 chosen to illustrate the extent of variability in mixing depths possible within and among days of the summer. The dashed lines represent the 0.1% depth for 399-nm irradiance (average of 29 July and 04 September 2009).

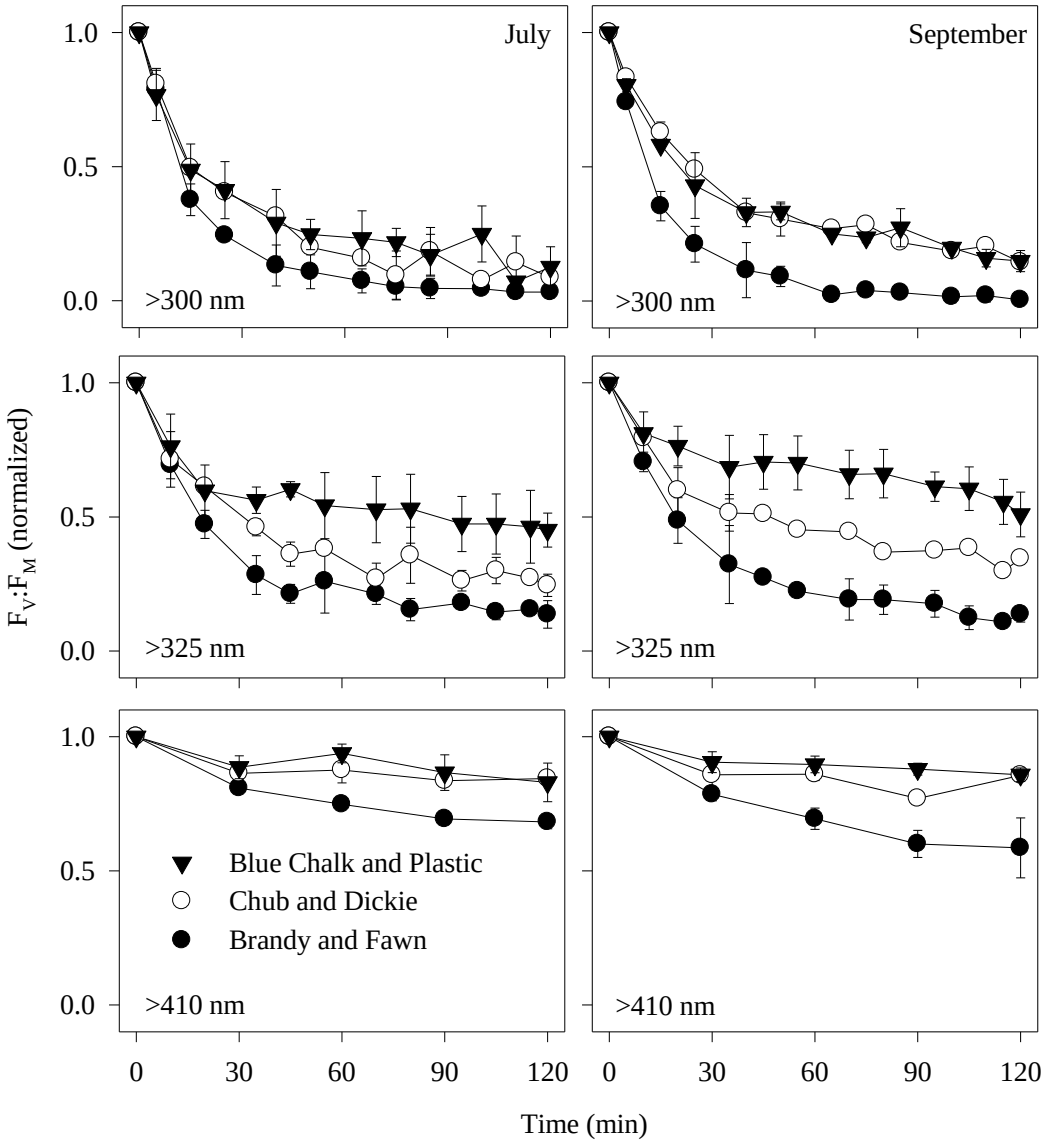

Figure 3.4. Change in $F_V:F_M$ over time (mean ± SD) of low (Blue Chalk and Plastic), medium (Chub and Dickie) and high (Brandy and Fawn) DOC lakes in response to 3 spectral treatments representative of solar irradiance (>300 nm), UVAR+PAR (>325 nm), and PAR-only (>410 nm) during July (left) and September (right) sampling periods. Due to equipment malfunction, the experiment on Dickie Lake phytoplankton lasted only 65 min in September; other data points without visible error bars had standard deviations smaller than the symbol size.

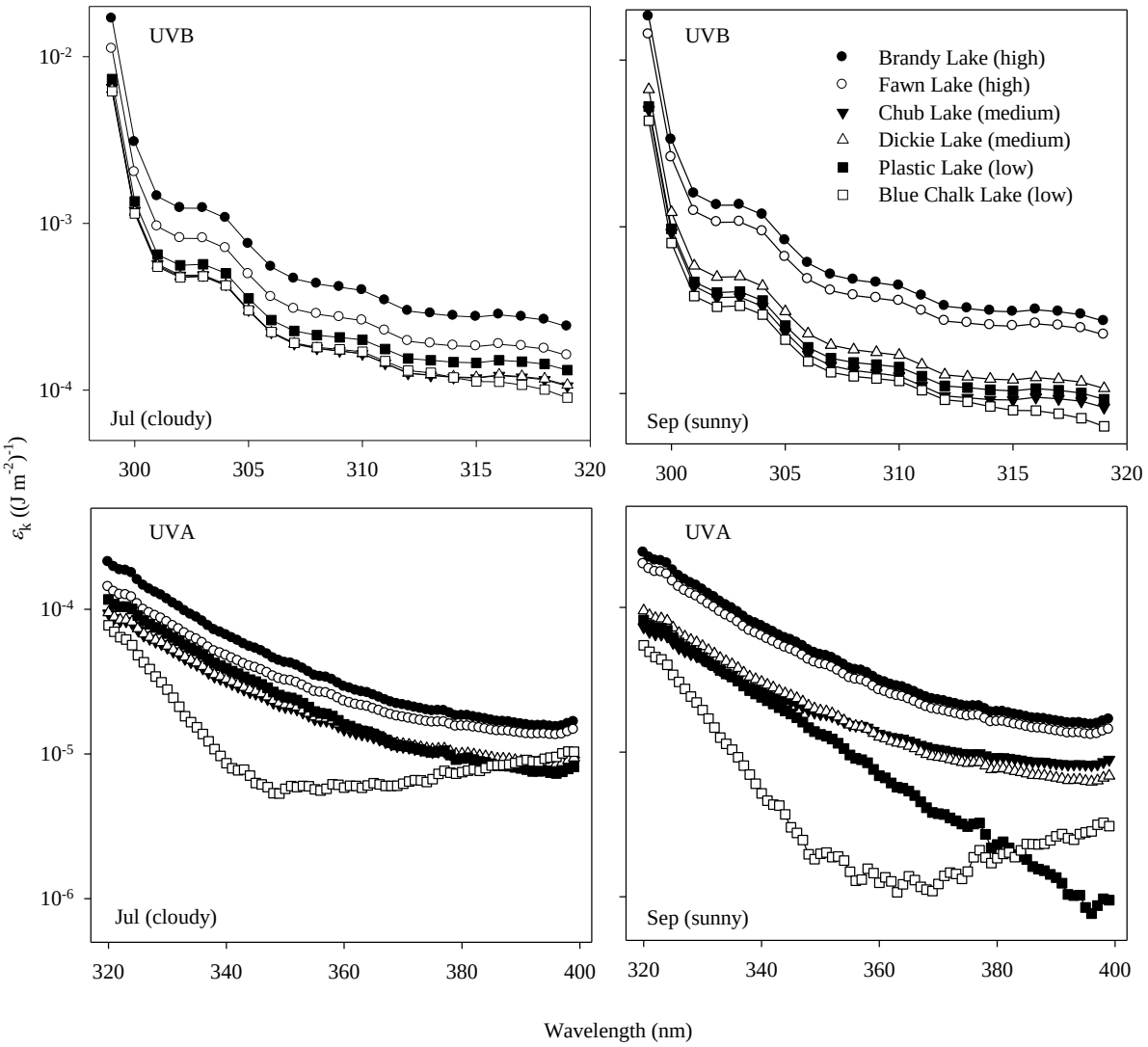

Figure 3.5. BWFs showing the spectral sensitivity of phytoplankton from six lakes of varying transparency to UVR-induced PSII reaction centre damage, as quantified by changes in F_V:F_M, in July (left panels) and September (right panels). The BWFs in the UVB and UVA spectral regions are displayed in the top and bottom panels, respectively (relative humicity of each lake is in parentheses).

Table 3.3. Percent variation in phytoplankton sensitivity to damage (ε_k) by various wavebands and recovery rates (r) explained by variation in either DOC or the natural logarithm of percent mean epilimnetic UVR using simple linear regression analyses (n = 6). Values are coefficients of determination (R^2) and symbols denote the level of significance: * for $p < 0.05$, ** for $p < 0.01$, *** for $p < 0.005$ and † for $p = 0.053$.

	Jul		Sep	
	DOC	ln ($\bar{E}\%_{UVR}$)	DOC	ln ($\bar{E}\%_{UVR}$)
$\varepsilon_{k(299–319\ nm)}$	0.85**	0.41	0.72*	0.49
$\varepsilon_{k(320–359\ nm)}$	0.83*	0.52	0.79*	0.59
$\varepsilon_{k(360–399\ nm)}$	0.93***	0.65†	0.96***	0.81*
$\varepsilon_{k(PAR)}$	0.36	0.18	0.45	0.35
recovery rate	0.66*	0.87**	0.26	0.22

The kinetics of the UVR responses were well described by Eq. 3.3 ($R^2 = 0.93 \pm 0.02$; mean ± SD.; n = 12) and lake DOC content was a significant predictor of model goodness-of-fit ($R^2 = 0.52$; $p < 0.01$; n = 12). The BWFs for UVR-induced damage I determined are similar in shape to previously determined BWFs (Neale *et al*. 2001*a*; Hiriart-Baer & Smith 2004), generally showing the photoinhibitory effects of irradiance to increase with decreasing wavelength (Figure 3.5). The July phytoplankton community of Blue Chalk Lake showed lower sensitivity to photodamage in the mid-UVA (~340–380 nm) spectral region relative to the other lakes, and in September this became more pronounced, at which time the Plastic Lake phytoplankton were also found to exhibit high UVAR resistance, although at longer wavelengths (380–400 nm). DOC was a significant predictor of the sensitivity to damage (ε_k) by UVBR, and short and long-wavelength UVAR, but not PAR (Table 3.3). The natural logarithm of percent mean epilimnetic UVR was a significant predictor of $\varepsilon_{k(360–399\ nm)}$ in September, and this relationship was nearly significant in July (Table 3.3). The most significant

relationships found were between DOC and $\varepsilon_{k(360–399\ nm)}$ (Figure 3.6). Seston C:P, C:N, C:Chl *a* and pre-exposure values of F_V:F_M were not significant predictors of $\varepsilon_{k(360–399\ nm)}$ in either month ($p > 0.05$).

3.4.5 Recovery

Lake DOC content was a significant predictor of rates of recovery under UVR exposure in July but not in September, as was mean epilimnetic UVR exposure (Table 3.3). The negative relationship between recovery rate and DOC was significant when both months were considered together (R^2 = 0.45; p = 0.018; n = 12), as was the log-linear relationship between recovery rate and $\bar{E}_{UVR}$ (R^2 = 0.49; p = 0.012; n = 12), although pooling data from both sampling periods could be considered a violation of the test's assumption of independence. Epilimnetic temperature varied little among lakes and dates (19.1–21.3°C) and did not significantly explain variation in recovery rates in either month ($p > 0.7$).

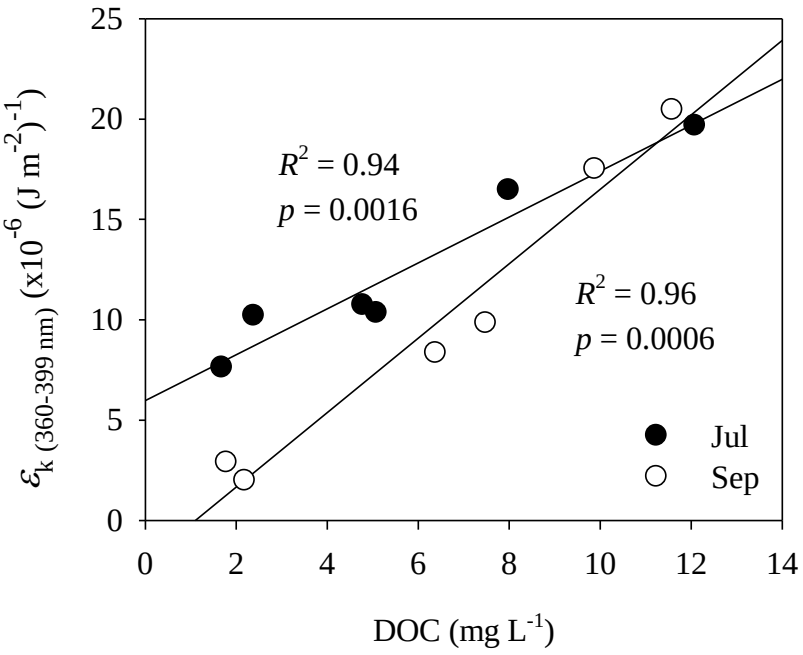

Figure 3.6. The relationship between sensitivity to PSII photoinhibition by long-wavelength UVAR (360–399 nm) and the DOC content of the lakes from which the algal communities were taken.

3.4.6 Reciprocal transfer experiments

Phytoplankton from Fawn Lake experienced greater losses of F_V:F_M than those from Plastic Lake when incubated in water from either lake, and phytoplankton from both lakes experienced greater losses of F_V:F_M when incubated in Plastic Lake water than when in Fawn Lake water, for all spectral exposure treatments (Figure 3.7). According to a 3-way ANOVA, cell origin was a significant factor

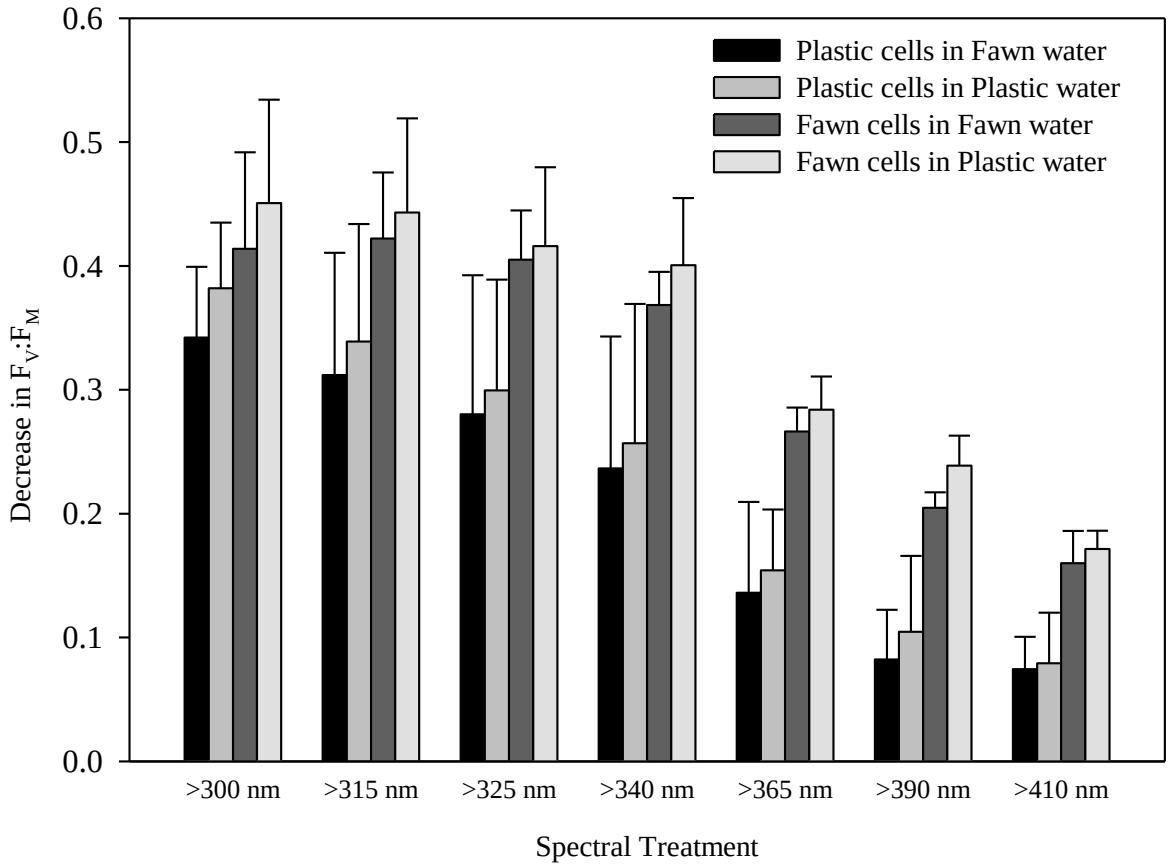

Figure 3.7. Loss of F_V:F_M after 1 h of spectral exposure (mean ± SD; n = 3) experienced by phytoplankton cells from Fawn and Plastic Lakes when incubated in clear water from Plastic Lake and humic water from Fawn Lake on 15 and 26 July, and 24 August in 2010.

for all spectral treatments; *i.e*., phytoplankton from Fawn Lake exhibited significantly greater losses of F_V:F_M than phytoplankton from Plastic Lake when variation associated with water type (humic *vs.* clear) and date was controlled for. The largest difference in loss of F_V:F_M between Fawn and Plastic Lake phytoplankton was in response to >340-nm irradiance. Water type was only a significant explanatory factor for the >305 nm and >390 nm spectral treatments. Date was a significant factor for all spectral treatments except >365 nm and >410 nm; phytoplankton from both lakes were significantly less photoinhibited on 15 July than on 26 July or 24 August.

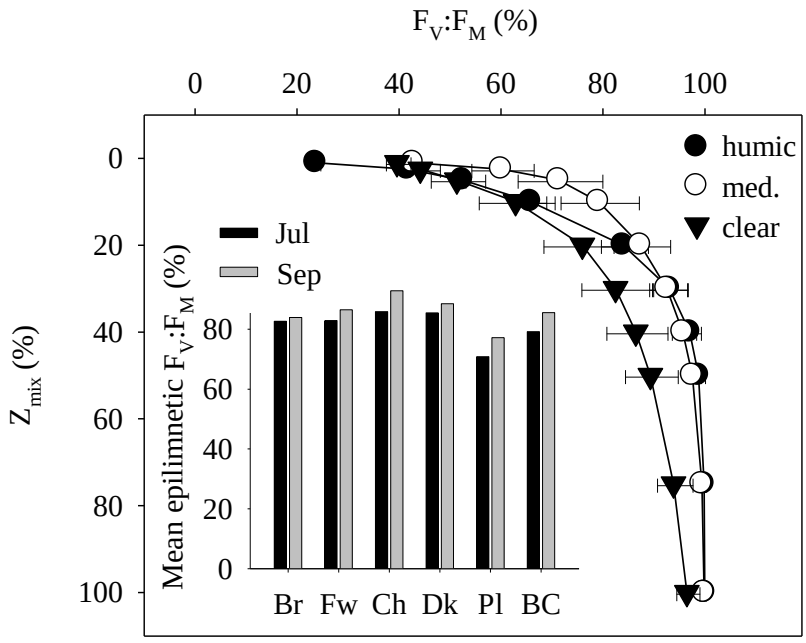

Figure 3.8. Vertical profiles of percent F_V:F_M remaining after 2 h of exposure to a representative surface incident spectrum, based on September BWF-ERC model predictions assuming a static water column and 2% surface reflectance in humic (Brandy and Fawn), medium DOC (Chub and Dickie), and clear (Plastic and Blue Chalk) lakes. Inset: mean epilimnetic values of percent F_V:F_M based on July and September BWF-ERCs; Br = Brandy, Fw = Fawn, Ch = Chub, Dk = Dickie, Pl = Plastic, and BC = Blue Chalk.

3.4.7 Estimated *in situ* photoinhibition

The BWF-Kok models predicted that F_V:F_M, as percent of maximal F_V:F_M, after a 2 hour mid-day sunlight exposure would increase with depth in the water column (Figure 3.8). The high-DOC lakes were predicted to show very high sub-surface photoinhibition, whereas the greatest losses of F_V:F_M at depth were predicted for the clearest lakes. The predicted mean epilimnetic F_V:F_M was generally high (avg. = 84% of maximal) and similar (range = 70–90%) among lakes and dates (Figure 3.8). In both July and September, predicted values were highest in Dickie (85%, 89%) and Chub (86%, 93%) and lowest in Plastic (71%, 77%) and Blue Chalk (79%, 86%). Mean epilimnetic F_V:F_M was predicted to be higher in all lakes in September (avg. = 86%) than July (avg. = 81%), due to both increases in Z_{mix} and decreases in susceptibility to photoinhibition. Neither DOC nor $\bar{E}\%_{360–399nm}$ were statistically significant predictors of predicted percent mean epilimnetic F_V:F_M in July, September, or across both months.

3.5 DISCUSSION

I found the phytoplankton of clear lakes to exhibit greater UVR resistance than those of humic lakes. The spectrally-resolved kinetic model was a good descriptor of the short-term responses of the phytoplankton communities to UVR exposure. When combined with knowledge of *in situ* irradiance, the model predicted that phytoplankton of clearer lakes were able to maintain photosynthetic competence (as assessed by F_V:F_M) comparable to that in the more humic lakes despite the major differences in water column transparency and resulting UVR exposure.

Although phytoplankton from clearer lakes were less susceptible to photoinhibition from all portions of the UV spectrum than those from more humic lakes (Figures 3.4, 3.5), the assemblages I examined showed similarly-high sensitivity to UVBR, but differed appreciably in how they responded to UVAR, especially the longer wavelengths (360–399 nm), which is consistent with the study of Moeller (1994). Sensitivity to PAR was generally low, but highest in the most humic lakes

(Figure 3.4, Table 3.3). The Kok model (Eq. 3.3) was successful (R^2 > 0.89) in describing the kinetics of UVR-induced photoinhibition, and revealed that variation in rates of both damage and recovery was responsible for differences in UVR response among phytoplankton communities. In July, for instance, the phytoplankton of Plastic Lake were equally sensitive to UVR damage relative to the Dickie and Chub Lake communities (Figure 3.5) but showed lower susceptibility to photoinhibition (Figure 3.4), due to higher recovery efficiency (*i.e.*, r = 4.37 x 10^{-4} s^{-1} for Plastic Lake, *vs*. r = 2.21 x 10^{-4} s^{-1} and 2.18 x 10^{-4} s^{-1}, for Dickie and Chub Lakes, respectively). Although the variability in model goodness-of-fit was relatively small among lakes and dates (R^2 = 0.89–0.97), the somewhat better fit in higher-DOC lakes probably reflects the greater losses of F_V:F_M incurred by the phytoplankton therein.

I quantified phytoplankton nutrient status using seston C:P and C:N ratios, and found neither to significantly explain variation in UVAR sensitivity. TP and SRP were correlated with $\varepsilon_{k(360–399nm)}$ (r = 0.91, 0.90) and r (r = -0.70, -0.59), but these higher damage rates and lower recovery rates at higher P concentrations likely reflect the covariance of P and DOC within the dataset rather than a synergistic negative effect of UVR and P supply on F_V:F_M. P-limitation has been found to increase susceptibility to UVR-induced photoinhibition by inhibiting recovery (Heraud *et al*. 2005). If P availability was in fact exerting the dominant effect, a positive rather than negative correlation between SRP and recovery rates would be expected. However, it is possible that the phytoplankton in the high-DOC systems would have experienced an even greater degree of photoinhibition due to UVR if SRP had been as low as it was in the clear lakes.

Based on existing literature, it appears unlikely that the among-lake differences in UVR response I observed were related to community composition. It has been suggested that cyanobacteria may be more UVR-resistant than other phytoplankton taxa (Laurion & Vincent 1998; Xenopoulos *et al.* 2009). However, I found the filamentous cyanobacteria communities of Brandy

and Fawn Lakes to exhibit the highest sensitivity to UVR-induced photoinhibition of any of the communities I examined. Likewise, the UVR-resistant communities of Plastic and Blue Chalk Lakes contained the greatest numbers of small unicells, which are considered intrinsically vulnerable to photodamage (Garcia-Pichel 1994; Key *et al*. 2010). The sensitivity of phytoplankton cells to UVR can reflect the interplay of many factors, such as cell size and morphology, nutrient status, taxonomy, and irradiance history (Harrison & Smith 2009). In this study, it is possible that subtle variation in UVR sensitivity related to taxonomic affiliation was obscured by more pronounced variation related to photoacclimation status, because the comparisons were made across a relatively strong transparency gradient. Indeed, the UVR resistance of cyanobacteria may be largely inducible; in addition to changes in photoprotective pigmentation (carotenoids), Jiang & Qiu (2005) found incremental decreases in the sensitivity of F_V:F_M to UVBR when cultures of *Microcystis aeruginosa* were conditioned to UVBR for 3 h per day over a 10-day period. The importance of taxonomy in determining the UVR response of the communities I sampled could be clarified by performing additional experiments. For instance, phytoplankton cells from the study lakes could be isolated and incubated in culture medium under identical spectral irradiance conditions for various durations prior to assessing their UVR responses, and the BWFs and recovery rates could then be compared with the data in this chapter. Such a comparison could help elucidate the extent to which the resistance of natural communities to UVR-induced photoinhibition of PSII function is inducible (*vs*. taxonomically-determined) and the length of time required for effective UVR acclimation to occur. Given that the capacity for phytoplankton UVR acclimation can itself be taxon-specific (Litchman & Neale 2005), this is clearly a question which requires further study.

DOC concentration explained 95% of the variation in $\varepsilon_{k(360–399nm)}$ among lakes (average R^2 for July and September) suggesting that irradiance history is a major determinant of community sensitivity to UVR-induced photoinhibition of PSII photochemistry. Plankton UVR exposure is a

function of both water column spectral transparency (*i.e.*, CDOM) and Z_{mix}, so it is surprising that $\varepsilon_{k(360–399nm)}$ showed higher correlation with DOC than mean epilimnetic irradiance in the UVA ($\bar{E}\%_{UVR}$). This may reflect uncertainty associated with my estimates of epilimnion depths based on early-morning temperature profiles. Indeed, thermal structure was highly dynamic in the one lake in which it was continuously monitored (Fawn Lake; Figure 3.3) and potential diurnal variation in the vertical distribution of phytoplankton due to phototactic motility (Tilzer 1973) introduces additional uncertainty into estimates of the spectral irradiance history of the epilimnetic communities I sampled. Alternatively, if the differences in ε_k that I determined reflect acclimation of phytoplankton to the *maximum* rather than *mean* irradiance experienced (Van Leeuwe *et al*. 2005), it would not be surprising that DOC was a better predictor of ε_k values than $\bar{E}\%_{UVR}$.

An additional possibility is that DOC and ε_k values were highly correlated because DOC contributed directly to photoinhibition; *i.e*., that PSII reaction centres were damaged by ROS, such as peroxide, produced *via* the interaction of UV photons with DOC compounds (Scully *et al*. 1996) during the incubations. F_V:F_M has been found to decrease in response to extracellular peroxide exposure, and cyanobacteria appear to be particularly sensitive to this stress, based on comparisons with diatoms and green algae (Drábková *et al*. 2007*a*, *b*). Addressing the role of toxicity from DOC photosensitization was therefore of particular importance to this study, as the two lakes with the highest concentrations of DOC were dominated by cyanobacteria. However, the results of the reciprocal transfer experiment (Figure 3.7) suggest that DOC protected phytoplankton from UVR *via* shading, and did not act as an indirect toxic stressor. It is important to note that light attenuation by DOC within the incubation vessels was corrected for (see section 3.3.5) and thus did not lead to an underestimation of the spectral sensitivity to photodamage (BWFs) of the phytoplankton from the humic lakes. This result is consistent with a comparison of UVR effects on the green alga

Selanastrum capricornutum in high- and low-DOC lake water (West *et al*. 1999), which found a protective effect of DOC on F_V:F_M and growth rates.

The large decreases in $\varepsilon_{k(360–399nm)}$ of the clear-lake assemblages observed during September, after several days of clear-sky conditions, supports the idea that physiological acclimation can play a large role in modulating phytoplankton UVR response (Van Leeuwe *et al*. 2005; Van de Poll *et al*. 2006). For instance, the predicted mean epilimnetic loss of F_V:F_M suffered by the Plastic Lake phytoplankton after 2 h of exposure to an incident solar spectrum (Figure 3.1) is 30% if the July BWF and recovery rate are applied, but only 23% based on the September BWF and recovery rate. This comparison serves not only to quantify the extent of acclimation achieved under increased UVR exposure, but also to draw attention to a potential source of error in modeling the biological effects of an altered UVR exposure regime: *i.e*., that the BWF determined for a phytoplankton assemblage with a given irradiance history, may no longer apply under the new irradiance conditions for which the predictions are being made.

A final important consideration is the appropriateness of F_V:F_M as a diagnostic of photoinhibition of PSII photochemistry; *i.e.*, how accurately changes in F_V:F_M, as measured in the present study, represented changes in the proportion of functional PSII reaction centres. While F_V:F_M has been used to monitor photodamage to PSII for some time (see Anderson *et al*. 1997), there is evidence that factors other than irradiance, such as nutrient limitation (Kolber *et al*. 1990; Shelly *et al*. 2005; but see Parkhill *et al*. 2001) and toxicity (Drábková *et al*. 2007*a*, *b*), can lower F_V:F_M *via* effects on PSII. While it is conceivable that these factors could help explain the sub-optimal (<0.65) pre-exposure values of F_V:F_M I found, the reciprocal transfer experiments confirmed that DOC-phototoxicity was not a factor, and it seems extremely unlikely that major changes in phytoplankton nutrient status sufficient to depress variable fluorescence could have occurred during the course of the 120-min UVR incubations. Non-photochemical quenching (NPQ) is an additional mechanism that

decreases the variable fluorescence of PSII, and all water samples were dark-adapted for 30 min prior to PAM analysis in order to control for this. However, there is emerging evidence suggesting that in certain diatom species low levels of PAR are required for complete relaxation of NPQ (Grouneva *et al*. 2008, 2009; Miloslavina *et al*. 2009). Given that these diatom species were not present in any of the phytoplankton communities that I examined, and that diatoms were a very minor component of the phytoplankton in the two lakes that exhibited the greatest losses of F_V:F_M under irradiance (Brandy and Fawn), it seems unlikely that residual NPQ appreciably affected the measurement of F_V:F_M.

Despite large differences in mean epilimnetic spectral irradiance, the model predicts relatively minor differences among lakes in the extent of photoinhibition occurring *in situ* (Figure 3.8). Although the comparison is simplistic, in that it assumes a static water column, it serves to illustrate that phytoplankton assemblages adjust to the UVR conditions that are characteristic of their habitats. I therefore conclude that changes in UVR transparency are unlikely to have drastic consequences for PSII function of freshwater phytoplankton. Further research should investigate how changes in water clarity will affect other aspects of phytoplankton physiology (*e.g*., dark reactions of photosynthesis, nutrient acquisition, respiration) and community composition in lakes.

Chapter 4: Effects of nutrients and irradiance on Photosystem II variable fluorescence of lake phytoplankton assemblages

4.1 SUMMARY

Phytoplankton from Lake Ontario and six small Canadian lakes (Dorset Lakes) were supplemented with nitrogen (N) and phosphorus (P) to determine how nutrients affect Photosystem II (PSII) variable fluorescence (VF) and photoinhibition in natural freshwater communities. Susceptibility of PSII to photoinhibition by PAR and UVR, as well as recovery potential, were quantified using changes in VF and compared among N- and P-supplemented (Nu+) and non-supplemented (Nu-) Lake Ontario phytoplankton. Nu+ communities exhibited slightly (≤10%) higher VF than Nu- when dark-adapted (F_V:F_M) or under constant illumination (F_Q':F_M'). Rates of relative electron transport (rETR) were up to 30% greater for Nu+ than Nu- phytoplankton, with higher non-photochemical quenching (NPQ) by Nu- samples. Nutrient supplementation increased rates of PAR- and UVR-dependent damage but also recovery, so that net PSII photoinhibition was equally severe as in the absence of added N and P. Additions of P, N, and N+P did not significantly alter F_V:F_M of Dorset Lakes phytoplankton. Compared to the range of VF observable over the diurnal cycle of photoinhibition and recovery in Lake Ontario, the effects of nutrients in this study were small, and F_V:F_M was routinely within ~15% of the nominal optimal value.

4.2 INTRODUCTION

Variable fluorescence (VF) techniques for assessing the quantum efficiency of Photosystem II (PSII) photochemistry have now been in use for over three decades (Butler & Kitajima 1975). Changes in the VF of PSII have been associated with exposure to damaging irradiance (Anderson *et al*. 1997; Harrison & Smith 2011*a*), toxins (Marwood *et al*. 1999; Drábková *et al*. 2007) and nutrient starvation

(Kolber *et al*. 1988; Graziano *et al*. 1996*a*). Consequently, the VF of PSII (often as F_V:F_M) has come to be viewed as a general indicator of phytoplankton physiological condition, or 'algal health' parameter (Kromkamp & Forster 2003).

Nutrient limitation of freshwater phytoplankton is typically quantified using seston particulate stoichiometry (Healey & Hendzel 1980), nutrient enrichment assays (Healey & Hendzel 1979*b*) or the alkaline phosphatase (AP) assay (Healey and Hendzel 1979*a*). While generally informative, these traditional assays have associated artefacts: heterotrophic bacterial biomass and particulate detritus unavoidably contribute to seston analysed for carbon (C), nitrogen (N), and phosphorus (P) content (C:N:P ratios), while uptake of N and P, and expression of AP by heterotrophic bacteria cannot be distinguished from that of phytoplankton. In contrast, the VF of PSII originates only from phototrophs, and can be determined rapidly and easily, using only a small volume of sample water (~3 mL). Depressed VF has been associated with N limitation in laboratory cultures (Kolber *et al*. 1988) and oceanic waters (Kolber *et al*. 1990), and it has similarly been concluded that P limitation can measurably decrease the VF of phytoplankton in culture (Graziano *et al*. 1996*a*; Shelly *et al*. 2005) and in estuarine systems (Sylvan *et al*. 2007). To date, the only published study that purposefully investigated the relationship between nutrient status and PSII VF in freshwaters is that of Rattan *et al*. (in press), who reported correlations between phytoplankton VF and N and P status in Lake Erie. Such findings suggest VF could supplement, or potentially replace, traditional proxies for the nutrient status of lake phytoplankton. However, contrary evidence exists (Parkhill *et al*. 2001; Moore *et al*. 2008; Suggett *et al*. 2009) and variations in methodology can have a large influence on the apparent VF characteristics of natural communities (Fuchs *et al*. 2002; Kromkamp & Forster 2003; Laney 2003). Changes in VF can also be confounded by other stresses such as photoinactivation of PSII (Campbell & Tyystjärvi 2011). In light of these factors, and because I am not presently aware of any studies other than that of Rattan *et al*. (in press) that have

examined this topic, more research is needed to elucidate how nutrient status influences the PSII VF of freshwater phytoplankton communities

Nutrient limitation is one of several factors, including irradiance history, taxonomy and temperature, thought to modulate the UVR sensitivity of freshwater phytoplankton (Harrison & Smith 2009). N-limited phytoplankton have been shown to exhibit increased sensitivity to UVR whether assessed in culture (Litchman *et al*. 2002; Shelley *et al*. 2002) or in nature (Hiriart *et al*. 2002; Bouchard *et al*. 2008). P-limited phytoplankton have similarly been found more susceptible to UVR-stress than P-sufficient phytoplankton (Heraud *et al*. 2005; Shelley *et al*. 2005); however, other studies have shown no apparent effect of nutrient limitation on UVR response (Furgal & Smith 1997; Hiriart-Baer & Smith 2004).

This study was conducted to supplement the paucity of research on the relationship between phytoplankton VF and nutrient status in lakes, and to provide additional insight into how nutrient availability influences the susceptibility of natural phytoplankton communities to UVR-induced photoinhibition of PSII function.

4.3 METHODS

4.3.1 Study lakes

Epilimnetic phytoplankton communities were sampled from one oligotrophic Laurentian Great Lake, Lake Ontario, and six small (32–108 ha) Canadian Shield lakes of the Dorset-Haliburton area of northern Ontario (Blue Chalk, Brandy, Chub, Dickie, Fawn, and Plastic; hereafter referred to as the 'Dorset Lakes') with total P (TP) values ranging from 3.1–24.2 μg L^{-1}. Additional limnological characteristics of the Dorset Lakes can be found in Table 3.2. The samples from Lake Ontario were collected from a site located 2 km south of the north shore (43°47'N 79°04'W), near the city of

Pickering, where the water column is ~20 m deep. Samples from all lakes were collected using a Niskin bottle and were screened through a 200-µm mesh prior to storage.

4.3.2 Nutrient amendments (L. Ontario)

Experiments were performed on 17 & 26 June, 15 July, 6, 13 & 27 August, 18 September, and 1 October in 2008. In the field, two 18-L water samples comprising equal volumes from 2 m, 5 m, and 10 m were collected at ~18:00 h and stored in two acid-washed (10% HCl) plastic carboys in a cooler. Upon return to the laboratory (~22:00 h), 90 mL of 1-mM KH_2PO_4 and 90 ml of 1-mM NH_4Cl were added to the water in one carboy ('Nu+') for final concentrations of approximately 5 µM, or approximately 155 µg-P L^{-1} and 90 µg-N L^{-1} (depending upon the ambient N and P concentrations initially present).

4.3.3 Variable fluorescence measurements (L. Ontario)

Prior to commencement of spectral exposure experiments, F_V:F_M, F_Q':F_M', and rETR measurements were made using Nu- and Nu+ samples to determine the effects of nutrient supplementation on VF and to obtain initial (pre-exposure) F_V:F_M values against which to compare the values measured during exposure to UVR and PAR. All data were obtained using a pulse amplitude modulation (PAM) fluorometer designed for use with phytoplankton cells in suspension (Water-PAM; Heinz Walz GmbH, Eichenring, Effeltrich, Germany). PSII VF assessed under dark conditions (F_V) was calculated as $F_V = F_M - F_O$, where F_O is the minimum fluorescence yield of PSII determined by a measuring pulse of light insufficient to cause PSII reaction centre (RC) closure, and F_M is the maximum fluorescence yield of PSII, determined after application of a saturating light pulse sufficient to temporarily close all PSII RCs (3650 µmol m^{-2} s^{-1} red light for 0.8 s). The ratio F_V:F_M represents the *maximum* quantum efficiency of PSII. Measurements of PSII VF were also made under constant illumination to determine the *effective* quantum efficiency of PSII, F_Q':F_M' ($F_Q' = F_M'$ -

F′, where F′ is the fluorescence yield under actinic illumination, and F_M' is the maximum fluorescence yield under actinic illumination). Using the instrument software, fluorescence Induction Curves (ICs) were determined. ICs consist of an initial measurement of F_V:F_M, followed by multiple successive measurements of F_Q':F_M' at a regular interval; a 15-s interval was used in this study. The photon flux density (PFD) of irradiance used was either 349, 498 or 696 µmol m^{-2} s^{-1} PAR, depending on the PFD required to saturate linear electron flow, as determined by visual inspection of Rapid Light Curves (RLCs; see below). The F_Q':F_M' values reported are averages of the last four F_Q':F_M' values from each IC. ICs were measured for a maximum duration of 3.5 min, but were terminated if a steady-state was obtained sooner, as early as 3 min (average = 3.25 min). Separate subsamples were used for the determination of F_V:F_M and F_Q':F_M' values. Dissolved fluorescence (<0.2 µm) was corrected for with gently-filtered water (<100 mmHg), so that all data represent the fluorescence emitted by phytoplankton only, with no interference from abiotic fluorophores.

Additionally, RLC measurements were obtained using the Water-PAM. RLCs consisted of an initial assessment of F_V:F_M followed by 8 assessments of F_Q':F_M' over 4 min, during which time the sample was exposed to progressively-increasing levels of illumination (103, 151, 234, 349, 498, 696, 1158 and 1737 µmol m^{-2} s^{-1} PAR; 30 s exposure per irradiance level). For each irradiance level a relative electron transport rate (rETR) was then calculated automatically by the instrument software as

$$\mathrm{rETR} = \frac{F_Q'}{F_M'} \cdot \mathrm{PAR} \cdot 0.5 \cdot \mathrm{ETRfactor} \qquad (4.1)$$

where 0.5 corresponds to the approximate fraction of light energy directed to PSII (*vs*. PSI) and ETRfactor is equal to 0.84, the default value provided by the software, corresponding to the approximate fraction of incident light absorbed by a standard leaf. Because the ETRfactor value does not accurately describe light absorption by phytoplankton cells, the absolute values of the electron transport rates calculated are not meaningful. However, values of rETR can be compared and useful

information about relative changes in electron transport obtained. The RLC data were fitted to the photosynthesis-irradiance model of Jassby & Platt (1976):

$$\mathrm{rETR} = \mathrm{rETR_{max}} \cdot \tanh(\alpha \cdot \frac{\mathrm{E}}{\mathrm{rETR_{max}}}) \quad (4.2)$$

where rETR is the rETR value at irradiance E, and $rETR_{max}$ is the maximum potential rETR value of the sample, and is equal to the product of the initial slope of the curve, α, and the saturating irradiance for rETR, E_K. Values of E_K were then calculated from estimates of $rETR_{max}$ and α (*i.e.*, $E_K = rETR_{max} / \alpha$) and confidence intervals for E_K were calculated using error propagation.

The model of Platt *et al*. (1982) includes a term, β, which quantifies the degree of inhibition experienced by a sample at high irradiance. Some samples did exhibit photoinhibition at the highest irradiance value used (1737 μmol m^{-2} s^{-1}). However, fitting RLC data to this model consistently generated absurd estimates of $rETR_{max}$ and β (*e.g.*, 166007, 136, respectively, for 17 June, Nu+), despite many adjustments of the starting estimates, and other parameters of the nonlinear regression analysis. Because all data were fitted to the simpler model, $rETR_{max}$ was likely underestimated when inhibition was apparent at the highest irradiance level. The nonlinear regression analyses were therefore also applied to a subset of the RLC data from each sampling date and treatment in which inhibition was never apparent (*i.e.*, F_Q':F_M' values obtained under 0–1158 μmol m^{-2} s^{-1}). Nonlinear regression analysis was performed using Systat (v. 10). Data from different sampling dates were treated as replicate measurements (n = 8) and paired t-tests were used to test for significant differences between initial F_V:F_M values of the Nu- and Nu+ samples.

4.3.4 Spectral exposure experiments and biological weighting functions (L. Ontario)

Experimental UVR and high-PAR (damage) and low-PAR (recovery) incubations were conducted as described in Chapter 2, with some minor methodological differences. The damage phase of the experiments began 17.5 h after addition of N and P, except on 26 June, when N and P were added

18.4 h in advance. Prior to the damage phase, a 2-L volume from the carboy was poured into a Pyrex culture flask and placed in a conventional incubator (wherein the scalar PAR was ~20 µmol m^{-2} s^{-1}) for 2 h to help repair any PSII damage (Greer *et al*. 1986) incurred *in situ* prior to sample collection. From the flask, 14 subsamples of 100 mL were distributed among 14 beakers and incubated for 90 min at *in situ* temperate, each under a different spectral treatment in the incUVator. The 14 irradiance treatments were generated using the same optical cut-off filters used for the work reported in Chapters 2 & 3, but the power supplied to the arc lamp was ~10% higher (compare Figure 2.2 with Figure 4.1). Over the course of the 90-min incubations, F_V:F_M was determined at 10, 20, 30, 45, 60, 75, and 85

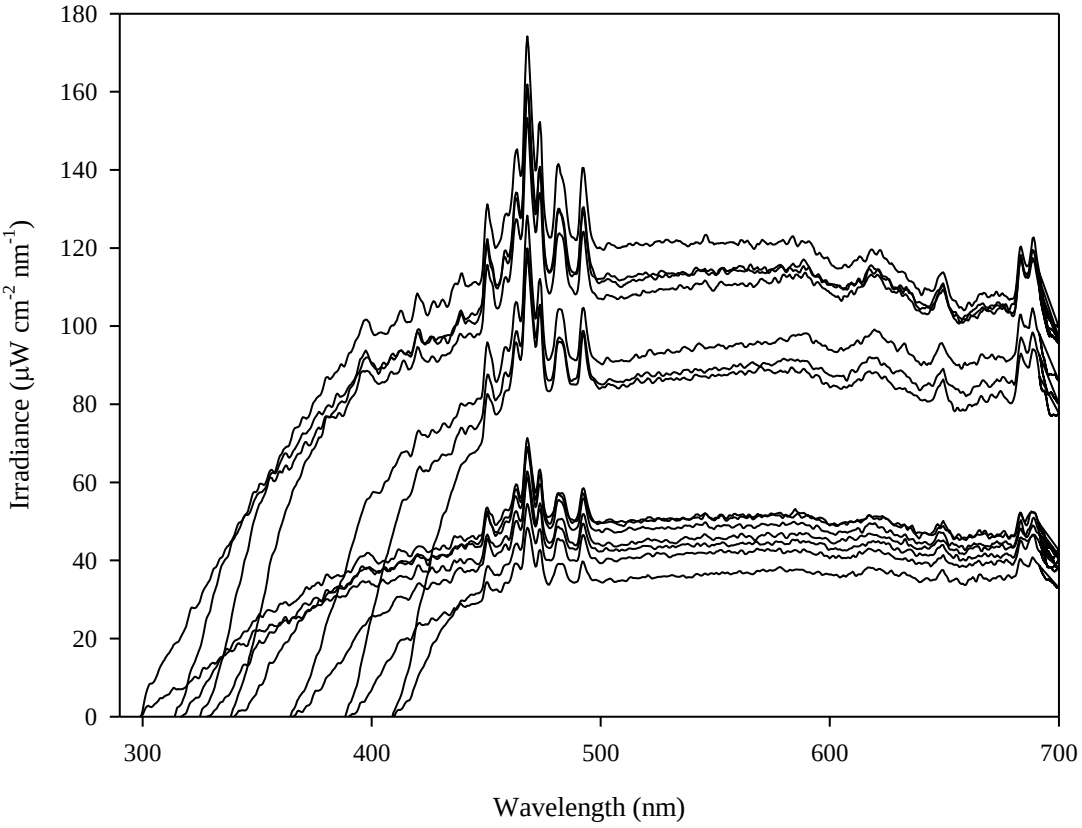

Figure 4.1. Spectral exposure treatments generated by UVR incubator ('incUVator') used for damage phase of experiments.

min for the >300 nm and >315 nm treatments, at 15, 25, 40, 55, 70, and 80 min for the >325 nm, >340 nm, and >365 nm treatments, and at 35, 65, and 90 min for the >390 nm and >410 nm treatments. All samples were dark adapted for 30 min prior to determination of F_V:F_M. At the conclusion of the damage phase, the 3 samples exposed to the high-PFD treatments representative of UVBR+UVAR+PAR (>300 nm), UVAR+PAR (>325 nm) and PAR (>410 nm) were placed in the conventional incubator for 180 min, during which time F_V:F_M was assessed every 30 min to monitor recovery from photoinhibition. Because the demands of the protocol precluded performing the experiments simultaneously, the Nu+ experiments were performed 6 h after the Nu- experiments. During this time the Nu+ sample remained in a plastic carboy in a dark incubator at *in situ* temperature (average temperature of water at 0.5 m, 1 m, and 2 m).

Biological weighting functions (BWFs) for damage by UVR, *i.e.* to quantify the wavelength-dependence of the loss of F_V:F_M in response to irradiance, and recovery rates were determined using the instructions of Cullen & Neale (1997), as in Chapter 3.

4.3.5 Seston C, N, and P content (Dorset Lakes)

Particulate organic C (POC) and N (PN) concentrations were quantified by filtering 100–200 mL of water from the carboy onto pre-combusted (4 h at 450°C) 25-mm GF/F filters which were then stored frozen at -20°C in plastic Petri dishes until return to the University of Waterloo. Filters were then dried in a dessicator, acid-fumed (10% HCl for 24 h) and analysed (980°C combustion, 700°C reduction) using a CE-440 Elemental Analyzer (Exter Analytical, Inc., North Chelmsford, Massachusetts, USA). Particulate P (PP) was calculated as the difference between total P (TP) and dissolved P (DP). Samples for DP were filtered at low vacuum pressure (<100 mm Hg) through polycarbonate filters (0.2-µm pore size) and these filtrates, along with whole-water samples for TP determination, were stored frozen (-20°C) in 60-mL polyethylene bottles until the time of analysis. P concentrations were determined spectrophotometrically using the ammonium molybdate method

(Stainton *et al*. 1977), after chemical digestion with potassium persulphate in an autoclave (30 min at 120°C). Phytoplankton were considered to be moderately N-limited when particulate C:N > 8.3 (molar), and severely P-limited when particulate C:P > 258 (molar), based on the criteria of Healey & Hendzel (1980).

4.3.6 Nutrient amendments (Dorset Lakes)

The Dorset Lakes were each sampled once during 24–29 July and once during 2–7 September in 2009. Data collected from Fawn Lake in July were subsequently lost, so that $n = 5$ in July and $n = 6$ in September. One lake was sampled each day, 3 h after sunrise. Samples of equal volume were collected from 0.5 m, 1 m, and 2 m depths and combined to create an integrated epilimnetic sample for each lake. Thermal profiles revealed that, among lakes, the average epilimnion depth was 3.8 m in July and 4.8 m in September, and the minimum epilimnion depth measured (2.5 m) was greater than the deepest depth from which water was collected, so that no sample ever included (potentially nutrient-rich) metalimnetic water. From each of these integrated epilimnetic samples, four 1-L volumes were poured into opaque plastic bottles (Nalgene). These bottles were acid-washed with 5% HCl prior to each of the two sampling trips and rinsed thoroughly with distilled water after use each day of each trip. A 20-µL volume of 50-mM KH_2PO_4 solution was added to one bottle ('+P'), 100 µL of 50-mM NH_4Cl solution was added to a second bottle ('+N'), and 20 µL of 50-mM KH_2PO_4 and 100 µL of 50-mM NH_4Cl solutions were added to a third bottle ('+N+P'). These supplementations resulted in final concentrations of 31 µg-P L^{-1} and 70 µg-N L^{-1}, in addition to the ambient (pre-existing) soluble N and P concentrations found in the lake water. A fourth bottle was not supplemented with N or P and served as a control. The same bottle was used for each treatment on each date, so that N and P were never added to the control bottle. Bottles were inverted 20 times to mix and then stored in a cooler until return to the laboratory (3.5 h), at which time they were placed in a dark incubator and kept at *in situ* temperature until analysis. Measurements of $F_V:F_M$ were made 8 h

after addition of KH_2PO_4 and NH_4Cl. To correct for instrument noise, 3 separate subsamples were analysed per treatment, and the average values were reported and used in statistical analyses. Using SigmaPlot (v. 11.0), a one-way repeated measures ANOVA was performed on the pooled data for both July and September for all lakes, followed by Tukey t-tests for pair-wise multiple comparisons, to test for significant differences between the 4 treatments, within the entire dataset (n = 44). Assumptions of normality and homoscedasticity were tested and met. Additionally, within two subsets of the data, those samples exhibiting moderate N limitation (n = 5) and those exhibiting extreme P limitation (n = 8), paired t-tests were used to compare the treatment (+N, +P) values of F_V:F_M to control values.

4.3.7 Ambient F_V:F_M (Dorset Lakes)

In addition to the nutrient amendment experiments, values of F_V:F_M were measured before and after exposure to low PAR to assess the extent to which suboptimal values of F_V:F_M (< 0.65; Falkowski & Raven 2007) reflected photoinhibition from irradiance exposure *in situ* prior to sample collection, rather than nutrient stress. A 2-L volume of lake water was poured from the carboy into a culture flask and placed in a cooler equipped with a fluorescent light bulb for 1 h, after which time F_V:F_M was determined ('light' value) and compared to a sample taken directly from the carboy, that had no exposure to light ('dark' value). Scalar PAR at the top of the flask was ~55 μmol m^{-2} s^{-1}. Linear regression analyses were performed with seston C:P as the predictor variable and the dark and light values of F_V:F_M as response variables; separate analyses were performed using the data from July (n = 5) and September (n = 6).

4.4 RESULTS

4.4.1 Effects of nutrient supplementation on phytoplankton variable fluorescence

F_V:F_M was slightly higher for Lake Ontario phytoplankton given supplemental nutrients (0.638 ± 0.030; avg. ± s.d.; n = 8) than for those that were not (0.623 ± 0.030). However, the differences were not quite significant (p = 0.065), and both Nu- and Nu+ F_V:F_M values approximated the nominal optimum value (0.65) and were similar across dates (Figure 4.2). Nu+ F_Q':F_M' values were significantly higher than Nu- values (p = 0.004), but the means were not greatly different (0.321 ±

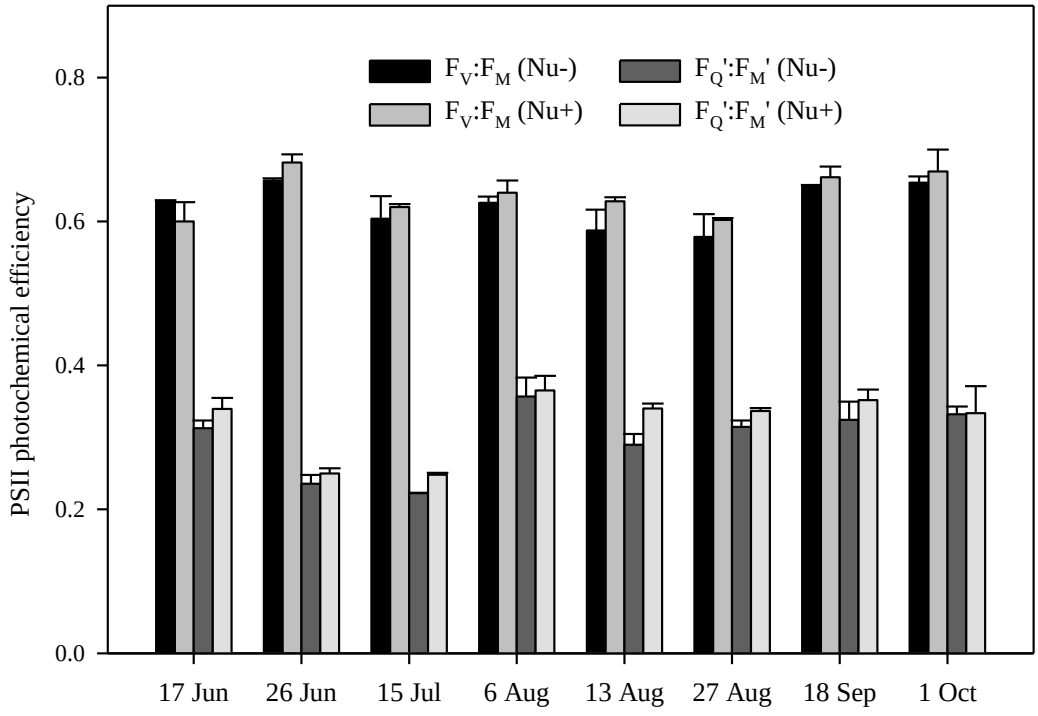

Figure 4.2. Maximum (F_V:F_M) and functional (F_Q':F_M') quantum yields of PSII photochemistry for Lake Ontario phytoplankton during the summer of 2008. F_V:F_M values are averages from RLCs and ICs (n = 2). F_Q':F_M' values are averages of the last 4 data from ICs (n = 4). Error bars represent standard deviations from mean values.

0.047 *vs*. 0.299 ± 0.045). Values of qP were similar between treatments, but Nu+ samples exhibited lower NPQ, and were therefore able to maintain somewhat higher values of F_Q':F_M' and rETR than Nu- samples when exposed to stepwise increases in PAR (Figure 4.3). When Equation 4.2 was

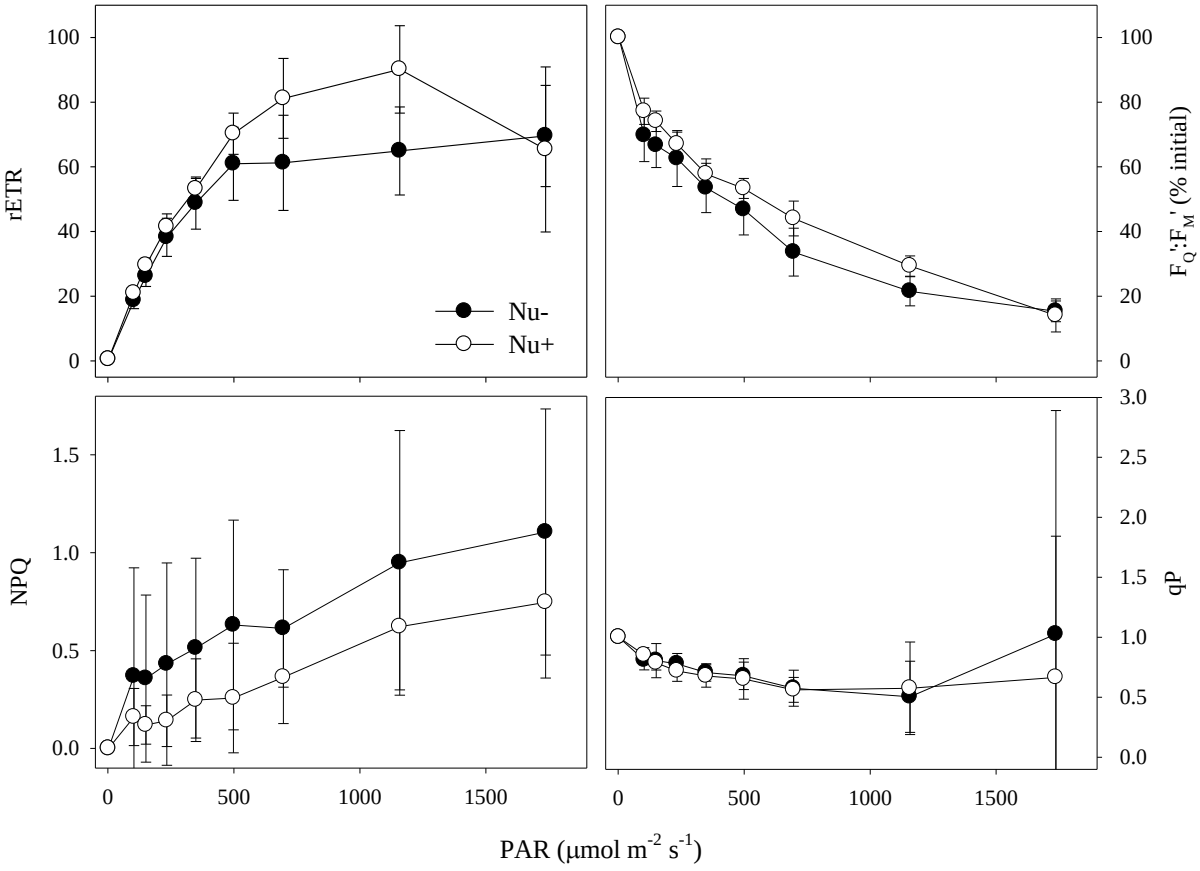

Figure 4.3. Summer average variable fluorescence parameters for Lake Ontario phytoplankton with (Nu+) and without (Nu-) added N and P. Average values of qP (lower right panel) do not include 15 July data (*i.e.*, n = 7) as the Nu- data on this date included 3 outliers (304, 963, and 2902% of the means from all other dates). For all other panels n = 8. Error bars represent standard deviations from mean values.

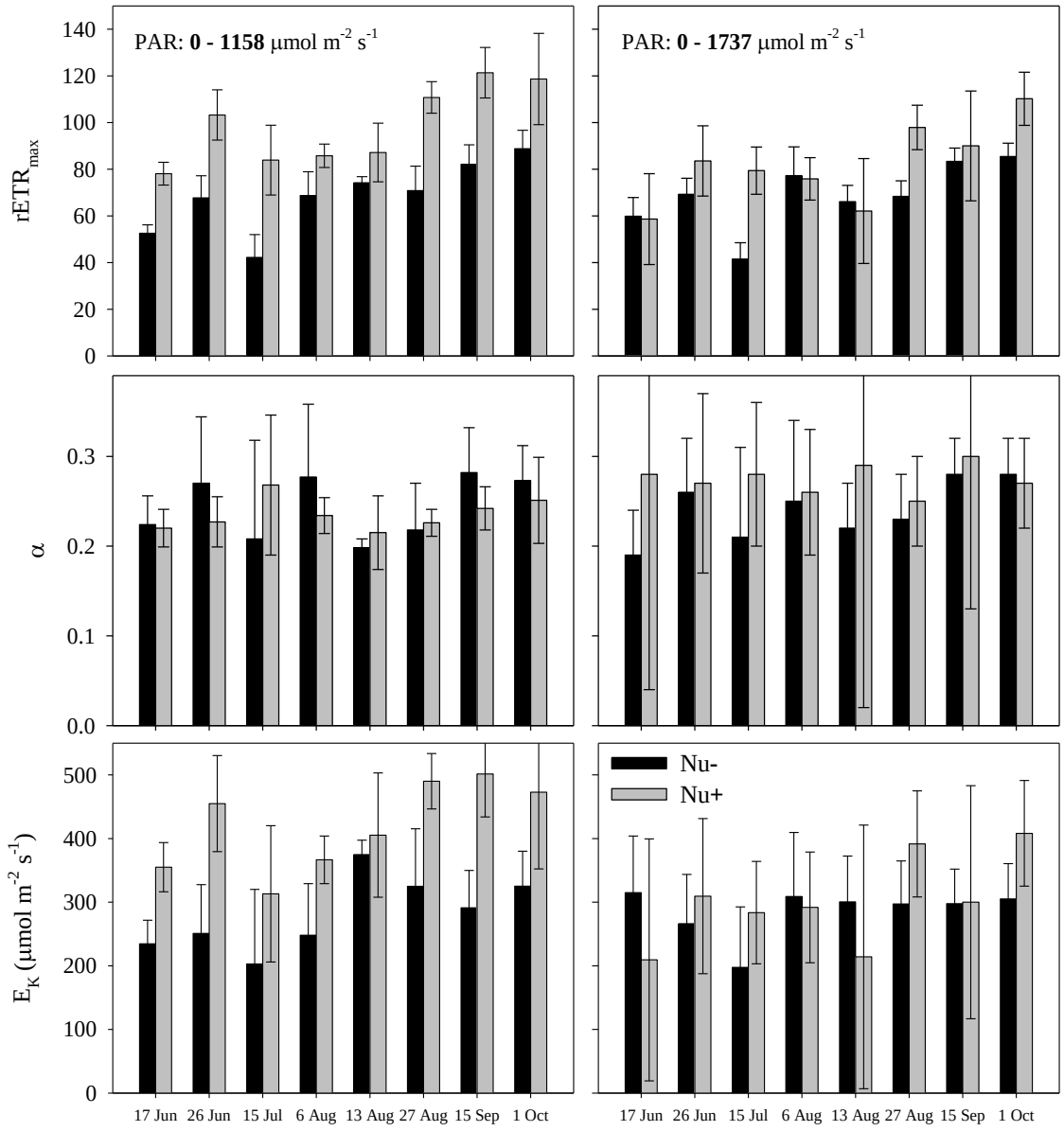

Figure 4.4. Photosynthetic parameters ($rETR_{max}$, α, E_k) of Lake Ontario phytoplankton with (Nu+) and without (Nu-) added N and P during the summer of 2008, estimated from RLCs spanning 0–1737 μmol m^{-2} s^{-1} PAR (right panels) and from the same RLCs from which the highest irradiance step was excluded during analysis (*i.e.*, PAR spanned only 0–1158 μmol m^{-2} s^{-1}; left panels). The error bars represent 95% confidence intervals of the estimates.

applied to RLC data spanning 0–1158 µmol m^{-2} s^{-1}, $rETR_{max}$ was significantly higher for Nu+ samples on all dates except 13 August (Figure 4.4). E_K was also consistently higher for Nu+ samples, and significantly so on 17 & 27 June, 27 August and 15 September, but there was no consistent pattern in α. When fluorescence data obtained under the highest irradiance level (1737 µmol m^{-2} s^{-1}) were included during curve fitting, Nu+ values of $rETR_{max}$ were significantly greater only on 15 July, 27 August and 1 October. Including the highest irradiance level substantially increased the error associated with estimates of α, which broadened the confidence intervals around estimates of E_K (*i.e.*, $E_K = rETR_{max} / \alpha$), so that no differences between Nu- and Nu+ values of α or E_K were significant.

Nutrient supplementation did not exert a large effect on the dark-adapted variable fluorescence of phytoplankton from the Dorset Lakes (Figure 4.5). $F_V:F_M$ was significantly lower

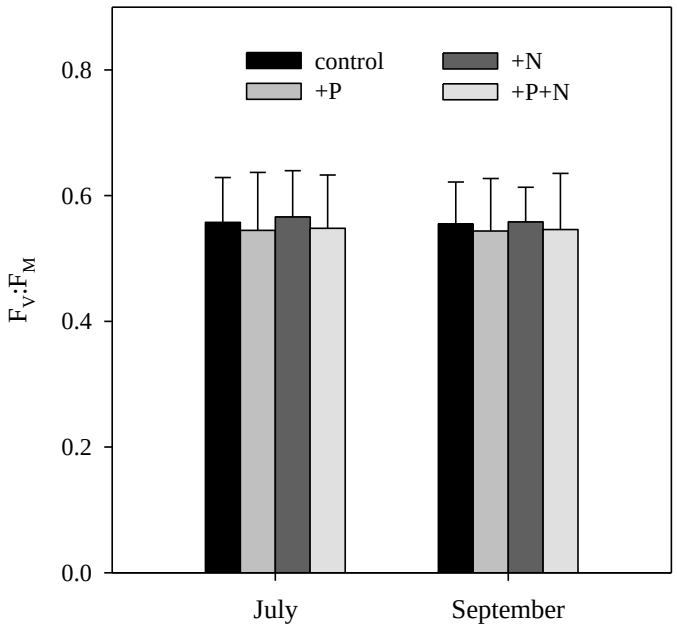

Figure 4.5. Variable fluorescence of phytoplankton from the Dorset Lakes after 8 h of dark incubation with and without supplemental nutrients. Values are among-lake averages (n = 5 in July, n = 6 in September) and error bars represent standard deviations.

after 8 h of dark incubation with added P than with added N (p = 0.045), but the difference in means was small (0.018), and there were no significant differences between treatments (+P, +N, +N+P) and the control (all p > 0.2). Within the subset of samples exhibiting moderate N limitation, F_V:F_M was not significantly different between the control and +N treatments (p = 0.28). Within the subset of samples showing extreme P limitation, mean +P values of F_V:F_M were slightly *lower* than control values, and this difference was nearly significant (p = 0.051). F_V:F_M could be weakly predicted by seston C:P in July and September (Figure 4.6). The slope of the relationship was negative, and it decreased after 1 h of low-PAR exposure in both months.

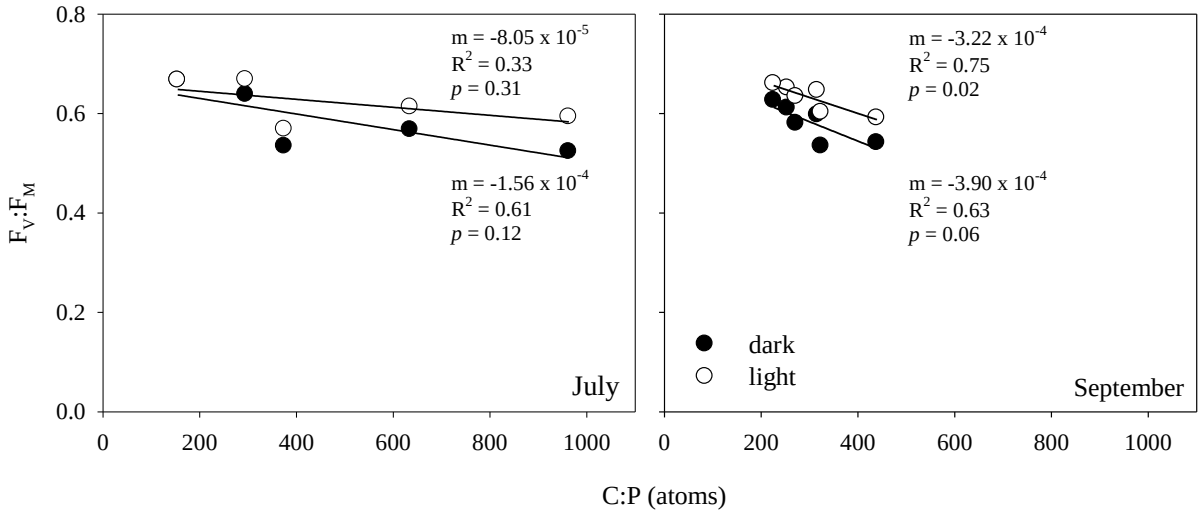

Figure 4.6. F_V:F_M of Dorset Lakes phytoplankton before (dark) and after 1 h of low-PAR exposure (light), as a function of seston P content. Note the differences in slope (m) of the trend-lines fitted to the 'dark' versus 'light' data.

4.4.2 Effects of nutrient supplementation on phytoplankton UVR response

Nu- and Nu+ phytoplankton exhibited similar decreases in F_V:F_M when exposed to irradiance. For both nutrient treatments, PAR (>410 nm) effects were very mild, full spectrum (>300 nm) effects very severe, and the response to UVAR+PAR (>325 nm) was intermediate in magnitude, and was most variable among dates (Figure 4.7). Nutrient supplementation increased rates of both damage and recovery under irradiance exposure, so that the net response of F_V:F_M to irradiance was similar among nutrient treatments relative to the variability among dates (Figure 4.7). When normalized to

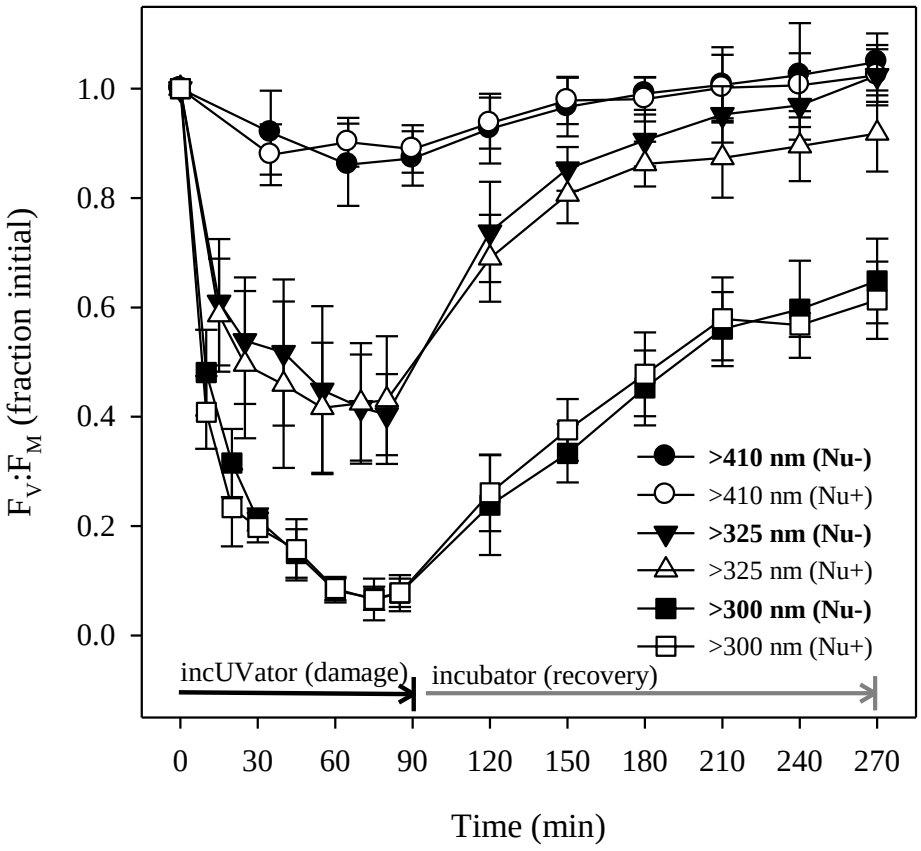

Figure 4.7. Photoinhibition of Lake Ontario phytoplankton, with (Nu+) and without (Nu-) supplemental N and P, under damaging irradiance, and subsequent recovery of F_V:F_M under low PAR. Values are summer averages (n = 8) with standard deviations represented by error bars.

pre-exposure values, summer average post-exposure F_V:F_M values were slightly higher (average = 4%, for all dates and spectral treatments) for Nu+ than Nu- samples, although this difference was not significant ($p > 0.05$) for any spectral treatment. Normalized summer average post-exposure F_Q':F_M' values of Nu+ phytoplankton were generally higher (average = 13%, for all dates and spectral treatments) than those of Nu- phytoplankton but the Nu+ post-exposure F_Q':F_M' was significantly ($p < 0.05$) higher than the Nu- value only for the >340-nm spectral treatment.

The relative spectral sensitivity of Lake Ontario phytoplankton to PSII photodamage was not affected by nutrient supplementation; *i.e.*, the Nu- and Nu+ BWFs had the same shape (Figure 4.8). However, Nu+ samples showed higher sensitivity to damage by UVR at all wavelengths. For the Nu+ phytoplankton, this higher vulnerability to damage by UVR was offset by higher rates of recovery, so that estimates of photoinhibition occurring during a 2-h exposure to a typical midday summer incident spectrum were very similar for Nu- and Nu+ phytoplankton (Figure 4.8; inset).

4.5 DISCUSSION

Reports of PSII VF in temperate oligotrophic lakes are not presently abundant, but are growing in number as more researchers use fast repetition rate fluorometry (FRRF) and PAM fluorometry in freshwaters. In eutrophic lakes, F_V:F_M measured by PAM fluorometry may be >0.60 and close to the nominal optimum value of 0.65 much of the time, when not suppressed by photoinhibition (*e.g.*, Oliver *et al*. 2003; Kromkamp *et al*. 2008). Marwood *et al*. (1999, 2000) used PAM to measure values mostly in the 0.30–0.50 range for summer phytoplankton in oligo-mesotrophic Lake Erie. Pemberton *et al*. (2007) used FRRF to profile VF in oligotrophic Lake Ontario, and estimated that F_V:F_M for unconfined phytoplankton near the base of the surface mixed layer was in the range of 0.35–0.50 during a late summer survey. Rattan *et al*. (in press) reported a very wide range of F_V:F_M, from 0.1–0.6, in oligo-mesotrophic Lake Erie, with values <0.3 being typical in late spring and mid-summer. The lower values were associated with symptoms of N or P deficiency (Rattan *et al*. in

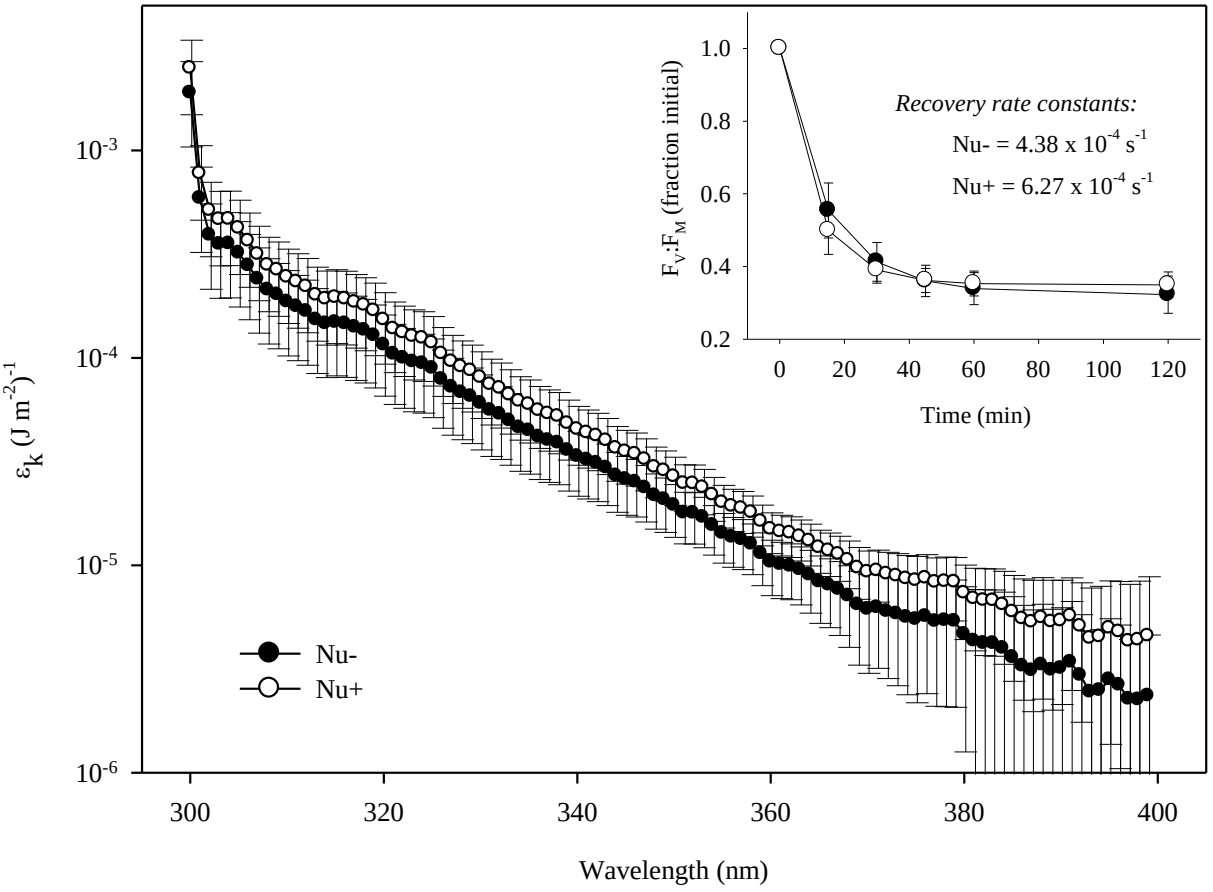

Figure 4.8. Summer average BWFs (n = 8) quantifying the spectral sensitivity to photodamage (ε_k) of Lake Ontario phytoplankton with (Nu+) and without (Nu-) supplemental N and P. Inset: estimated photoinhibition occurring during 2 h exposure to a typical midday summer incident solar spectrum (recorded at the University of Waterloo, 29 August 2010, under clear-sky conditions), based on damage rates calculated using the BWFs and the summer average recovery rates. All error bars represent standard deviations from mean values.

press), and nutrient supplementation led to significantly higher F_V:F_M values (Rattan 2009). Similarly low values of F_V:F_M (0.3 ± 0.03; mean ± SD) were recorded along a 180-km stretch of the St. Lawrence River using FRRF (Twiss *et al*. 2010). Twiss & MacLeod (2008) found a range of values of PSII VF in Lake Ontario, and attributed lower values to the effects of nutrient limitation. The present results indicate, by contrast, that F_V:F_M, and other VF metrics, were typically quite high and only weakly responsive to nutrient supplementation, even in lakes that would be characterized as highly oligotrophic and strongly P-limited (*e.g.*, Blue Chalk and Plastic Lakes). However, our results are consistent with those of Pemberton *et al*. (2007), who found no relationship between F_V:F_M or F_Q':F_M' and phytoplankton nutrient status (C:N:P) in Lake Ontario.

Nutrient-supplemented phytoplankton from Lake Ontario exhibited higher F_V:F_M, F_Q':F_M', and $rETR_{max}$, and lower NPQ values than communities with access to only ambient nutrients. However, the differences were small, especially in F_V:F_M, which generally approximated the optimum value prior to nutrient supplementation; for Lake Ontario phytoplankton, F_V:F_M was 0.579–0.657, and it was similarly high in the Dorset Lakes after 1 h of low-PAR exposure (Figure 4.6). Furthermore, it can only be tentatively concluded that nutrient supplementation caused the observed changes in the VF of the Lake Ontario phytoplankton. As previously mentioned, the Nu+ experiments were conducted 6 h after the Nu- experiments. While rates of recovery from photoinhibition can be approximately an order of magnitude lower in the dark than under dim illumination, they are nonetheless measureable (*e.g.*, Harrison & Smith 2011*a*), and may have caused the small differences in VF observed between Nu- and Nu+ treatments. When a similar nutrient supplementation protocol was followed using phytoplankton from the Dorset Lakes, but treatments and controls were analysed simultaneously, there were no significant increases in F_V:F_M due to N, P, or N & P additions. This possible artefact could have been avoided by conducting the two Lake Ontario experiments in a randomized order; however, this would have introduced uncertainty into the relationship between

irradiance history and UVR sensitivity, which is the subject of Chapter 5. The nutrient supplementation treatments were relatively brief, and more sustained changes in nutrient supply may have revealed additional effects, but similar treatments have been reported to improve PSII efficiency in other studies (*e.g.*, Holland *et al*. 2004; Sylvan *et al*. 2007), and VF metrics were close to optimal, even in controls.

The correlation between seston C:P and F_V:F_M found among phytoplankton assemblages from the Dorset Lakes appears to support the theory that VF responds to nutrient stress, but as with the Lake Ontario data, these findings must be interpreted carefully. When the samples were exposed to dim light for 1 h the lowest F_V:F_M values increased disproportionately relative to the higher values, suggesting that the lower values of F_V:F_M were in part reflective of photodamage to PSII accumulated *in situ* prior to sample collection rather than nutrient stress. Based on the least conservative interpretation of the findings from these lakes, I conclude that nutrient supply exerts a relatively small influence on F_V:F_M of the phytoplankton communities examined, although the differences between nutrient treatments were somewhat larger when PSII VF was measured under illumination (F_Q':F_M', $rETR_{max}$, and NPQ).

Independent evidence on the nutrient status of the phytoplankton sampled here is limited to C:N:P ratios for the Dorset Lakes and in Lake Ontario is based on sampling in previous years. It is nonetheless reasonable to assume that summer phytoplankton in the Dorset Lakes were strongly nutrient limited. Chub, Dickie, Plastic and Blue Chalk Lakes all had P concentrations in the oliotrophic range (*i.e.*, TP < 10 µg L^{-1}; Nürnberg & Shaw 1999), and while stoichiometric ratios are imperfect and variable indicators of nutrient status (*e.g.*, Sterner *et al*. 2008), most of the Dorset Lakes had seston C:P values in a range considered to represent severe limitation (molar C:P > 258; Healey & Hendzel 1980). Phosphate turnover times measured in Brandy and Plastic Lakes in July of 2007 (3–5 min; Sereda *et al*. 2009) and in Dickie Lake in June of 2009 (10.6 min; W.D. Taylor,

person. comm.), are indicative of strong P limitation of the phytoplankton communities in these lakes (Lean *et al*. 1987). Particle stoichiometry was measured as part of a study of Lake Ontario during 14 May–22 Oct 2007, and C:P ratios for a site within 0.5 km of the current study site were representative of moderate to severe P limitation (C:P = 120–385, mean = 250; Smith, unpub. data). In the 1980s, offshore Lake Ontario phytoplankton were characterized as strongly P-limited by measurements of P- and C-cycling (Lean *et al*. 1987; Millard *et al*. 1996), and since that time P concentrations have declined and the oligotrophic nature of the lake has strengthened (Dove *et al*. 2009).

It has been proposed that natural communities acclimated to chronic nutrient stress, despite imbalanced nutrient and energy income, are able to acclimate sufficiently to protect PSII function and maintain high F_V:F_M (Parkhill *et al*. 2001; Suggett *et al*. 2009). However, it can also be argued that natural communities, unlike experimental lab cultures, generally experience an environment that is sub-optimal not only in the variable of interest (*e.g*., P supply) but often others as well (*e.g*., N supply, light availability, temperature), and that this could constrain their ability to allocate resources for maintenance of optimal PSII function (Rattan *et al*. in press). While my dataset does not include direct physiological measures of nutrient stress or growth rate reductions due to nutrient limitation, the results do support the idea that phytoplankton can maintain high VF function in situations where nutrient (specifically P) limitation should be severe. These results are in strong contrast to Rattan *et al*. (in press), and may partly reflect chemical and/or biological differences between the lakes studied.

Methodological differences could also be important. The Water-PAM used in the present study is a high-sensitivity instrument designed for use on phytoplankton, whereas previous studies that have reported lower values of PSII VF in oligo-mesotrophic systems have used other instruments, such as the PAM-101 (Marwood *et al*. 1999), PAM-2000 (Marwood *et al*. 2000), FRRF (Twiss & MacLeod 2008; Twiss *et al*. 2010), or Diving-PAM (Rattan *et al*. in press). It is well established that the FRRF technique yields consistently lower VF values than PAM fluorometry, because the former

uses single turnover flashes of light to determine F_M and the latter uses multiple turnover flashes (see review by Kromkamp & Forster 2003). Furthermore, the presence of cyanobacterial species lacking phycoerythrin in samples can lead to spuriously low measurements of VF by FRRF, because the instrument uses excitation flashes of a wavelength (470 nm) not absorbed by phycoerythrocyanin (Raateoja *et al*. 2004). To conduct measurements on phytoplankton with a PAM-101, PAM-2000,

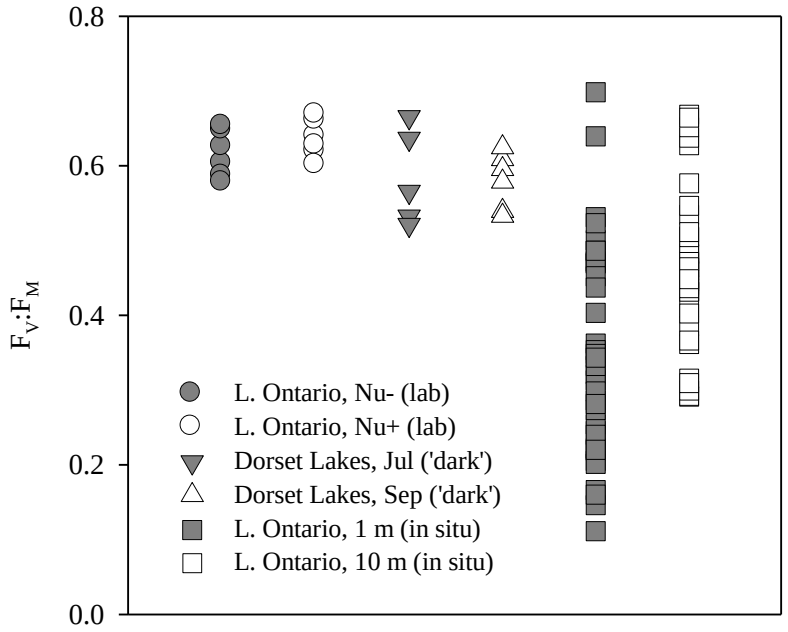

Figure 4.9. F_V:F_M of Lake Ontario phytoplankton measured with (Nu+) and without (Nu-) supplemental N and P under laboratory conditions, of phytoplankton from six Dorset Lakes spanning a gradient in seston C:P (188–963 by atoms) and of Lake Ontario phytoplankton in the field at 0 m and 10 m depths at 6 times of day (7:30, 9:30, 11:30, 13:30, 15:00 and 18:00 h; see Chapter 5). Lake Ontario data are for 6 dates spanning 15 Jul–1 Oct 2008; Nu- and Nu+ samples were collected at ~18:00 h and constituted equal volumes from 2 m, 5 m, and 10 m. Samples from Dorset Lakes were collected 3 h after sunrise and kept in a dark carboy until analysis (‘dark’).

or Diving-PAM, samples must be concentrated on filters so that the relatively low-sensitivity fibre optic system can obtain sufficient signal intensity for measurement. It is possible that in previous studies phytoplankton have been damaged by such filtration, causing underestimation of $F_V:F_M$ and other VF metrics, although this effect should have been minimal at low vacuum pressure (*e.g.*, <5 mmHg; Marwood *et al*. 2000). Direct comparisons are needed to assess the possible role of instrument bias. It is clear that, with the Water-PAM, the measurable variations of $F_V:F_M$ are subtle and would not suggest great potential as a diagnostic of nutrient stress for the communities that were sampled. Even the modest variation tentatively attributed to nutrient effects in the current study needs to be disentangled from the much larger influence of solar irradiance on $F_V:F_M$ (Figure 4.8). The 10–30 min of 'dark adaptation' conventionally used in VF studies facilitates the relaxation of non-photochemical (thermal) quenching of fluorescence, but for appreciable repair of damaged PSII RCs to occur, low levels of PAR are required (Greer *et al*. 1986). Because VF can show strong diel variation *in situ* due to photoinhibition (Oliver *et al*. 2003; Villafañe *et al*. 2007; Chapter 5), I recommend that any study using PSII VF to infer the nutrient status of freshwater phytoplankton controls for the confounding influence of solar irradiance. At the very least, the conditions under which data are obtained should be made explicit; *i.e.*, sampling depth(s) and time(s), weather conditions, and optical properties of the water column (or some proxy, *e.g.*, Secchi depth), so that PSII VF data can be interpreted in a meaningful context.

Nutrient supplementation had small effects on the UVR and PAR responses of Lake Ontario phytoplankton, as measured by PSII VF. During spectral exposure, rates of recovery were generally higher under enhanced nutrient conditions. However, because rates of damage were also higher, and proportionately so, differences in VF under irradiance were negligible between Nu- and Nu+ treatments. Several studies have shown rates of recovery from photodamage to be higher under nutrient-replete conditions relative to nutrient-deprived conditions (*e.g.*, Litchman *et al*. 2002; Heraud

et al. 2005), although Shelly *et al*. (2002) document the opposite effect. Higher availability of the elements required for amino acid and ATP synthesis would be expected to facilitate *de novo* synthesis and insertion of functional D1 protein, resulting in a greater fraction of functional PSII RCs and therefore increased VF. The higher recovery rates measured under nutrient supplementation are consistent with this account, but a mechanistic explanation for nutrient supplementation increasing rates of UVR-induced PSII damage is less obvious. It has been suggested that the rapid turnover of D1 protein helps to prevent net photoinactivation of (entire) PSII RCs, and hence represents a photoprotective strategy (Anderson *et al*. 1997). However, the similar rates of recovery observed during low-PAR exposure suggest that the Nu+ and Nu- phytoplankton had experienced comparable rates of PSII RC inactivation in response to UVR exposure, and recovery of Nu+ phytoplankton from >325-nm irradiance was actually slightly less complete after 3 h exposure to low PAR (Figure 4.7). It therefore does not appear that nutrient supplementation prevented longer-lasting photodamage (RC inactivation) by enhancing the rate of easily-repairable photodamage (D1 degradation).

In nature, UVR and nutrient stress may interact such that UVR alters nutrient assimilation (*e.g.*, Xenopoulos *et al*. 2002), and my experiments were not designed to investigate such effects. It would be desirable to include measures of nutrient cycling and physiological nutrient stress, as well as additional end points for response to UVR (Andreasson & Wängberg 2006), to gain a more complete picture of UVR-nutrient interactions. The present results nonetheless point to a limited influence of short-term nutrient availability on the response of freshwater phytoplankton PSII function to acute PAR and UVR stress.

Chapter 5: Modeling diurnal photoinhibition of Photosystem II

5.1 SUMMARY

The Kok model for photoinhibition was calibrated with BWFs and recovery rate constants determined for Lake Ontario phytoplankton communities during summer and autumn of 2008 and applied to water column spectral irradiance data to make date- and time-specific estimates of *in situ* F_V:F_M at various depths. Model estimates of F_V:F_M integrated throughout the upper half (0–10 m) of the water column showed good agreement with the diurnal pattern of observed values, but the model generally overestimated photoinhibition near the lake surface and underestimated it at depth. It is surmised that the addition of a model for vertical water column mixing to the model presented here would increase the accuracy of depth-specific predictions of *in situ* F_V:F_M. Surface incident irradiance alone explained 98% of the variation in daily integrated *in situ* photoinhibition among dates, suggesting that other factors such as temperature or nutrients did not modulate the UVR-response of the phytoplankton at the study site in Lake Ontario. The irradiance history of the phytoplankton that I sampled was positively correlated with their sensitivity to UVBR, but negatively correlated with their sensitivity to long-wavelength UVAR; this may reflect residual photodamage in the former case, and a short-term photoacclimation response in the latter.

5.2 INTRODUCTION

The photon flux density (PFD) of incident solar irradiance varies over the course of each day, increasing to a maximum at solar noon and subsequently waning until sunset. Certain photobiological effects, such as the formation of cyclobutane pyrimidine dimers (*i.e.*, DNA damage) in bacterioplankton (Visser *et al.* 2002) and inhibition of bacterioplankton productivity (Wilhelm & Smith 2000), are essentially cumulative functions of photon dose, so that net damage steadily

increases during a photoperiod under natural conditions. In contrast, when the repair of damage is rapid, such as for the D1-protein of Photosystem II (PSII) (Bouchard *et al.* 2006), net recovery from photodamage is possible if the rate of repair exceeds that of damage for a sufficient duration. As might therefore be expected, a diurnal pattern in photosynthetic efficiency has been observed in terrestrial plants (see Long *et al.* 1994), corals (Brown *et al.* 1999), macroalgae (Coutinho & Zingmark 1987; Sagert *et al.* 1997) and phytoplankton (Oliver *et al.* 2003; Villafañe *et al.* 2007), in which there is a midday depression of photosynthetic efficiency, followed by recovery in the latter part of the photoperiod.

The spectral irradiance environment of phytoplankton is determined not only by the PFD of incident irradiance, and spectral transparency of the aquatic system, but also by the speed and depth of vertical mixing, which determine the vertical position of the organisms in the water column (Neale *et al.* 2003). Water clarity has increased in Lake Ontario over the past several decades as turbidity has declined because of reductions in phosphorus loading to the lake (Nicholls *et al.* 2001), and the invasion of the filter-feeding Dreissenid mussels (Binding *et al.* 2007). Changes in climate can also have strong effects on the underwater light field. Under certain atmospheric conditions, severe Arctic ozone loss, such as was observed in the spring of 2011, has the potential to increase UVBR at lower latitudes (Manney *et al.* 2011), and this could in turn have the additional indirect effect of enhancing the photodegradation of UVR-attenuating dissolved organic carbon (Morris & Hargreaves 1997), further augmenting *in situ* UVR. There is evidence for a long-term warming trend in the Laurentian Great Lakes (McCormick & Fahnenstiel 1999), and it is predicted that climate change will lead to longer duration and greater stability of stratification in the lakes (Lehman 2002), which would modify the mean spectral irradiance climate of the plankton in Lake Ontario.

Because changes in limnological conditions brought on by natural and anthropogenic forces, such as those described above, can influence (1) the underwater spectral irradiance regime, and (2)

the mixing regime, an attempt to predict the effects of such changes on phytoplankton photosynthetic efficiency *in situ* will require a model that (1) is spectrally-resolved, and (2) that faithfully describes the kinetics of both damage and recovery. Here, as in the preceding chapters of this thesis, the Kok model (Equations 2.1, 3.3) is the exposure-response curve (ERC) used to describe changes in the maximum quantum efficiency of PSII (F_V:F_M) of phytoplankton exposed to irradiance. The damage term of the model is calibrated in a spectrally-specific manner using the Biological Weighting Function (BWF) approach, whereas the recovery rate constant is irradiance-independent, but is specific to the phytoplankton assemblage for which predictions are being made. Though it has been attempted (*e.g.*, Oliver *et al.* 2003), the drawback of the variable fluorescence (VF) approach is that, because changes in F_V:F_M become uncoupled from changes in carbon fixation at saturating irradiance (Behrenfeld *et al.* 1998), losses of primary production cannot generally be reliably modeled. However, F_V:F_M is a useful UVR response metric, especially in the context of rapid changes in irradiance related to diurnal variation and water column mixing, because it offers an instantaneous assessment of the state of PSII (*vs.* the lengthy incubations required to measure carbon fixation or oxygen evolution), and is a sensitive indicator of PSII photoinhibition (Anderson *et al.* 1997).

Many studies have quantified the diurnal time course of *in situ* photoinhibition of PSII (see Behrenfeld *et al.* 1998, and references therein) and some have specifically examined the role of UVR in lakes (Oliver *et al.* 2003; Villafañe *et al.* 2007). Köhler *et al.* (2001) used a BWF for Lake Lucerne (derived by Neale *et al.* 2001) to calibrate an irradiance-dependent (*i.e.*, steady-state) model of photoinhibition ('E model'; Cullen *et al.* 1992), and made predictions of *in situ* rates of carbon assimilation for different mixing depths. Their estimates showed reasonable agreement with measured data from the same system, however, because of the constraints of the ^{14}C methodology, the measured data were not from freely-circulating phytoplankton, but rather samples in bottles that were mechanically circulated to simulate vertical mixing. To my knowledge, no study has yet validated

spectrally-resolved model predictions of *in situ* photoinhibition with empirical data obtained from truly *in situ* (unconstrained) phytoplankton assemblages.

In this study, I performed such a comparison, by calibrating the kinetic model of Kok (1956) with BWFs and recovery rate constants estimated for Lake Ontario phytoplankton communities during summer and autumn of 2008, and applying it to underwater spectral irradiance data to generate date- and time-specific estimates of F_V:F_M at various depths *in situ*. The model predictions were made assuming no mixing and then compared to observed F_V:F_M data for Lake Ontario to test how well this simple, static water column, approach could capture the *in situ* dynamics.

There is evidence that prior exposure to UVR can decrease the susceptibility of phytoplankton to UVR-induced photoinhibition. For example, assemblages from shallow mixed layers have been found to exhibit high UVR resistance relative to those mixed more deeply (Neale *et al.* 1998*b*; Xenopoulos & Schindler 2003), and communities from clear lakes appear to be more UVR-resistant than communities from turbid or humic lakes (Chapter 3, and references therein). Similar findings have come from laboratory-based studies (*e.g.* Jiang & Qiu 2005), suggesting that phytoplankton have the capacity to acclimate to UVR effectively, although this may vary taxonomically (Litchman & Neale 2005). Bouchard *et al.* (2005) found that while UVBR effects on Antarctic phytoplankton were dependent on light history, UVAR and PAR were the dominant contributors to photoinhibition of PSII *in situ*, and that incident PAR alone explained 99% of the variation among dates in photoinhibition. This suggests that the inhibition of PSII function of natural communities can be directly proportional to solar exposure, with no apparent influence of photoacclimation status. However, unlike Lake Ontario during the duration of my study, the Antarctic site was rich in nutrients, and varied little in water clarity or temperature among sampling dates. To help clarify the factors contributing to inhibition of PSII function in natural phytoplankton, additional objectives of this study were to elucidate the factors controlling variation in photoinhibition

of Lake Ontario phytoplankton *in situ*, and to determine the factors responsible for variation in their spectral sensitivity to photodamage and their recovery potential.

5.3 METHODS

5.3.1 Field Sampling

Samples were collected from Lake Ontario at the same site described in Chapter 4 (near Pickering; 43°47'N 79°04'W) on 29 May, 17 & 26 June, 15 July, 6, 13 & 27 August, 18 September and 1 October 2008. Due to inconsistent sampling times among dates and missing field measurements, data from May and June were not included in analyses related to the modeling of *in situ* photoinhibition. However, the BWF data determined for these dates were used to examine the relationship between irradiance history and UVR sensitivity (section 5.4.3). On each of the 6 sampling dates during 15 July–1 October, water was collected from various depths at the study site over the course of the day to measure diurnal variation in phytoplankton PSII VF. Six-litre samples were collected from depths of 1 m, 2.5 m, 5 m, 7.5 m, and 10 m using a Niskin bottle, and from each 6-L sample a 1-L volume was poured into an opaque, acid-washed plastic bottle (Nalgene). A subsurface ("0 m") sample was also collected by placing a bottle immediately below the surface of the lake and allowing it to fill with water. Samples from these 6 depths were collected at 7:30 h, 9:30 h, 11:30 h, 13:30 h, 15:00 h, and 18:00 h on each date. After a dark-adaptation period of at least 30 min (typically ~45 min), PSII VF parameters (F_V:F_M, RLCs, ICs) were measured as described in section 4.3.3 of this document. Samples collected at 18:00 h were analyzed only for F_V:F_M, and not the other VF metrics, due to time constraints. Shortly after 18:00 h an integrated water column sample (equal volumes from 2 m, 5 m, & 10 m) for laboratory experiments was collected and stored as described in the preceding chapter (from 29 May–1 October). Several vertical profiles of temperature and spectral fluorescence were measured over the course of each sampling date using the aforementioned FluoroProbe.

5.3.2 Radiometry

Profiles of down-welling irradiance were recorded at wavelengths of 305 nm, 320 nm, 340 nm, and for broadband-PAR using a BIC-2104 radiometer (Biospherical Instruments Inc.), and at wavelengths of 380 nm and 399 nm using a Satlantic OCI-200 radiometer (Satlantic Inc.). Vertical attenuation coefficients (KD_λ) were then calculated as the magnitude of the slope obtained by regression of the natural logarithm of irradiance versus depth. Using the linear relationship between the natural logarithm of KD_λ and wavelength, determined for each sampling date (average $R^2 = 0.97$), attenuation coefficients for each wavelength from 299–399 nm were estimated by interpolation.

On sampling days, surface incident UVR (305 nm, 320 nm, and 340 nm) and broadband-PAR were monitored at the study site using the BIC-2014 radiometer. These data were recorded at approximately 30-min intervals between approximately 8:00–18:30 h each sampling day (average n = 18). Additionally, total solar radiation (UVR, PAR & infrared; hereafter 'TSR') data were obtained from a meteorological station situated onshore, approximately 2 km north of the study site (43°48'22"N, 79° 3'39"W). Measurements were taken every 5 s, averaged every 10 min, and the averages were recorded. These data were collected by the National Water Research Institute of Environment Canada (NWRI), and made available by Dr. Ram Yerubandi.

5.3.3 Laboratory Experiments

F_V:F_M data obtained during spectral exposures in the incUVator are those reported in the preceding chapter ('Nu-' treatment), and the details of the 90-min exposures to UVR and PAR can be found there. Biological weighting functions (BWFs) and recovery rates were estimated as described in section 3.3.5.

5.3.4 Quantifying *in situ* photoinhibition

For each sampling depth (0 m, 1 m, 2.5 m, 5 m, 7.5 m & 10 m) and for the average between 0 and 10 m, daily *in situ* photoinhibition (DIPI) was calculated by applying the 'Area Below Curves' macro of

SigmaPlot (v. 11.0) to line-plots of $IPI_{(t,z)}$ *vs.* time for each date. For a given depth, z, $IPI_{(t)}$ was calculated as the difference between the F_V:F_M value at time t and the value of F_V:F_M at 7:30 h at that depth; *i.e.*, $IPI_{(t,z)}$ is the net decrease in F_V:F_M since 7:30 h at a particular depth on that day. $DIPI_{(z)}$ is therefore the loss of F_V:F_M integrated over the majority of the photoperiod (7:30–18:30 h) at depth z.

5.3.5 Modeling of *in situ* F_V:F_M

Surface incident spectral radiation (299–399 nm) on the sampling dates was estimated by scaling a previously-recorded incident solar spectrum to surface incident 340-nm irradiance measured at the study site at approximately 30-min intervals with the BIC radiometer previously described. The incident solar spectrum was recorded at the University of Waterloo on 29 August 2010 at 13:28 (*i.e.*, the approximate middle of the photoperiod; see Figure 3.1). Reflectance at the air-water interface, RF, was calculated according to Kirk (1983), as

$$RF = \frac{1}{2}\frac{sin^2(\theta_a-\theta_w)}{sin^2(\theta_a+\theta_w)} + \frac{1}{2}\frac{tan^2(\theta_a-\theta_w)}{tan^2(\theta_a+\theta_w)} \quad (5.1)$$

where θ_a is the zenith angle of the incident light in air, and θ_w is the angle to the downward vertical of the transmitted beam in water. The θ_a value corresponding to each time of day was calculated using online software provided by the Earth System Research Lab of the National Oceanic and Atmospheric Administration (http://www.srrb.noaa.gov/highlights/ sunrise/azel.html). Assuming a refractive index of 1.33 for water (Kirk 1983), values of θ_w were then calculated from Snell's Law

$$\frac{\sin\theta_a}{\sin\theta_w} = 1.33 \quad (5.2)$$

Spectra (299–399 nm) at depths of 0 m, 1 m, 2.5 m, 5 m, 7.5 m, and 10 m were then estimated using the equation

$$E_{Z,\lambda} = E_{I,\lambda} \cdot e^{-KD_\lambda \cdot z} \quad (5.3)$$

where $E_{I,\lambda}$ is the incident irradiance at wavelength λ after correction for surface reflectance, KD_λ is the vertical attenuation coefficient for wavelength λ, and z is depth. Broadband PAR at different depths

was estimated in the same fashion, using incident radiation data and attenuation coefficients that were measured directly. Additionally, estimates were made of the irradiance history of the sample (E_S) used in laboratory experiments. E_S was calculated as the mean *in situ* irradiance, from sunrise until 18:00 h, at 2 m, 5 m, and 10 m; *in situ* irradiance at the various depths was calculated using the TSR data from the meteorological station and values of KD_{PAR}. No radiometric profile was taken on 17 June, so KD_{PAR} was calculated as the quotient of 1.7 and the secchi depth on this date (Kalff 2002).

Using the calculated spectral irradiance data, predictions of $F_V:F_M$ at 0 m, 1 m, 2.5 m, 5 m, 7.5 m, and 10 m were made for each time of day at which incident UVR data were collected; data were generally recorded at an interval of ~30 min. For the first time interval for which model predictions were made (7:30 h to ~8:00 h), the starting value of $F_V:F_M$ was set to the 7:30 h value measured (*i.e.*, the observed value; $F_V:F_{M(7:30)}$), and the value at the end of the time interval was calculated using the model of Kok (1956), as expressed by Equation 2.1. $F_V:F_M$ at the end of each subsequent time interval, $F_V:F_{M(t)}$, was calculated as

$$F_V:F_{M(t)} = F_V:F_{M(p)} - L + G \qquad (5.4)$$

where $F_V:F_{M(p)}$ is $F_V:F_M$ from the end of the previous time interval, and L and G are the decrease and increase, respectively, in $F_V:F_M$ during the present time interval (Figure 5.1). L was calculated using Equation 2.1 and assuming no recovery (*i.e.*, r = 0). G was calculated using Equation 2.2, in which the previously-accumulated damage, d, was equal to the difference between $F_V:F_{M(7:30)}$ and $F_V:F_{M(p)}$. This modeling approach does not account for the influence of vertical mixing on $F_V:F_M$; it assumes a static water column in which phytoplankton spend the entire photoperiod at a single depth. In an attempt to quantify the influence of the mixing regime on $F_V:F_M$ *in situ*, and therefore on the accuracy of the model predictions, multiple linear regression analyses were performed using the magnitude of the difference between observed and predicted values of DIPI as the dependent variable, and the strength of stratification and wind speed as independent variables. The strength of stratification was

equated to the daily average difference in temperature between 2 m and 12 m depths, calculated using data from a chain of TidBit temperature loggers (Onset Computer Co.) moored 1.3 km south of the study site by NWRI. Wind speed data were measured at the aforementioned meteorological station. All linear regression and Pearson correlation analyses were performed using SigmaPlot (v. 11.0).

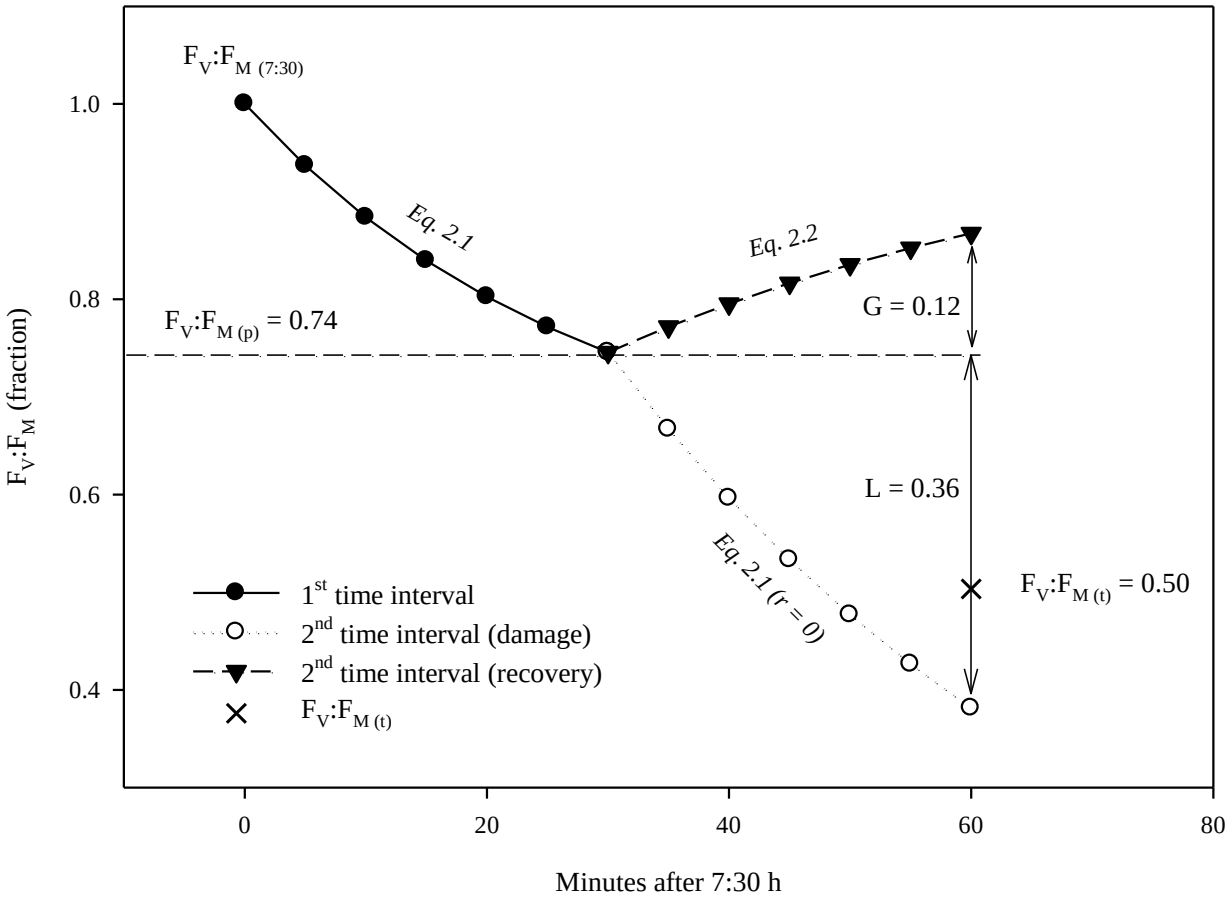

Figure 5.1. A schematic of how Equations 2.1 & 2.2 were used to predict diurnal changes in $F_V:F_M$ *in situ*. The $F_V:F_M$ value of 0.50 at 60 min is the final value ($F_V:F_{M(t)}$) of the second time interval (30–60 min), and would therefore be the starting value ($F_V:F_{M(p)}$) for the third time interval, and so forth.

5.4 RESULTS

5.4.1 Optical quality of Lake Ontario & F_V:F_M *in situ*

Table 5.1. 1%-irradiance depths at the study site on Lake Ontario for several UV wavelengths and for broadband PAR for individual dates and as an average of all dates during 15 July–1 October 2008; standard deviations are shown in parentheses.

	305 nm	320 nm	340 nm	380 nm	399 nm	PAR
15 July	2.53	3.71	5.48	11.0	12.8	19.2
6 August	1.84	2.64	3.74	6.13	7.54	12.8
13 August	2.36	3.93	6.13	13.5	17.7	21.9
27 August	2.24	3.38	4.87	6.46	7.73	14.9
18 September	1.70	2.75	3.93	6.87	8.36	17.0
1 October	2.04	3.41	4.84	10.7	13.1	18.4
AVG	2.12 (0.32)	3.30 (0.51)	4.83 (0.91)	9.11 (3.04)	11.2 (4.05)	17.4 (3.22)

Water clarity at the study site in Lake Ontario was generally high, and while UVBR-transparency was relatively consistent among dates, UVAR- and PAR-transparency showed considerable temporal variation (Table 5.1). F_V:F_M was typically ~0.5 in the early morning (7:30 h) and decreased thereafter, generally reaching a minimum at midday when solar irradiance was highest, and showed some recovery in the late afternoon as incident irradiance waned (Figure 5.2). F_V:F_M was generally much higher on 1 October than on the earlier sampling dates (Figure 5.2). The diurnal depression of PSII VF was highly depth-dependent: midday losses of F_V:F_M were approximately twice as high in the top metre of the water column than at depths 7.5–10 m (Figure 5.3). (Only the F_V:F_M data are reported and discussed in this chapter, but associated values of F_Q':F_M', $rETR_{max}$, E_K, and α can be found in Appendix A.) The BWF-model predictions of *in situ* F_V:F_M approximated the pattern of diurnal variation present in the observed data (Figures 5.2 & 5.3). The model usually underestimated F_V:F_M (*i.e.* overestimated photoinhibition) near the surface of the lake (0–1 m) and overestimated

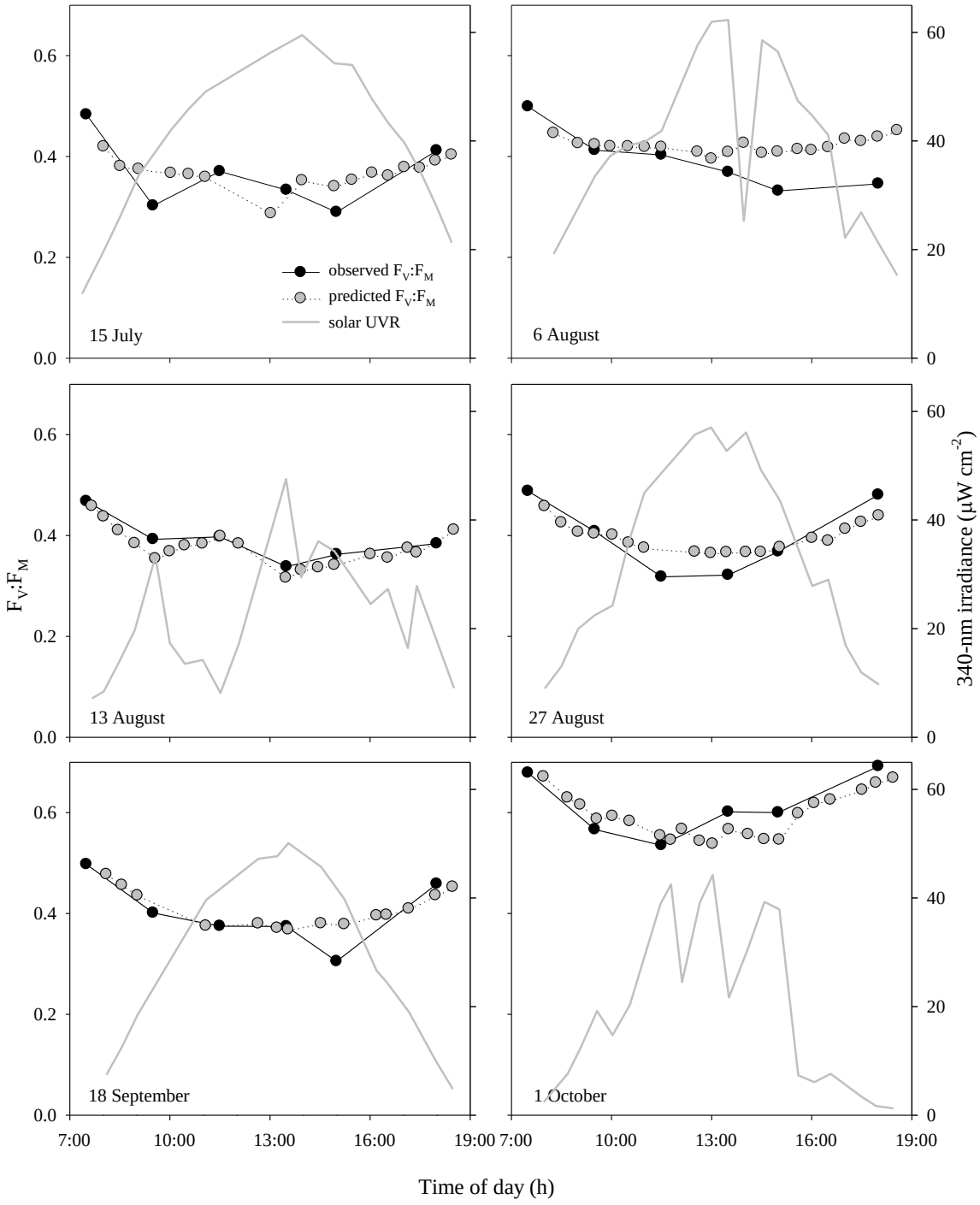

Figure 5.2. Diurnal variation in observed and predicted water column (0–10 m) average F_V:F_M, as well as incident solar irradiance at the study site on Lake Ontario in 2008.

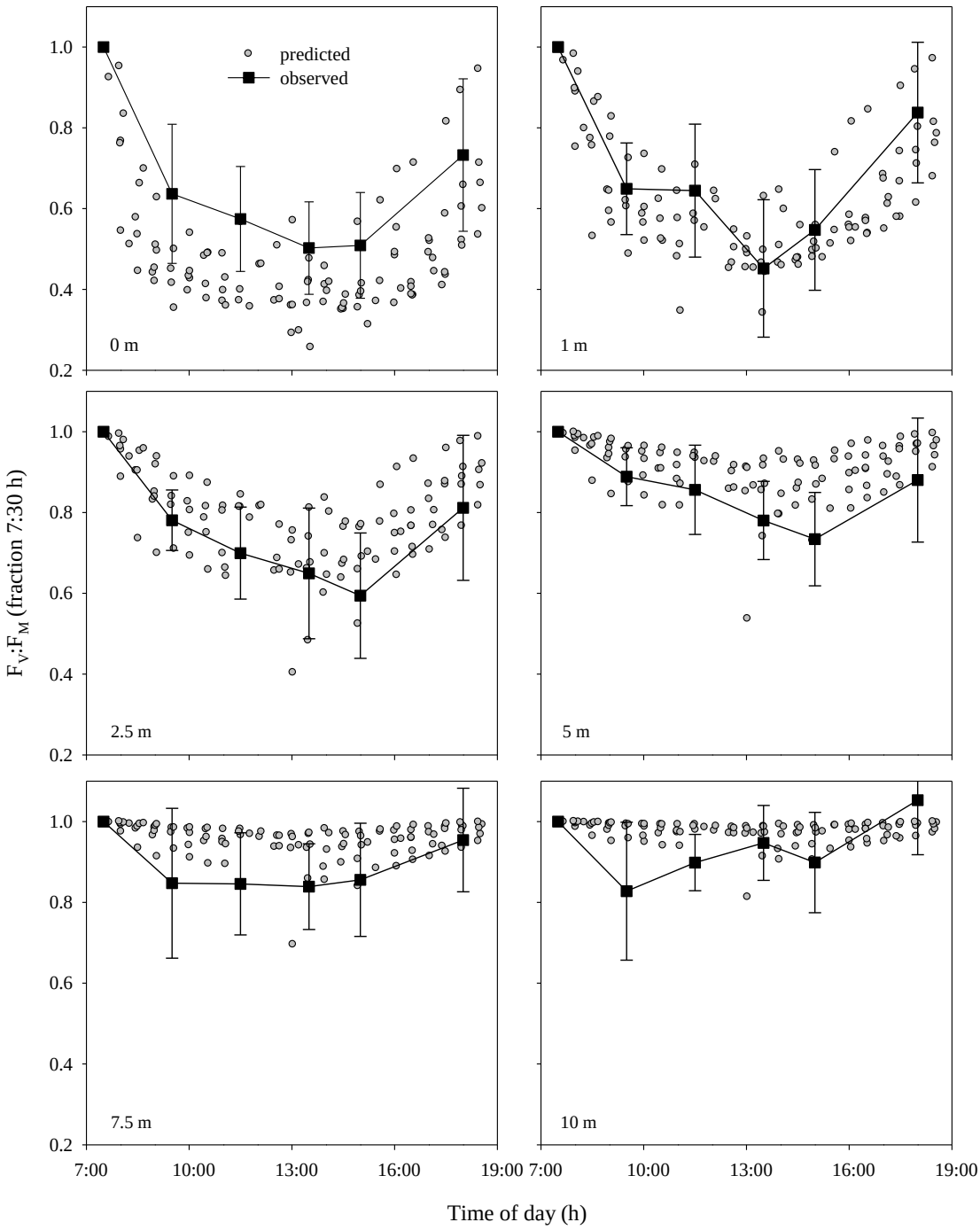

Figure 5.3. Diurnal variation in observed and predicted F_V:F_M, at 6 depths spanning 0–10 m at the study site on Lake Ontario, 15 July–1 October 2008. Observed data are averages of all dates (n = 6) with standard deviations represented by error bars.

F_V:F_M at depths 2.5–10 m (Figure 5.3). Predicted and observed values of the average F_V:F_M between 0 and 10 m depths showed good correlation over the photoperiod, although the predictive accuracy of the model varied among dates (Figure 5.2); in particular, the model did not predict the lack of late-afternoon recovery observed on 6 August.

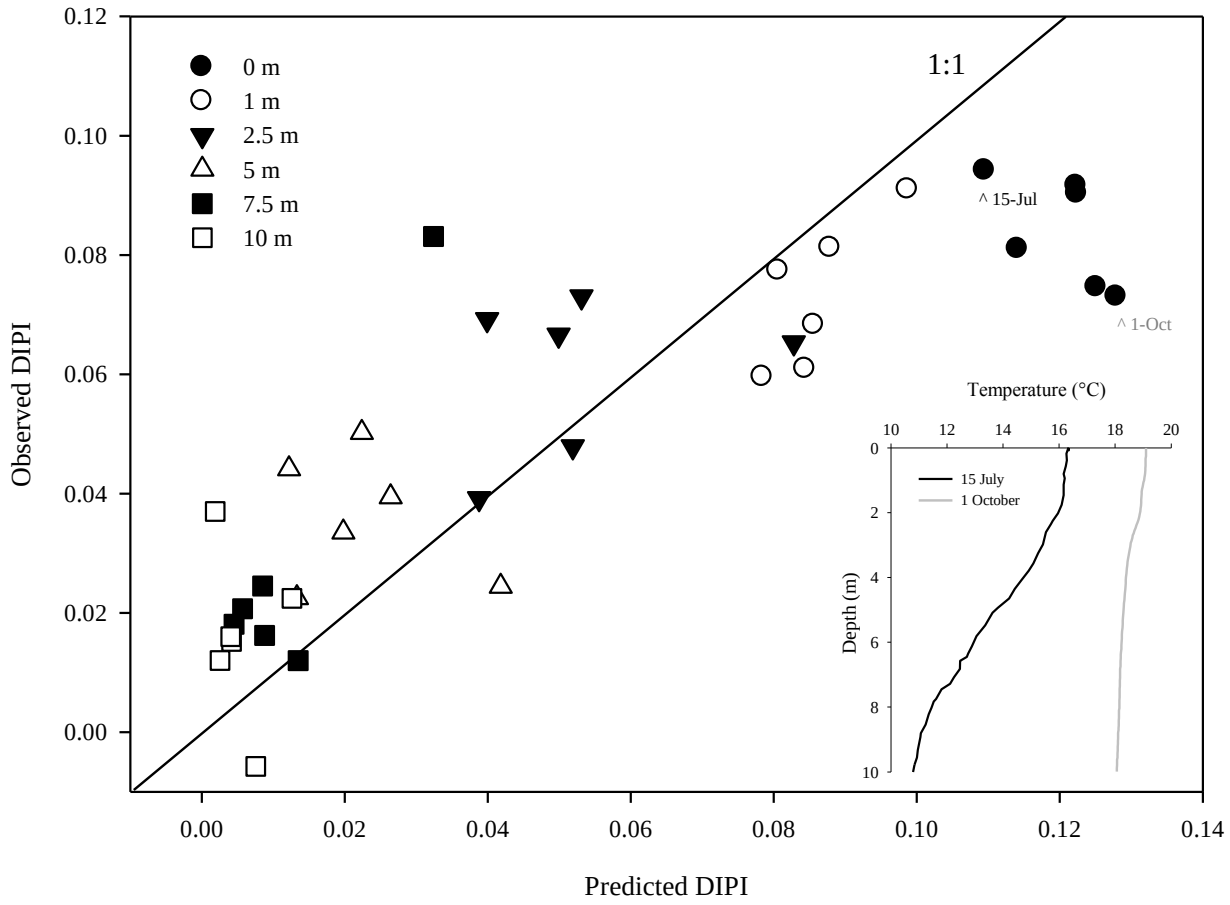

Figure 5.4. Observed vs. predicted daily *in situ* photoinhibition (DIPI) of PSII in Lake Ontario, for all depths and dates. Inset: Vertical profiles of temperature at the study site on Lake Ontario for two dates in 2008 on which there was pronounced stratification (15 July) and an almost isothermal water column (1 October). Note the positions of the 0-m points for 15 July and 1 October relative to the 1:1 line on the main figure.

5.4.2 Daily *in situ* photoinhibition (DIPI)

Almost all of the variation among dates in observed $DIPI_{(0–10\ m)}$ was explained by variation in surface incident TSR (R^2 = 0.987, p < 0.001, n = 6). The predicted and observed values of $DIPI_{(z)}$ for all dates and depths (Figure 5.4) were significantly correlated (r = 0.86, p < 0.001, n = 36). However, when the predictive power of the model was tested in a depth-specific manner by using data from different dates as replicates, and correlating observed and predicted values of $DIPI_{(z)}$, the only

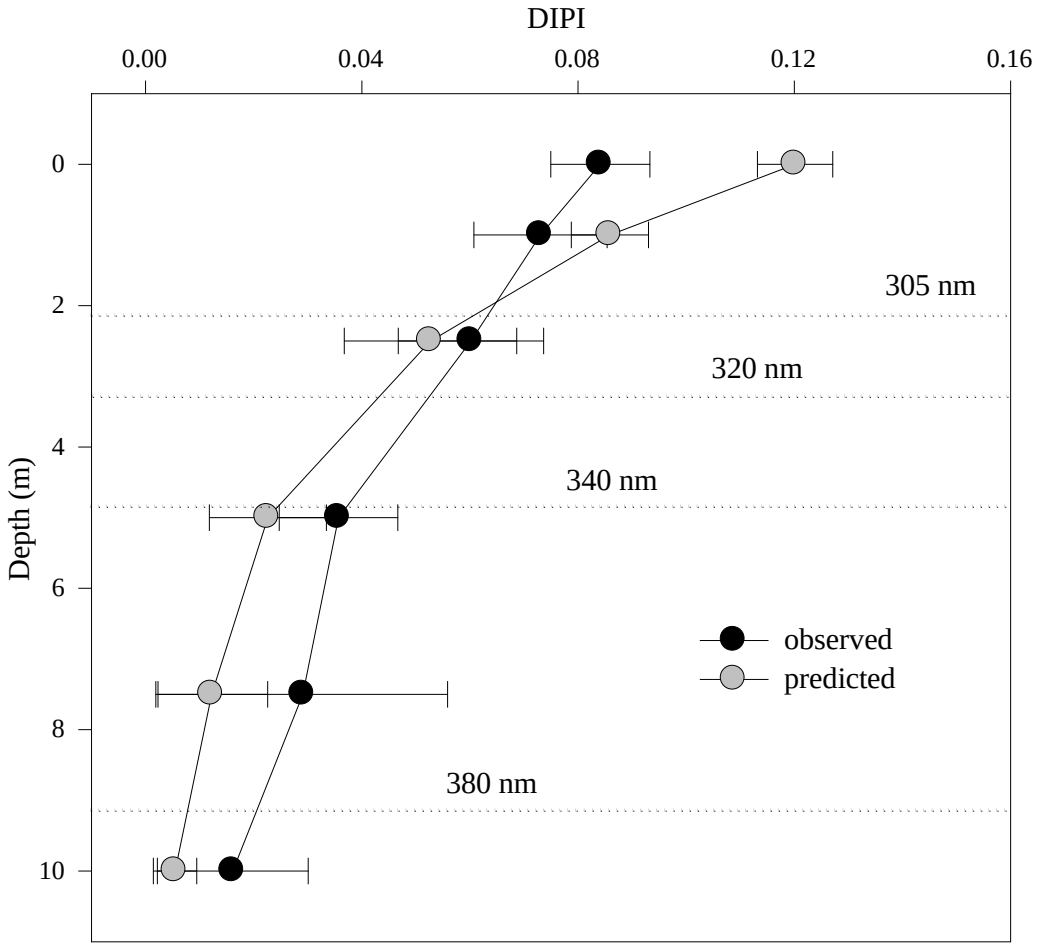

Figure 5.5. Vertical profile of observed and predicted DIPI (averaged for all dates; n = 6) with 1%-irradiance depths for several UV wavelengths indicted by dotted lines.

significant relationship was at 7.5 m (r = 0.92, p = 0.011), although the correlation was almost significant at 1 m (r = 0.78, p = 0.066). The correlation between observed and predicted values of $DIPI_{(0–10\ m)}$ was not significant (p = 0.27, n = 6). DIPI was overestimated near the surface (0 m and 1 m) and was generally underestimated at deeper depths (Figure 5.4), so that the observed vertical profile of DIPI was more uniform than was predicted (Figure 5.5). The best agreement between predicted and observed values of $DIPI_{(0–10\ m)}$ was on 15 July, and the worst on 6 August (Figure 5.6).

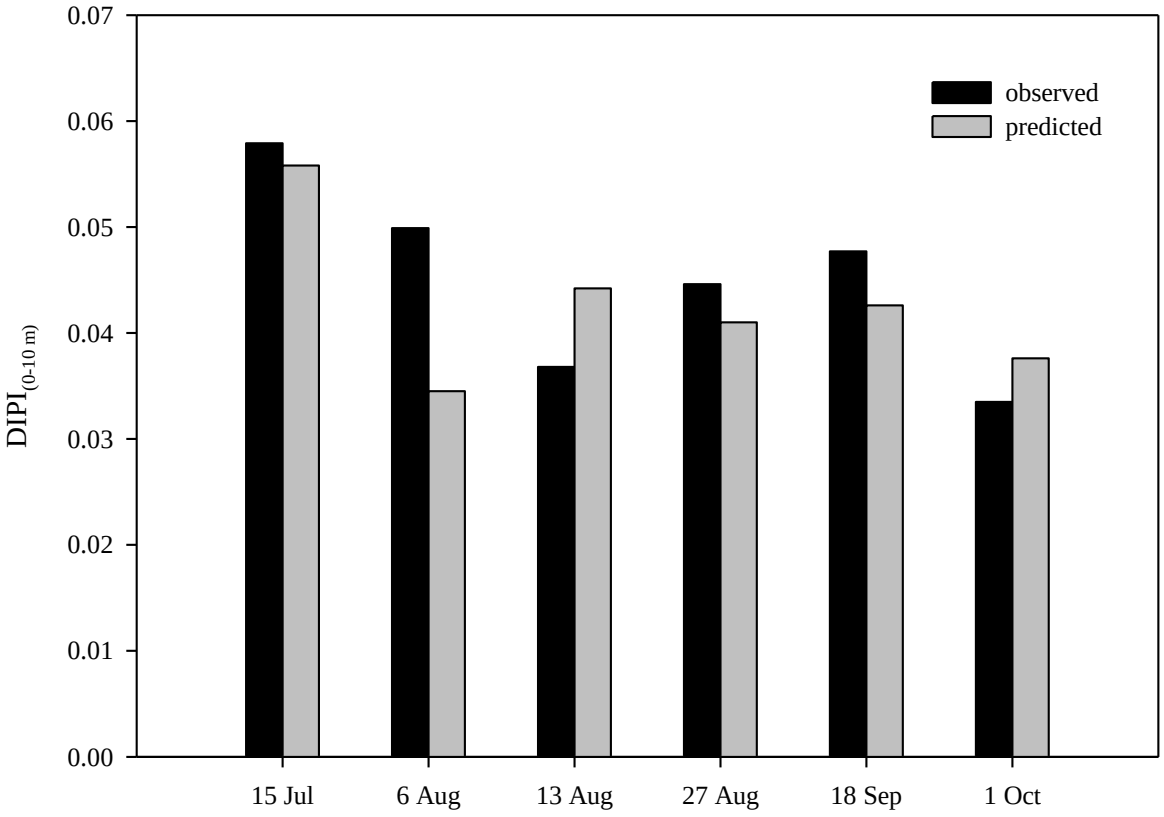

Figure 5.6. Predicted and observed daily *in situ* photoinhibition as an average for 0-10 m depths, for 15 July–1 October 2008 at the study site in Lake Ontario.

The model did not consistently overestimate or underestimate $DIPI_{(0–10\ m)}$ (Figure 5.6). Strength of stratification (as inferred by the temperature difference between 2 m and 12 m) and wind speed were not significant co-predictors of model performance (difference between observed and predicted values of DIPI) at any depth, or for $DIPI_{(0–10\ m)}$. However, it is noteworthy that the best agreement between predicted and observed $DIPI_{(0\ m)}$ occurred on 15 July, when temperature stratification was pronounced, whereas the worst agreement between predicted and observed $DIPI_{(0\ m)}$ occurred on 1 October, when the water column was essentially isothermal (Figure 5.4).

5.4.3 Variation in phytoplankton UVR sensitivity

The shape of the BWFs was very consistent across sampling dates, while the magnitude of the BWF coefficients showed a modest degree of variability (see Figure 4.8). Recovery rate constants ranged from 1.72–9.45 x 10^{-4} s^{-1}. Because the rate constants for damage and recovery were highly correlated (R^2 = 0.96), the net sensitivity to photoinhibition under a representative midday solar spectrum was fairly similar among dates (Figure 5.7). In response to this spectrum, the estimated damage and recovery rate constants for the 15 July assemblage were much larger than for the other dates, leading to predictions of a more rapid attainment of a steady state level of PSII VF (Figure 5.7).

The irradiance history of the sample (E_S) explained much of the variation in sensitivity to damage by the UVB ($\varepsilon_{K(299\ nm)}$, $\varepsilon_{K(309\ nm)}$, & $\varepsilon_{K(319\ nm)}$) and long-wavelength UVA ($\varepsilon_{K(389\ nm)}$ & $\varepsilon_{K(399\ nm)}$) spectral regions, but there was no relationship between sensitivity to damage by mid-wavelength UVAR ($\varepsilon_{K(339\ nm)}$ $\varepsilon_{K(349\ nm)}$ $\varepsilon_{K(359\ nm)}$) and E_S (Figure 5.8). These relationships between sensitivity to photodamage and irradiance history were positive in the 299–339 nm range of the spectrum, but negative for wavelengths 349–399 nm (Figure 5.8). For comparison, E_S was also calculated as the average value for the day of sampling and the previous day, to determine whether BWF coefficients might integrate the effects of exposure over longer periods; the slopes of the relationships were the

same, but the irradiance history of the previous two days explained less (~20%) of the variation in each BWF coefficient than the irradiance on the day of sampling alone.

5.5 DISCUSSION

The relatively high early-morning values of $F_V:F_M$ (~0.5) suggest that nutrient limitation was not acting to strongly depress PSII VF in Lake Ontario, consistent with the results reported in Chapter 4.

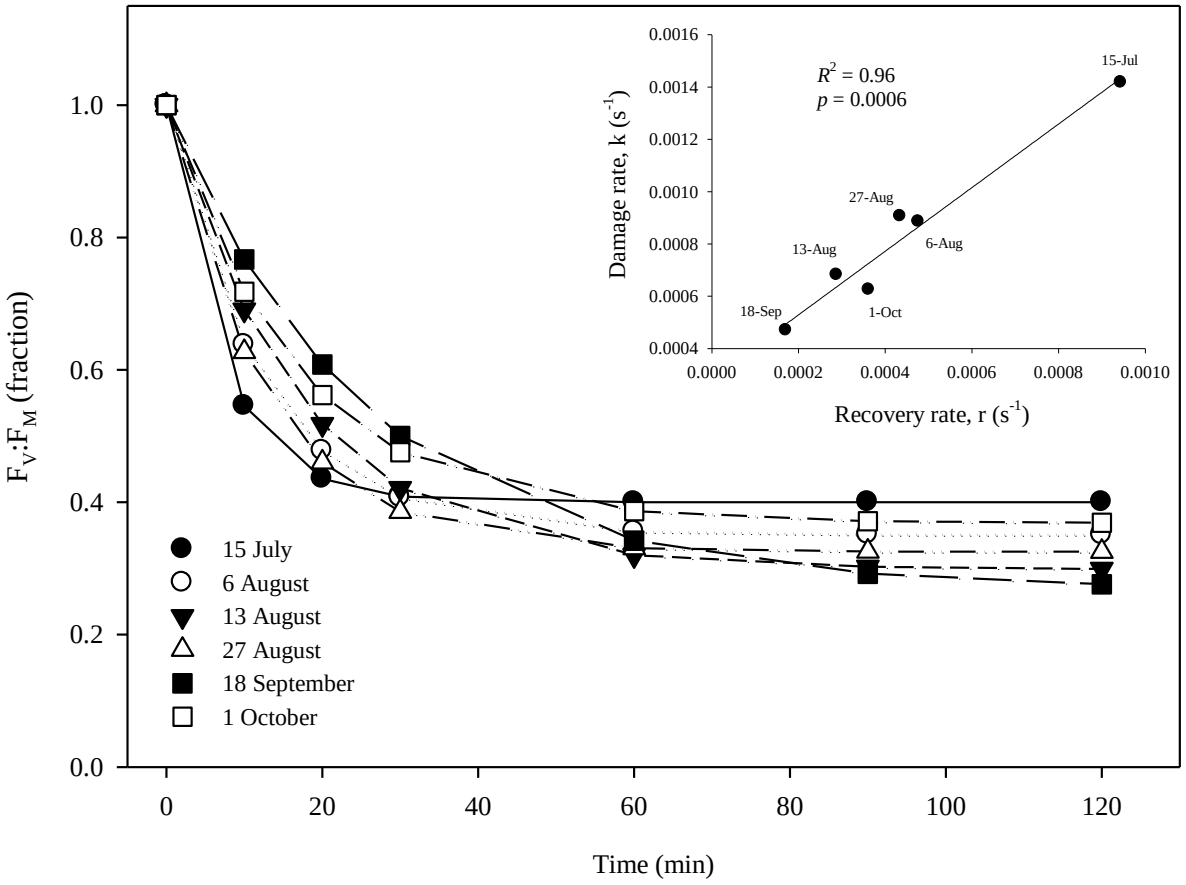

Figure 5.7. Predicted response of $F_V:F_M$ to a midday surface incident spectrum based on modeled recovery rates and damage rates from BWFs. Inset: the relationship between the predicted damage and recovery rates for each sampling date.

However, F_V:F_M was lower than the nominal maximum value for phytoplankton (~0.65–0.70) on most dates, even at 7:30 h, so it is possible that the slight depression of VF could have been related to the nutritional status of the phytoplankton. Alternatively, on some dates photoinhibition may already have occurred by 7:30 h, as the time of sunrise varied from 5:51 h on 15 July to 7:16 h on 1 October. Indeed, the highest early morning values of F_V:F_M (~0.70) were observed on 1 October, when

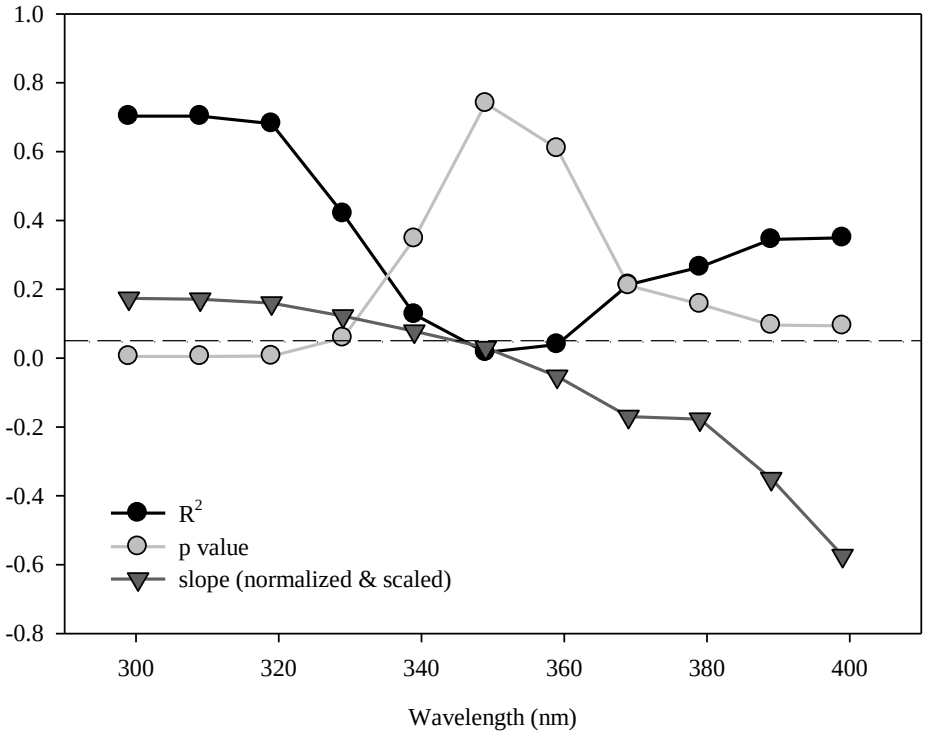

Figure 5.8. Results of 11 linear regression analyses (n = 6) performed using E_S as the independent variable and BWF coefficients as dependent variables ($\varepsilon_{K(299\ nm)}$, $\varepsilon_{K(309\ nm)}$, $\varepsilon_{K(319\ nm)}$, $\varepsilon_{K(329\ nm)}$, $\varepsilon_{K(339\ nm)}$, $\varepsilon_{K(349\ nm)}$, $\varepsilon_{K(359\ nm)}$, $\varepsilon_{K(369\ nm)}$, $\varepsilon_{K(379\ nm)}$, $\varepsilon_{K(389\ nm)}$, $\varepsilon_{K(399\ nm)}$) for 15 July – 1 October data. The slope from each analysis (*i.e.*, for each wavelength) was normalized by dividing it by the mean BWF coefficient for that wavelength, and then scaled (x20) for this figure. Wavelengths at which the grey circles are found below the dashed line had significant linear relationships between E_S and $\varepsilon_{K(\lambda)}$.

conditions were overcast, and the sun rose only minutes prior to the collection of the first samples used for PAM analysis. It is also possible that suboptimal F_V:F_M values measured in the early morning could partially have reflected residual photoinhibition from the preceding photoperiod, as has been previously documented (Villafañe *et al*. 2007). As the final set of *in situ* F_V:F_M data on each date were collected at 18:00 h in this study, it is unknown how complete the recovery of PSII function was on a given date in Lake Ontario prior to the end of the photoperiod; at the latitude of the study site, the sun sets at 20:57 h on 15 July and at 18:58 h on 1 October. Some recovery could also have taken place overnight, but dark recovery of Lake Ontario phytoplankton under laboratory conditions was found to be approximately an order of magnitude slower than under low PAR (data not shown), consistent with the data obtained for the phytoplankton communities from Blue Chalk and Plastic Lakes (see section 2.4.4).

The observed depth-dependent pattern in F_V:F_M, *i.e.*, lower values closer to the surface, is consistent with the role of UVR (and very high PAR PFDs) in promoting photoinhibition, and reflects the disproportionately high attenuation of the most harmful (short) UV wavelengths with depth in the water column, relative to the longer-wavelength UVAR, and PAR. The overestimation of photoinhibition near the surface of the lake and underestimation at depth by the BWF-Kok model as applied here likely reflects the admittedly unrealistic assumption of a static water column. This supposition is supported by the results of Villafañe *et al.* (2007), who used a PAM fluorometer to compare the PSII VF of actively-mixing freshwater phytoplankton assemblages with those incubated *in situ* at fixed depths; they observed that mixing mitigated photoinhibition at the lake's surface. Similarly, Oliver *et al.* (2003) found that freely-circulating samples had higher PSII VF than static samples near the surface, but lower values at depth. Here, the improved agreement between observed and predicted values of F_V:F_M for 0–10 m, compared to the systematic underestimation and overestimation of F_V:F_M in the near-surface waters and at depth, respectively, supports the idea that

results of the BWF-Kok model of photoinhibition would be improved if a mixing model was used to describe vertical motions and associated *in situ* irradiance variations. This entails a substantial effort, but future work will focus on the incorporation of such a mixing model (*e.g.* Patterson 1991) into the theoretical framework established here.

The question of ecological importance, which is not addressed by the study of Villafañe *et al.* (2007), is how the mixing regime affects photoinhibition integrated throughout the photoactive zone of the water column, as opposed to merely at the surface. Faster mixing within the photic zone has been shown to exacerbate water column photoinhibition in Antarctic phytoplankton (Neale *et al.* 1998*a*), and model scenarios of both slow and fast mixing (0.5 and 5 h cycle rates) were predicted to approximately double the integrated (0–10 m) photoinhibition in Lake Erie relative to static conditions (Hiriart-Baer & Smith 2005). However, rapid mixing of tropical, coastal phytoplankton caused UVAR to enhance rather than inhibit photosynthesis (Helbling *et al.* 2003). The net influence of the mixing regime on water-column effects of UVR depends in part on the efficiency of recovery processes. If recovery is absent and effects are a cumulative function of photon dose (*e.g.*, at extremely low temperature), fast mixing can increase photoinhibition by exposing a greater portion of the plankton to high near-surface UVR PFDs during a given period; however, if rates of recovery and damage are proportional, such that a steady-state is rapidly achieved, vertical mixing will have limited influence on the water column integrated effects of UVR (Neale *et al*. 2003). For a given *in situ* irradiance climate, the effect of mixing speed on UVR effects depends additionally on the mixing depth (Neale *et al*. 1998*a*; Oliver *et al.* 2003), because it is one determinant of the mean irradiance experienced by the plankton. In the present study, recovery was active and, under exposure to a midday solar spectrum, the predicted time required to reach a near-steady state was approximately 30 min on most dates (see Figure 5.7). The model did not consistently overestimate $DIPI_{(0–10\ m)}$, as would be expected if mixing alleviated photoinhibition integrated throughout the top 10 m of the

water column; nor did it consistently underestimate $DIPI_{(0–10\ m)}$, as would be expected if mixing enhanced water column photoinhibition. It is noteworthy that the highest recovery and damage rate constants (and therefore shortest time needed to establish a steady state under spectral exposure) were observed on 15 July, the date on which predicted and observed $DIPI_{(0–10\ m)}$ values showed the best agreement. The high rate constants on 15 July may reflect the high incident irradiance conditions that prevailed on that day.

The rate constants for recovery of PSII VF estimated for Lake Ontario phytoplankton using laboratory incubations in this study (1.72–9.45 x 10^{-4} s^{-1}) are comparable in range and magnitude to those reported by Oliver *et al.* (2003) for *in situ* populations of an Australian reservoir (0.7–9.1 x 10^{-4} s^{-1}). They are also comparable to those reported by Hiriart-Baer & Smith (2004) for carbon fixation by Lake Erie phytoplankton during May–August 1997 (0.14–7.96 x 10^{-4} s^{-1}), but less variable than recovery rates determined by Hiriart-Baer & Smith (2004) for Lake Erie during June–August 1998 (0.014–18.25 x 10^{-4} s^{-1}). The lack of recovery observed during the latter half of the photoperiod on 6 August in Lake Ontario is intriguing, as the 'U-shaped' diurnal pattern in PSII VF occurred on all other dates, and has been observed in many other aquatic systems (Behrenfeld *et al*. 1998; Oliver *et al*. 2003; Villafañe *et al*. 2007). It is possible that on 6 August the water at the study site that was sampled during 7:30–13:30 h was, *via* advection, replaced by a nearshore water mass later that day. If the shallow depth of such a water mass had resulted in more extreme photoinhibition earlier in the day, its transport to the location of the study site could have caused the low F_V:F_M ratios observed there at 15:00 h and 18:00 h. In their study of Lake Titicaca, Neale & Richerson (1987) observed a lack of afternoon recovery of PSII VF by near-surface populations subjected to lengthy exposure to high PFDs, whereas populations at the bottom of diurnal thermoclines exhibited rapid, complete recovery during the latter half of the photoperiod.

The extremely strong predictive relationship between TSR and $DIPI_{(0–10\ m)}$ suggests that, during the study period, incident solar radiation was the dominant factor controlling the among-date variability in inhibition of PSII at the study site in Lake Ontario. This finding is consistent with the study of Bouchard *et al.* (2005), who found incident irradiance (PAR) during the first half of the photoperiod to be a similarly strong predictor (R^2 = 0.99, n = 5) of the decrease in F_V:F_M (from 7:00 h to 13:00 h) among dates in the Antarctic. That surface-incident irradiance explained such a high proportion of the variation in DIPI is somewhat surprising, because the mean irradiance in a body of water is also a function of the spectral transparency of the water column. Water clarity at the study site in Lake Ontario showed considerable temporal variation in the UVA spectral region; for instance, on 6 August $KD_{380\ nm}$ was 0.75 m^{-1}, whereas on 13 August $KD_{380\ nm}$ was 0.34 m^{-1}. Consequently, the 1% irradiance depths for 380-nm irradiance differed considerably on 6 August and 13 August: 6.1 m *vs*. 13.5 m, respectively. Likewise, the mean 380-nm irradiance in the top 10 m of the water column was 13.3% *vs*. 28.4% of the immediately-subsurface PFD on 6 August and 13 August, respectively. Water temperature is another factor that can control the susceptibility of phytoplankton to photoinhibition of PSII, by slowing enzymatic repair of D1 protein (Bouchard *et al*. 2006), but, not surprisingly, epilimnetic temperature did not show extreme variability from 15 July to 1 October (range: 14–22°C, n = 6). Thus, it would not be expected to exert a strong influence on D1 repair rates, as is the case in extreme environments, such as the Antarctic (Neale 1988), and was not found to be a significant predictor (R^2 = 0.02; p = 0.79) of recovery rates in this study. An experiment conducted with winter phytoplankton assemblages from Lake Erie demonstrates the potential for temperature to exert an effect on the sensitivity of F_V:F_M to photoinhibition from UVAR but not UVBR (Figure C.1 of Appendix C).

The daily average total solar irradiance experienced by plankton sampled for laboratory experiments (E_S) was a significant predictor of the UVBR sensitivity of the assemblages, and a

nearly-significant predictor of the long-wavelength UVAR sensitivity of the assemblages. Interestingly, the predictive relationships were positive in the UVB spectral region and negative in the UVA. To explain this, I propose that two distinct mechanisms are responsible. The high sensitivity of phytoplankton to UVBR, following dates on which the *in situ* irradiance was high, suggests that residual physiological stress induced *in situ* may have increased the sensitivity of the communities to damage by UVBR when they were exposed to it the following day in the laboratory. By contrast, the decreased sensitivity to UVAR-induced damage, following days with high solar radiation, is suggestive of a short-term acclimation response, by which sensitivity to damage caused by UVAR is minimized. That phytoplankton should acclimate more effectively to UVAR than UVBR stress is consistent with the spectral nature of the acclimation accomplished by epilimnetic phytoplankton relative to metalimnetic communities (Chapter 2), and of clear-lake relative to humic-lake phytoplankton (Chapter 3). The physiological and ecological reasons why the PSII acclimation potential of lake phytoplankton should exhibit a spectral bias are fully considered in the concluding section of this thesis (Chapter 6).

Chapter 6: Synthesis, Conclusions, & Outlook

The foregoing chapters have described a number of experimental comparisons made among phytoplankton communities from different freshwater habitats. It was observed that metalimnetic phytoplankton were more susceptible to UVR-induced photoinhibition of PSII than epilimnetic phytoplankton from the same lakes (Chapter 2), that the UVR sensitivity of several epilimnetic communities was strongly influenced by water transparency (Chapter 3), and that sensitivity to PSII damage by UVR varies according to recent solar radiation at a single site (Chapter 5). Taken together, these results strongly suggest that prior irradiance conditions exert a strong influence on the sensitivity of the algal assemblages to PSII inactivation.

The data presented in this document do not provide strong support for the use of PSII VF as a diagnostic of nutrient stress in natural communities of phytoplankton. Some effects of nutrient status were observed (Chapter 4), but the results were somewhat equivocal, and the magnitude of the inferred effects quite small. If these putative effects were in fact genuine, the problem remains that any minor depression of $F_V:F_M$ related to phytoplankton nutrient stress must somehow be distinguished from the substantial variability in $F_V:F_M$ related to diurnal changes in solar radiation *in situ*. Night surveys could help circumvent the difficulties related to photoinhibition, but residual inhibition from the previous photoperiod could still be present, and the practical problems of conducting fieldwork at night are obvious. Collecting samples from depths at which photoinhibition is absent (or at least minimal) is another potential solution, but in many systems this depth would be near or within the metalimnion, where concentrations of soluble nutrients are typically much higher than in epilimnetic waters. I tentatively suggest that $F_V:F_M$ not be used to infer the nutritional status of natural phytoplankton assemblages. A more definitive answer could be provided by additional research which assesses the nutrient demand of phytoplankton in a more robust fashion, *i.e.*, using multiple indicators such as APA, C:N:P ratios, uptake assays, *etc*., while at the same time carefully

controlling for the influence of solar radiation and quantifying the influence of taxonomic variability on PSII variable fluorescence. Other fluorescence metrics obtained using PAM fluorometry, such as NPQ, appear to be more responsive to changes in nutrient availability (Figure 4.3), and may therefore have greater potential than F_V:F_M to serve as reliable indicators of phytoplankton nutrient status in lakes.

Based on the existing literature, the differences in UVR sensitivity that I observed among phytoplankton assemblages were not likely related to differences in community composition. Differential sensitivity to UVR among taxa has previously been reported (see Harrison & Smith 2009), as have shifts in community composition of natural communities under altered UVR exposure (Xenopoulos & Frost 2003). In the former case, apparent differences in UVR response among taxa depend partially on the physiological process being affected; for example, the quantum efficiency of PSII *vs*. C fixation (Andreasson & Wängberg 2006). Moreover, it is possible that subtle taxon-specific differences in UVR response were present but undetectable, because the differences in sensitivity related to light history were so great. The results presented here do not necessarily imply that UVR cannot act as a selective agent in structuring phytoplankton communities in lakes, in contradiction to previous studies. The overall fitness of the organisms is a function not strictly of PSII photochemical efficiency, but of other photosynthetic processes (Calvin Cycle, *etc*.) as well as metabolic functions related to growth, gene expression, and behaviour (*e.g.* motility). In nature, UVR also affects heterotrophic bacteria and zooplankton, leading to complex food-web interactions (Sommaruga 2003). The lack of variation in sensitivity to UVR-induced photoinhibition of PSII related to community composition reported here does not therefore imply that the net effect of UVR on the fitness of phytoplankton does not vary taxonomically.

The capacity for acclimation to UVR I have observed is consistent with results from laboratory experiments (Litchman & Neale 2005; Jiang & Qiu 2005) and previous studies conducted

with natural assemblages (Neale *et al.* 1998*b*; Xenopoulos & Schindler 2003), all of which suggest that high exposure of sufficient duration can effectively induce UVR resistance in phytoplankton. I did not assay for specific photoprotective pigments such as MAAs, but these compounds are known to be photo-inducible by UVR (Hannach & Sigleo 1998; Klisch & Häder 2000) and have been found in high concentrations in clear lakes, especially in near-surface waters (Laurion *et al.* 2002). An interesting pattern, found throughout this thesis, is the high degree of variability in the phytoplankton community response to UVAR; whether among strata (Figures 2.5, 2.6), among lakes (Figures 3.4, 3.5), or through time at the same site (Figure 4.7). By contrast, a striking lack of variation was observed in the response of the phytoplankton communities to UVBR (>300 nm). UVAR (*vs.* UVBR or PAR) is the dominant contributor to photoinhibition *in situ* (*e.g.*, Neale *et al.* 2001*b*; Hiriart-Baer & Smith 2004, 2005), so it is perhaps not surprising that natural phytoplankton assemblages should acclimate specifically to this waveband. UVAR is efficient in eliciting MAA synthesis (Roy 2000); however, the absorption maxima of the common MAAs range from 310–360 nm (Nakamura *et al.* 1982), whereas the strongest correlations between prior UVR exposure and changes in sensitivity to photodamage by UVAR were in the 360–399 nm range (*e.g.*, Table 3.3, Figure 5.8). The tolerance of the more resistant communities could reflect enhanced recovery efficiency in response to UVAR but not UVBR, because under full spectrum (>300 nm) exposure the D1 repair process is severely inhibited by UVBR (Bouchard *et al.* 2005, 2006). Sensitivity to photodamage was modeled in a spectrally-specific manner by weighting UVR with BWFs, but the recovery rate constants I determined were not spectrally-specific (*i.e.*, the model assumes that the same recovery rate constant applies under any irradiance conditions), so some uncertainty remains here. However, this explanation is consistent with the results of the experiments conducted with winter phytoplankton from Lake Erie. Incubation under >300-nm irradiance elicited comparable levels of PSII inhibition at cold (~5°C) and moderate (20°C) temperatures, whereas there was a distinct low-temperature effect

on F_V:F_M during UVAR+PAR exposure, in the absence of UVBR (Figure C.1). The recovery rates observed under cold and moderate temperatures differed largely under UVAR+PAR exposure (7.18 x 10^{-3} s^{-1} *vs.* 27.7 x 10^{-3} s^{-1}, respectively) but not under full spectrum (>300 nm) exposure (8.17 x 10^{-3} s^{-1} *vs.* 8.26 x 10^{-3} s^{-1}, respectively), suggesting that UVBR did in fact have a strong inhibitory effect on the recovery process. In Lake Ontario and in the Dorset Lakes, temperature did not have a significant effect on recovery rates, as may have been expected for an enzymatic process such as D1 re-synthesis (Bouchard *et al.* 2006); but this was likely due to the relatively narrow range of epilimnetic temperatures encountered in the datasets (14–22°C, excluding Appendix C).

I conclude that further changes in UVR exposure caused by climate change (DOC, stratification) or other factors (dreissenid mussels) are unlikely to have catastrophic consequences for PSII function of freshwater phytoplankton due to their apparent ability to readily acclimate. However, having only measured PSII VF, it remains unclear what the metabolic tradeoffs of the apparent acclimation are; nor is it clear how UVR is affecting downstream photosynthetic processes, nutrient uptake and assimilation, motility, FA profiles, *et cetera*.

This dissertation represents a substantial effort on my part, and fully addresses the proposed objectives. However, further questions can be answered with my dataset by taking the following additional steps: 1) analysis of F_Q':F_M' and RLC data from the Dorset Lakes, and from Lake Ontario (*in situ*), 2) quantify the spectral dependence of recovery of PSII by fitting the Kok model to the ERCs from individual spectral treatments, 3) using the thermistor data obtained in Fawn Lake, model the impact of micro-stratification on PSII inactivation *in situ*, 4) add a mixing model to the BWF-ERC model employed for Lake Ontario, and 5) use the aforementioned model to determine the relative contributions of different spectral regions to *in situ* photoinhibition of PSII, and to make predictions of PSII function under altered scenarios of mixing and transparency that are likely to result from impending climatic changes.

The research described in this dissertation was highly specific with regards to the physiological process that was studied. The efficiency of photochemistry at Photosystem II is but one of several aspects of phytoplankton physiology, and complimentary assessments of carbon fixation, oxygen evolution, cellular respiration, alkaline phosphatase expression, lipid peroxidation, changes in light-harvesting and photoprotective pigmentation, or even PSII variable fluorescence parameters obtained using FRRF, such as the functional absorption cross-section of PSII (σ_{PSII}), would have clearly led to more robust, general conclusions as to the effects of UVR on phytoplankton physiology in temperate lakes. However, the highly-focused experimental approach I employed, *i.e.*, the determination of PAM-fluorometry derived PSII VF as the sole indicator of UVR stress, was advantageous in several ways. The substantial breadth of this study—the number of phytoplankton communities that were examined, and how often they were examined—would have been impractical0 if various, more numerous physiological responses to UVR had been measured as part of each experimental protocol. Secondly, having used the PAM fluorometer exclusively (and frequently), I have complete confidence in the quality of the data generated by its use; superficial familiarity with the procedures for operation of laboratory equipment, or an inadequate appreciation of its underlying theory, can lead to datasets partially reflective of artefacts, rather than genuine eco-physiological processes or patterns.

At the time of my writing, Environment Canada has recently dismissed ~300 employees, and the future of the Canadian ozone and UVR monitoring program, which is a substantial contributor to the international database known as the World Ozone and Ultraviolet Radiation Data Centre (WOUDC), looks bleak (Schiermeier 2011). While the current political and economic climate casts a gloomy shadow over the future of UVR-research in Canada, an 'ozone hole' has just recently appeared for the first time in recorded history over the Arctic (Manney *et al.* 2011). Many research questions remain unanswered. There is clearly ample scope to augment the PSII VF results presented

here with data on various other aspects of phytoplankton physiology (nutrient uptake and assimilation, fatty acids, respiration, interactions with bacteria and zooplankton, *etc.*), by conducting complementary investigations along the same conceptual lines but with different physiological endpoints for UVR stress; an obvious next step would be to conduct the clear *vs.* humic lake comparison as I did, but measure susceptibility to UVR-induced photoinhibition of C fixation and growth rather than F_V:F_M. The UVR incubators ('incUVators') could also be used to answer ecological questions of a photobiological nature that are less closely related to the subject matter of this thesis. For instance, the effects of UVBR on interactions between bacteria and phytoplankton in humic lakes, with special attention to the role of UVR-induced bacterial mortality in liberating P stores for phytoplankton assimilation, and the role of UVR-induced excreted organic carbon from phytoplankton in supporting bacterial metabolism (Medina-Sánchez *et al.* 2006). Some uncertainty no doubt remains, but the direct effects of UVR on phytoplankton photosynthesis have at this time been studied rather exhaustively; it is my recommendation that future studies focus on the synergistic effects of UVR and other stressors (*e.g.*, increased temperature) on phytoplankton physiology, or on indirect effects of UVR on food-web interactions in lakes.

Bibliography

Allen, C.D. & Smith, R.E.H. 2002. The response of planktonic phosphate uptake and turnover to ultraviolet radiation in Lake Erie, *Canadian Journal of Fisheries and Aquatic Sciences*, 59: 778–786.

Alpert, P. & Kishcha, P. 2008. Quantification of the effect of urbanization on solar dimming. *Geophysical Research Letters*, **35**: L08801.

Anderson, J.M., Park, Y.-I., & Chow, W.S. 1997. Photoinactivation and photoprotection of photosystem II in nature. *Physiologia Plantarum*, **100**: 214–223.

Andreasson, K.I.M. & Wängberg, S.-Å. 2006. Biological weighting functions as a tool for evaluating two ways to measure UVB radiation inhibition on photosynthesis. *Journal of Photochemistry and Photobiology B: Biology*, **84**:111–118.

Aro, E.-M., Virgin, I. & Andersson, B. 1993. Photoinhibition of Photosystem II. Inactivation, protein damage and turnover. *Biochimica et Biophysica Acta*, **1143**: 113–134.

Arts, M.T. & Rai, H. 1997. Effects of ultraviolet radiation on the production of lipid, carbohydrate, and protein in three freshwater algal species. *Freshwater Biology*, **38**: 597–610.

Banaszak, A.T. 2003. Photoprotective physiology and biochemical responses of aquatic organisms. In: *UV Effects in Aquatic Organisms and Ecosystems* (Eds E.W. Helbling & H. Zagarese), pp. 329–358. Comprehensive Series in Photochemical & Photobiological Sciences, Vol. 1. The Royal Society of Chemistry, Cambridge.

Barbiero, R.P. & Tuchman, M.L. 2001. Results from the USEPA's biological open water surveillance program of the Laurentian Great Lakes: II. Deep chlorophyll maxima. *Journal of Great Lakes Research*, **27**:155–166.

Behrenfeld, M.J., Prasil, O., Kolber, Z.S., Babin, M. & Falkowski, P.G. 1998. Compensatory changes in Photosystem II electron turnover rates protect photosynthesis from photoinhibition. *Photosynthesis Research*, **58**: 259–268.

Binding, C.E., Jerome, J.H., Bukata, R.P. & Booty, W.G. 2007. Trends in water clarity of the Lower Great Lakes from remotely sensed aquatic color. *Journal of Great Lakes Research*, **33**: 828–841.

Bouchard, J.N., Roy, S., Ferreyra, G., Campbell, D.A. & Curtosi, A. 2005. Ultraviolet-B effects on Photosystem II efficiency of natural phytoplankton communities from Antarctica. *Polar Biology*, **28**: 607–618.

Bouchard, N.J., Roy, S. & Campbell, D.A. 2006. UVB effects on the photosystem II-D1 protein of phytoplankton and natural phytoplankton communities. *Photochemistry and Photobiology*, **82**: 936–951.

Bouchard, J.N., Longhi, M.L., Roy, S., Campbell, D.A. & Ferreyra, G. 2008. Interaction of nitrogen status and UVB sensitivity in a temperate phytoplankton assemblage. *Journal of Experimental Marine Biology and Ecology*, **359**:67–76.

Brown, B.E., Ambarsari, I., Warner, M.E., Fitt, W.K., Dunne, R.P., Gibb, S.W. & Cummings, D.G. 1999. Diurnal changes in photochemical efficiency and xanthophylls concentrations in shallow water reef corals: evidence for photoinhibition and photoprotection. *Coral Reefs*, **18**: 99–105.

Butler, W.L. & Kitajima, M. 1975. Fluorescence quenching in photosystem II of chloroplasts. *Biochimica et Biophysica Acta*, **376**:116–125.

Cabrera, S., López, M. & Tartarotti, B. 1997. Phytoplankton and zooplankton response to ultraviolet radiation in a high-altitude Andean lake: short- *versus* long-term effects. *Journal of Plankton Reseach*, **19**: 1565–1582.

Camacho, A. 2006. On the occurrence and ecological features of deep chlorophyll maxima (DCM) in Spanish stratified lakes. *Limnetica*, **25**: 453–478.

Campbell, D.A. & Tyystjarvi, E. 2011. Parameterization of photosystem II photoinactivation and repair. *Biochimica et Biophysica Acta*, **in press**, doi:10.1016/j.bbabio.2011.04.010

Carpenter, S.R. 1996. Microcosm experiments have limited relevance for community and ecosystem ecology. *Ecology*, **77**: 677–680.

Coutinho, R. & Zingmark, R. 1987. Diurnal photosynthetic responses to light by macroalgae. *Journal of Phycology*, **23**: 336–343.

Cullen, J.J. 1982. The deep chlorophyll maximum: comparing vertical profiles of chlorophyll a. *Canadian Journal of Fisheries and Aquatic Sciences*, **39:** 791–803.

Cullen, J.J., Neale, P.J. & Lesser, M.P. 1992. Biological weighting function for the inhibition of phytoplankton photosynthesis by ultraviolet radiation. *Science*, **258**: 646–650.

Cullen, J.J. & Neale, P.J. 1997. Biological weighting functions for describing the effects of ultraviolet radiation on aquatic systems. In: *The effects of ozone depletion on aquatic ecosystems* (Ed D.-P. Häder), pp. 97–118. Environmental Intelligence Unit. R. G. Landes, Georgetown.

De Lange, H.J. & Van Donk, E. 1997. Effects of UVB-irradiated algae on life history traits of *Daphnia pulex*. *Freshwater Biology*, **38*:*** 711–720.

De Lange, H.J. & Lürling, M. 2003. Effects of UV-B irradiated algae on zooplankton grazing. *Hydrobiologia*, **491**: 133–144.

De Lange, H.J. & Van Reeuwijk, P.L. 2003. Negative effects of UVB-irradiated phytoplankton on life history traits and fitness of *Daphnia magna*. *Freshwater Biology*, **48**: 678–686.

Dove, A. 2009. Long-term trends in major ions and nutrients in Lake Ontario. *Aquatic Ecosystem Health & Management*, **12**:281–295.

Drábková, M., Admiraal, W. & Maršálek, B. 2007*a*. Combined exposure to hydrogen peroxide and light–Selective effects on cyanobacteria, green algae, and diatoms. *Environmental Science & Technology*, **41**: 309–314.

Drábková, M., H. C. P. Matthijs, W. Admiraal, & B. Maršálek. 2007*b*. Selective effects of H_2O_2 on cyanobacterial photosynthesis. *Photosynthetica*, **45**: 363–369.

Fahnenstiel, G.L. & Scavia, D. 1987. Dynamics of Lake Michigan phytoplankton: the deep chlorophyll layer. *Journal of Great Lakes Research*, **13**: 285–295.

Falkowski, P.G. & Raven, J.A. 2007. *Aquatic Photosynthesis*. 2nd ed. Princeton University Press, Princeton, New Jersey.

Fee, E.J. 1976. The vertical and seasonal distribution of chlorophyll in lakes of the Experimental Lakes Area, northwestern Ontario: Implications for primary production estimates. *Limnology and Oceanography*, **21**: 767–783.

Fennel, K. & Boss, E. 2003. Subsurface maxima of phytoplankton and chlorophyll: Steady-state solutions from a simple model. *Limnology and Oceanography*, **48**: 1521–1534.

Ferreyra, G.A, Mostajir, B., Schloss, I.R., Chatila, K., Ferrario, M.E., Sargian, P., Roy, S., Prod'homme, J. & Demers, S. 2006. Ultraviolet-B radiation effects on the structure and function of lower trophic levels of the marine planktonic food web. *Photochemistry and Photobiology*, **82**: 887–897.

Field, C.B., Behrenfeld, M.J., Randerson, J.T. & Falkowski, P.G. 1998. Primary production of the biosphere: Integrating terrestrial and oceanic components. *Science*, **281:** 237–240.

Fuchs, E., Zimmerman, R.C. & Jaffe, J.S. 2002. The effect of elevated levels of phaeophytin in natural waters on variable fluorescence measured from phytoplankton. *Journal of Plankton Research*, **24**:1221–1229.

Furgal, J.A. & Smith, R.E.H. 1997. Ultraviolet radiation and photosynthesis by Georgian Bay phytoplankton of varying nutrient and photoadaptive status. *Canadian Journal of Fisheries and Aquatic Sciences*, **54**: 1659–1667.

Gao, K., Guan, W. & Helbling, E.W. 2007*a*. Effects of solar radiation on photosynthesis of the marine red tide alga *Heterosigma akashiwo* (Raphidophyceae). *Journal of Photochemistry and Photobiology B: Biology*, **86**: 140–148.

Gao, K., Wu, Y., Li, G., Wu, H., Villafañe, V.E. & Helbling, E.W. 2007*b*. Solar UV radiation drives CO_2 fixation in marine phytoplankton: a double edged sword. *Plant Physiology*, **144**: 54–59.

Garcia-Pichel, F. 1994. A model for internal self-shading in planktonic organisms and its implications for usefulness of ultraviolet sunscreens. *Limnology and Oceanography*, **39**: 1704–1717.

Goes, J.I., Handa, N., Taguchi, S. & Hama, T. 1994. Effects of UV-B radiation on the fatty acid composition of the marine phytoplankter *Tetraselmis* sp.: Relationship to cellular pigments. *Marine Ecology Progress Series*, **114**: 259–274.

Graziano, L.M., La Roche, J. & Geider, R.J. 1996. Physiological responses to phosphorus limitation in batch and steady-state cultures of *Dunaliella tertiolecta* (Chlorophyta): A unique stress protein as an indicator of phosphate deficiency. *Journal of Phycology*, **32**: 825–838.

Greer, D.H., Berry, J.A. & Björkman, O. 1986. Photoinhibition of photosynthesis in intact bean leaves: role of light and temperature, and requirement for chloroplast-protein synthesis during recovery. *Planta*, **168**: 253–260.

Grouneva, I., Jakob, T., Wilhelm, C. & Goss, R. 2008. A new multicomponent NPQ mechanism in the diatom *Cyclotella meneghiniana*. *Plant and Cell Physiology*, **49**: 1217–1225.

Grouneva, I., Jakob, T., Wilhelm, C. & Goss, R. 2009. The regulation of xanthophylls cycle activity and of non-photochemical fluorescence quenching by two alternative electron flows in the diatoms *Phaeodactylum tricornutum* and *Cyclotella meneghiniana*. *Biochimica et Biophysica Acta*, **1787**: 929–938.

Guan, W. & Gao, K. 2008. Light histories influence the impacts of solar ultraviolet radiation on photosynthesis and growth in a marine diatom, *Skeletonema costatum*. *Journal of Photochemistry and Photobiology B: Biology*, **91**:151–156.

Hannach, G. & Sigleo, A.C. 1998. Photoinduction of UV-absorbing compounds in six species of marine phytoplankton. *Marine Ecology Progress Series*, **174**: 207–222.

Harrison, J.W. & Smith, R.E.H. 2009. Effects of ultraviolet radiation on the productivity and composition of freshwater phytoplankton communities. *Photochemical & Photobiological Sciences*, **8**: 1218–1232.

Harrison, J.W. & Smith, R.E.H. 2011*a*. Deep chlorophyll maxima and UVR acclimation by epilimnetic phytoplankton. *Freshwater Biology*, **56**: 980–992.

Harrison, J.W. & Smith, R.E.H. 2011*b*. The spectral sensitivity of phytoplankton communities to ultraviolet radiation-induced photoinhibition differs among clear and humic temperate lakes. *Limnology & Oceanography*, **56**: 2115–2126.

Healey, F.P. & Hendzel, L.L. 1979*a*. Fluorometric measurement of alkaline phosphatase activity in algae. *Freshwater Biology*, **9**:429–439.

Healey, F.P. & Hendzel, L.L. 1979*b*. Indicators of phosphorus and nitrogen deficiency in five algae in culture. *Journal of the Fisheries Research Board of Canada*, **36**:1364–1369.

Healey, F.P. & Hendzel, L.L. 1980. Physiological indicators of nutrient deficiency in lake phytoplankton. *Canadian Journal of Fisheries and Aquatic Science*, **37**: 442–453.

Helbling, E.W., Villafañe, V.E., Buma, A.G.J., Andrade, M. & Zaratti, F. 2001. DNA damage and photosynthetic inhibition induced by solar ultraviolet radiation in tropical phytoplankton (Lake Titicaca, Bolivia). *European Journal of Phycology*, **36**: 157–166.

Helbling, E.W., Gao, K.S., Gonçalves, R.J., Wu, H.Y. & Villafañe, V.E. 2003. Utilization of solar radiation by coastal phytoplankton assemblages off SE China when exposed to fast mixing. *Marine Ecology Progress Series*, **259**: 59–66.

Helbling, E.W., Farías, M.E., Zenoff, M.V.F. & Villafañe, V.E. 2006. In situ responses of phytoplankton from the subtropical Lake Lake Angostura (Tucumán, Argentina) in relation to solar ultraviolet radiation exposure and mixing conditions. *Hydrobiologia*, **559**: 123–134.

Heraud, P. & Beardall, J. 2000. Changes in chlorophyll fluorescence during exposure of *Dunaliella tertiolecta* to UV radiation indicate a dynamic interaction between damage and repair processes. *Photosynthesis Research*, **63**: 123–134.

Heraud, P., Roberts, S., Shelly, K. & Beardall, J. 2005. Interactions between UV-B exposure and phosphorus nutrition. II. Effects on rates of damage and repair. *Journal of Phycology*, **41**: 1212–1218.

Hernando, M., Schloss, I., Roy, S. & Ferreyra, G. 2006. Photoacclimation to long-term ultraviolet radiation exposure of natural sub-Antarctic phytoplankton communities: Fixed surface incubations versus mixed mesocosms. *Photochemistry and Photobiology*, **82**: 923–935.

Hessen, D.O., De Lange, H.J. & Van Donk, E. 1997. UV-induced changes in phytoplankton cells and its effects on grazers. *Freshwater Biology*, **38**: 513–524.

Hiriart, V.P., Greenberg, B.M., Guildford, S.J. & Smith, R.E.H. 2002. Effects of ultraviolet radiation on rates and size distribution of primary production by Lake Erie phytoplankton. *Canadian Journal of Fisheries and Aquatic Science*, **59**: 317–328.

Hiriart-Baer, V.P. & Smith, R.E.H. 2004. Models for ultraviolet radiation–dependent photoinhibition of Lake Erie phytoplankton. *Limnology and Oceanography*, **49**: 202–214.

Hiriart-Baer, V.P., & Smith, R.E.H. 2005. The effect of ultraviolet radiation on freshwater planktonic primary production: The role of recovery and mixing processes. *Limnology & Oceanography*, **50**: 1352–1361.

Jennings, E., Järvinen, M., Allott, N., Arvola, L., Moore, K., Naden, P., Aonghusa, C.N., Nõges, T. & Weyhenmeyer, G.A. 2010. Impacts of climate change on the flux of dissolved organic carbon from catchments. In: *The Impact of Climate Change on European Lakes* (Ed D.G. George), pp. 199–221. Aquatic Ecology Series, Vol. 4, Springer, New York.

Jiang, H., & Qiu, B. 2005. Photosynthetic adaptation of a bloom-forming cyanobacterium *Microcystis aeruginosa* (Cyanophyceae) to prolonged UV-B exposure. *Journal of Phycology*, **41**: 983–992.

Kaczmarska, I., Clair, T.A., Ehrman, J.M., MacDonald, S.L., Lean, D. & Day, K.E. 2000. The effects of ultraviolet B on phytoplankton populations in clear and brown temperate Canadian lakes. *Limnology & Oceanography*, **45**: 651–663.

Kalff, J.2002. *Limnology: inland water ecosystems*. Prentice-Hall Inc., Upper Saddle River, New Jersey.

Keller, W., Paterson, A.M., Somers, K.A., Dillon, P.J., Heneberry, J. & Ford, A. (2008) Relationships between dissolved organic carbon concentrations, weather, and acidification in small Boreal Shield lakes. *Canadian Journal of Fisheries and Aquatic Sciences*, **65**: 786–795.

Kerr, J.B. & McElroy, C.T. 1993. Evidence for Large Upward Trends of Ultraviolet-B Radiation Linked to Ozone Depletion. *Science,* **262**: 1032–1034.

Kirk, J.T.O. 1983. Light and photosynthesis in aquatic ecosystems. Cambridge University Press, Cambridge.

Klisch, M. & Häder, D.-P. 2002. Wavelength dependence of mycosporine-like amino acid synthesis in *Gyrodinium dorsum*. *Journal of Photochemistry and Photobiology B: Biology*, **66**: 60–66.

Key, T., McCarthy, A., Campbell, D.A., Six, C., Roy, S. & Finkel, Z.V. 2010. Cell size trade-offs govern light exploitation strategies in marine phytoplankton. *Environmental Microbiology*, **12**: 95–104.

Köhler, J., M. Schmitt, H. Krumbeck, M. Kapfer, E. Litchman & Neale, P.J. 2001. Effects of UV on carbon assimilation of phytoplankton in a mixed water column. *Aquatic Sciences*, **63**: 294–309.

Kok, B. 1956. On the inhibition of photosynthesis by intense light. *Biochimica et Biophysica Acta*, **21**: 234–244.

Kolber, Z., Zehr, J. & Falkowski, P.G. 1988. Effects of growth irradiance and nitrogen limitation on photosynthetic energy conversion in Photosystem II. *Plant Physiology*, **88**:923–929.

Kolber, Z., Wyman, K.D. & Falkowski, P.G. 1990. Natural variability in photosynthetic energy conversion efficiency: A field study in the Gulf of Maine. *Limnology & Oceanography*, **35**: 72–79.

Korbee, N., Figueroa, F.L. & Aguilera, J. 2005. Effect of light quality on the accumulation of photosynthetic pigments, proteins and mycosporine-like amino acids in the red alga *Porphyra leucosticta* (Bangiales, Rhodophyta). *Journal of Photochemistry and Photobiology B: Biology*, **80**: 71–78.

Krause, G.H. & Weis, E. 1991. Chlorophyll fluorescence and photosynthesis: the basics. *Annual Review of Plant Physiology and Plant Molecular Biology*, **42**: 313–349.

Kromkamp, J. & Forster, R. 2003. The use of variable fluorescence measurements in aquatic ecosystems: differences between multiple and single turnover measuring protocols and suggested terminology. *European Journal of Phycology*, **38**:102–112.

Laurion, I., & Vincent, W.F. 1998. Cell size versus taxonomic composition as determinants of UV-sensitivity in natural phytoplankton communities. *Limnology & Oceanography*, **43**: 1774–1779.

Laurion, I., Lami, A. & Sommaruga, R. 2002. Distribution of mycosporine-like amino acids and photoprotective carotenoids among freshwater phytoplankton assemblages. *Aquatic Microbial Ecology*, **26**: 283–294.

Lean, D.R.S., Abbott, A.A. & Pick, F.R. 1987. Phosphorus deficiency of Lake Ontario plankton. *Canadian Journal of Fisheries and Aquatic Sciences*, **44**:2069–2076.

Lehman, J.T. 2002. Mixing patterns and plankton biomass of the St. Lawrence Great Lakes under climate change scenarios. *Journal of Great Lakes Research*, **28**: 583–596.

Leu, E., Færøvig, P. & Hessen, D.O. 2006. UV effects on stoichiometry and PUFAs of *Selenastrum capricornutum* and their consequences for the grazer *Daphnia magna*. *Freshwater Biology*, **51**: 229 6–2308.

Leu, E., Falk-Petersen, S. & Hessen, D.O. 2007. Ultraviolet radiation negatively affects growth but not food quality of arctic diatoms. *Limnology & Oceanography*, **52**: 787–797.

Liang, Y., Beardall, J. & Heraud, P. 2006. Effects of nitrogen source and UV radiation on the growth, chlorophyll fluorescence and fatty acid composition of *Phaeodactylum tricornutum* and *Chaetoceros muelleri* (Bacillariophyceae). *Journal of Photochemistry and Photobiology, B: Biology*, **82**: 161–172.

Liley, J.B. 2009. New Zealand dimming and brightening. *Journal of Geophysical Research*, **114**:D00D10.

Litchman, E., Neale, P.J. & Banaszak, A.T. 2002. Increased sensitivity to ultraviolet radiation in nitrogen-limited dinoflagellates: Photoprotection and repair. *Limnology & Oceanography*, **47**:86–94.

Litchman, E., & Neale, P.J. 2005. UV effects on photosynthesis, growth and acclimation of an estuarine diatom and cryptomonad. *Marine Ecology Progress Series*, **300**: 53–62.

Long, S.P., Humphries, S. & Falkowski, P.G. 1994. Photoinhibition of photosynthesis in nature. *Annual Review of Plant Physiology and Plant Molecular Biology*, **45**: 633–662.

Manney, G.L. & 28 others. 2011. Unprecedented Arctic ozone loss in 2011. *Nature*, doi: 10.1038/nature10556

Marwood, C.A., Smith, R.E.H., Solomon, K.R., Charlton, M.N. & Greenberg, B.M. 1999. Intact and photomodified polycyclic aromatic hydrocarbons inhibit photosynthesis in natural assemblages of Lake Erie phytoplankton exposed to solar radiation. *Ecotoxicology and Environmental Safety*, **44**:322–327.

McKenzie, R.L., Aucamp, P.J., Bais, A.F., Björn, L.O., Ilyas, M. & Madronich, S. 2011. Ozone depletion and climate change: impacts on UV radiation. *Photochemical & Photobiological Sciences*, **10**: 182–198.

McCormick, M.J. & Fahnenstiel, G.L. 1999. Recent climatic trends in nearshore water temperatures in the St. Lawrence Great Lakes. *Limnology & Oceanography*, **44**: 530–540.

Medina-Sánchez, J.M., Villar-Argaiz, M. & Carrillo, P. 2006. Solar radiation–nutrient interaction enhances the resource and predation algal control on bacterioplankton: A short-term experimental study. *Limnology & Oceanography*, **51**: 913–924.

Millard, E.S., Myles, D.D., Johannsson, O.E. & Ralph, K.M. 1996. Seasonal phosphorus deficiency of Lake Ontario phytoplankton at two index stations: light versus phosphorus limitation of growth. *Canadian Journal of Fisheries and Aquatic Sciences*, **53**:1112–1124.

Miloslavina, Y., Grouneva, I., Lambrev, P.H., Lepetit, B., Goss, R., Wilhelm, C. & Holzwarth, A.R. 2009. Ultrafast fluorescence study on the location and mechanism of non-photochemical quenching in diatoms. *Biochimica et Biophysica Acta*, **1787**: 1189–1197.

Milot-Roy, V. & Vincent, W.F. 1994. UV radiation effects on photosynthesis: The importance of near-surface thermoclines in a subarctic lake. *Archiv für Hydrobiologie–Beiheft Ergebnisse der Limnologie*. **43**: 171–184.

Moeller, R.E. 1994. Contribution of ultraviolet radiation (UV-A, UV-B) to photoinhibition of epilimnetic phytoplankton in lakes of differing UV transparency. *Archiv für Hydrobiologie–Beiheft Ergebnisse der Limnologie*. **43**: 157–170.

Molina, M.J. & Rowland, F.S. 1974. Stratospheric sink for chlorofluoromethanes: chlorine atomc-atalysed [*sic*] destruction of ozone. *Nature*, **249**: 810–812.

Moore, C.M., Mills, M.M., Langlois, R., Milne, A., Achterberg, E.P., La Roche, J. & Geider, R.J. 2008. Relative influence of nitrogen and phosphorus availability on phytoplankton physiology and productivity in the oligotrophic sub-tropical North Atlantic Ocean. *Limnology & Oceanography*, **53**: 291–305.

Morris, D.P., Zagarese, H., Williamson, C.E., Balseiro, E.G., Hargreaves, B.R., Modenutti, B., Moeller, R. & Queimalinos, C. 1995. The attenuation of solar UV radiation in lakes and the role of dissolved organic carbon. *Limnology and Oceanography*, **40**: 1381–1391.

Morris, D.P. & Hargreaves, B.R. 1997. The role of photochemical degradation of dissolved organic carbon in regulating the UV transparency of three lakes on the Pocono Plateau. *Limnology & Oceanography*, **42**: 239–249.

Mousseau, L., Gosselin, M., Levasseur, M., Demers, S., Fauchot, J., Roy, S., Villegas, P.Z., & Mostajir, B. 2000. Effects of ultraviolet-B radiation on simultaneous carbon and nitrogen transport rates by estuarine phytoplankton during a week-long mesocosm study. *Marine Ecology Progress Series*, **199**: 69–81.

Murphy, T.M. 1983. Membranes as targets of ultraviolet radiation. *Physiologica Plantarum*, **58**: 381–388.

Nakamura, H., Kobayashi, J. & Hirata, Y. 1982. Separation of mycosporine-like amino acids in marine organisms using reversed-phase high-performance liquid chromatography. *Journal of Chromatography*, **250**: 113–118.

Neale, P.J. & Richerson, P.J. 1987. Photoinhibition and the diurnal variation of phytoplankton photosynthesis – I. Development of a photosynthesis-irradiance model from studies of *in situ* responses. *Journal of Plankton Research*, **9**: 167–193.

Neale, P.J., Davis, R.F. & Cullen, J.J. 1998*a*. Interactive effects of ozone depletion and vertical mixing on photosynthesis of Antarctic phytoplankton. *Nature*, **392**: 585–589.

Neale, P.J., Cullen, J.J., & Davis, R.F. 1998*b*. Inhibition of marine photosynthesis by ultraviolet radiation: Variable sensitivity of phytoplankton in the Weddell-Scotia Confluence during the austral spring. *Limnology and Oceanography*, **43**: 433–448.

Neale, P.J., Fritz, J.J. & Davis, R.F. 2001*a*. Effects of UV on photosynthesis of Antarctic phytoplankton: models and their application to coastal and pelagic assemblages. *Revista Chilena de Historia Natural*, **74**: 283–292.

Neale, P.J., Litchman, E., Sobrino, C., Callieri, C., Morabito, G., Montecino, V., Huot, Y., Bossard, P., Lehmann, C. & Steiner, D. 2001*b*. Quantifying the response of phytoplankton photosynthesis to ultraviolet radiation: Biological weighting functions versus in situ measurements in two Swiss lakes. *Aquatic Sciences*, **63:** 265–285.

Neale, P.J., Helbling, E.W. & Zagarese, H.E. 2003. Modulation of UVR exposure and effects by vertical mixing and advection. In: *UV Effects in Aquatic Organisms and Ecosystems* (Eds E.W. Helbling & H. Zagarese), pp. 107–134. Comprehensive Series in Photochemical & Photobiological Sciences, Vol. 1. The Royal Society of Chemistry, Cambridge.

Nicholls, K.H., Hopkins, G.J., Standke, S.J. & Nakamoto, L. 2001. Trends in total phosphorus in Canadian near-shore waters of the Laurentian Great Lakes: 1976–1999. *Journal of Great Lakes Research*, **27**: 402–422.

Nilawati, J., Greenberg, B.M. & Smith, R.E.H. 1997. Influence of ultraviolet radiation on growth and photosynthesis of two cold ocean diatoms. *Journal of Phycology*, **33**: 215–224.

Nürnberg, G.K. & Shaw, M. 1999. Productivity of clear and humic lakes: nutrients, phytoplankton, bacteria. *Hydrobiologia*, **382**:97–112.

Ohvril, H., Teral, H., Neiman, L., Kannel, M., Uustare, M., Tee, M., Russak, V., Okulov, O., Joeveer, A., Kallis, A., Ohvril, T., Terez, E.I., Terez, G.A., Gushchin, G.K., Abakumova, G.M., Gorbarenko, E.V., Tsvetkov, A.V. & Laulainen, N. 2009. Global dimming and brightening *versus* atmospheric column transparency, Europe, 1906–2007. *Journal of Geophysical Research*, **114**: D00D12.

Oliver, R.L., Whittington, J., Lorenz, Z. & Webster, I.T. 2003. The influence of vertical mixing on the photoinhibition of variable chlorophyll *a* fluorescence and its inclusion in a model of phytoplankton photosynthesis. *Journal of Plankton Research*, **25**: 1107–1129.

Parkhill, J.P., Maillet, G. & Cullen, J.J. 2001. Fluorescence-based maximal quantum yield for PSII as a diagnostic of nutrient stress. *Journal of Phycology*, **37**: 517–529.

Parsons, T.R. & Strickland, J.D.H. 1963. Discussion of spectrophotometric determination of marine-plant pigments, with revised equations for ascertaining chlorophylls and carotenoids. *Journal of Marine Research*, **21**: 155–163.

Patterson, J.C. 1991. Modelling the effects of motion on primary production in the mixed layer of lakes. *Aquatic Sciences*, **53**: 218–238.

Pfennig, N. 1989. Ecology of Phototrophic Purple and Green Sulfur Bacteria. In: *Autotrophic Bacteria* (Eds H.G. Schlegel & B. Bowien), pp. 97–116. Springer-Verlag, New York.

Pick, F.R., Nalewajko, C. & Lean, D.R.S. 1984a. The origin of a metalimnetic chrysophyte peak. *Limnology and Oceanography*, **29**: 125–134.

Pienitz, R. & Vincent, W.F. 2001. Effect of climate change relative to ozone depletion on UV exposure in subarctic lakes. *Nature*, **404**: 484–487.

Platt, T. & Jassby, A.D. 1976. The relationship between photosynthesis and light for natural assemblages of coastal marine phytoplankton. *Journal of Phycology*, **12:**421–30.

Platt, T., Harrison, W.G., Irwin, B., Horne, E.P. & Gallegos, C.L. 1982. Photosynthesis and photoadaptation of marine phytoplankton in the Arctic. *Deep-Sea Research*, **29**:1159–1179.

Raateoja, M., Seppälä, J., & Ylöstalo, P. 2004. Fast repetition rate fluorometry is not applicable to studies of filamentous cyanobacteria from the Baltic Sea. *Limnology & Oceanography*, **49**:1006–1012.

Rattan, K.J. 2009. Traditional and new fluorometric methods to determine phytoplankton nutrient status for freshwater ecosystems. Ph.D. dissertation, University of Waterloo, Waterloo, 187 pp.

Rattan, K.J., Taylor, W.D. & Smith, R.E.H. Nutrient status of phytoplankton in an oligo-mesotrophic lake (Lake Erie): Evidence from new fluorescence methods. *Canadian Journal of Fisheries and Aquatic Sciences*, in press.

Roy, S. 2000. Strategies for the minimisation of UV-induced damage. In: *The effects of UV radiation in the marine environment* (Eds S. de Mora, S. Demers & M. Vernet), pp. 177–205. Cambridge Environmental Chemistry Series, Vol. 10. Cambridge University Press, Cambridge.

Sagert, S., Forster, R. M., Feuerpfeil, P. & Schubert, H. 1997. Daily course of photosynthesis and photoinhibition in *Chondrus crispus* (Rhodophyta) from different shore levels. *European Journal of Phycology*, **32**: 363–371.

Saros, J.E., Interlandi, S.J., Doyle, S., Michel, T.J. and Williamson, C.E. 2005. Are the deep chlorophyll maxima in alpine lakes primarily induced by nutrient availability, not UV avoidance? *Arctic, Antarctic, and Alpine Research*, **37**: 557–563.

Schiermeier, Q. 2011. Canadian ozone network faces axe. *Nature*, **477**: 257–258.

Schindler, D.W., Curtis, P.J., Parker, B.R. & Stainton, M.P. 1996. Consequences of climate warming and lake acidification for UV-B penetration in North American boreal lakes. *Nature*, **379**: 705–708.

Schreiber, U. 1986*a*. Detection of rapid induction kinetics with a new type of high frequency modulated chlorophyll fluorometer. *Photosynthesis Research*, **9**: 261–272.

Schreiber, U., Schliwa, U. & Bilger, W. 1986*b*. Continuous recording of photochemical and non-photochemical chlorophyll fluorescence quenching with a new type of modulation fluorometer. *Photosynthesis Research*, **10**: 51–62.

Scott, J.D., Chalker-Scott, L., Foreman, A.E. & D'Angelo, M. 1999. *Daphnia pulex* fed UVB-irradiated *Chlamydomonas reinhardtii* show decreased survival and fecundity. *Photochemistry and Photobiology*, **70**: 308–313.

Scully, N.M., McQueen, D.J. & Lean, D.R.S. 1996. Hydrogen peroxide formation: The interaction of ultraviolet radiation and dissolved organic carbon in lake waters along a 43–75°N gradient. *Limnology & Oceanography*, **41**: 540–548.

Sereda, J.M., Hudson, J.J. & Taylor, W.D. 2009. Abiotic effects of UV on planktonic P kinetics. *Aquatic Sciences*, **71**:127–134.

Shelly, K., Heraud, P. & Beardall, J. 2002. Nitrogen limitation in *Dunaliella tertiolecta* (Chlorophyceae) leads to increased susceptibility to damage by ultraviolet-B radiation but also increased repair capacity. *Journal of Phycology*, **38**:713–720.

Shelly, K., Roberts, S., Heraud, P. & Beardall, J. 2005. Interactions between UV-B exposure and phosphorus nutrition. I. Effects on growth, phosphate uptake, and chlorophyll fluorescence. *Journal of Phycology*, **41**: 1204–1211.

Sinha, R. P. & Häder, D.-P. 2002. UV-induced DNA damage and repair: a review. *Photochemical & Photobiological Sciences*, **1**: 225–236.

Six, C., Sherrard, R., Lionard, M., Roy, S. & Campbell, D.A. 2009. Photosystem II and pigment dynamics among ecotypes of the green alga *Ostreococcus*. *Plant Physiology*, **151**: 379–390.

Smith, R.E.H., Allen, C.D. & Charlton, M.N. 2004. Dissolved organic matter and ultraviolet radiation penetration in the Laurentian Great Lakes and tributary waters. *Journal of Great Lakes Research*, **30**: 367–380.

Sobrino, C., Montero, O. & Lubián, L.M. 2004. UV-B radiation increases cell permeability and damages nitrogen incorporation mechanisms in *Nannochloropsis gaditana*. *Aquatic Sciences*, **66**: 421–429.

Sobrino, C., Neale, P.J., Montero, O. & Lubián, L.M. 2005. Biological weighting function for xanthophylls de-epoxidation induced by ultraviolet radiation. *Physiologia Plantarum*, **125**: 41–51.

Sobrino, C., Ward, M.L. & Neale, P.J. 2008. Acclimation to elevated carbon dioxide and ultraviolet radiation in the diatom *Thalassiosira pseudonana*: Effects on growth, photosynthesis, and spectral sensitivity of photoinhibition. *Limnology and Oceanography*, **53**: 494–505.

Sommaruga, R. 2003. UVR and its effects on species interactions. In: *UV Effects in Aquatic Organisms and Ecosystems* (Eds E.W. Helbling & H. Zagarese), pp. 485–508. Comprehensive Series in Photochemical & Photobiological Sciences, Vol. 1. The Royal Society of Chemistry, Cambridge.

Stainton, M.P., Capel, M.J. & Armstrong, F.A.J. 1977. *The Chemical Analysis of Fresh Water*. Fisheries and Marine Service Special Publication, 25. Department of Fisheries and Oceans, Winnipeg.

Sterner, R.W. 1990. Lake morphometry and light in the surface layer. *Canadian Journal of Fisheries and Aquatic Sciences*, **47**: 687–692.

Sterner, R.W., Anderson, T., Elser, J.J., Hessen, D.O., Hood, J.M., McCauley, E. & Urabe, J. 2008. Scale-dependent carbon: nitrogen: phosphorus seston stoichiometry in marine and freshwaters. *Limnology and Oceanography*, **53**: 1169–1180.

Stockner, J. G., Callieri, C. & Cronberg, G. 2000. Picoplankton and other non-bloom-forming cyanobacteria in lakes. In: *The Ecology of Cyanobacteria* (Eds B.A. Whitton & M. Potts), pp. 195–231. Kluwer Academic Publishers, Dordrecht, the Netherlands.

Sommaruga, R. 2003. UVR and its effects on species interactions. In: *UV Effects in Aquatic Organisms and Ecosystems* (Eds E.W. Helbling & H. Zagarese), pp. 485–508. Comprehensive Series in Photochemical & Photobiological Sciences, Vol. 1. The Royal Society of Chemistry, Cambridge.

Strid, Å., Chow, W.S. & Anderson, J.M. 1994. UV-B damage and protection at the molecular level in plants. *Photosynthesis Research*, **39**: 475–489.

Suggett, D.J., Moore, C.M., Hickman, A.E. & Geider, R.J. 2009. Interpretation of fast repetition rate (FRR) fluorescence: signatures of phytoplankton community structure versus physiological state. *Marine Ecology Progress Series*, **376**:1–19.

Sylvan, J.B., Quigg, A., Tozzi, S., & Ammerman, J.W. 2007. Eutrophication-induced phosphorus limitation in the Mississippi River plume: evidence from fast repetition rate fluorometry. *Limnology and Oceanography*, **52:** 2679–2685.

Tank, S.E., Schindler, D.W. & Arts, M.T. 2003. Direct and indirect effects of UV radiation on benthic communities: epilithic food quality and invertebrate growth in four montane lakes. *Oikos*, **103**: 651–667.

Tilzer, M.M. 1973. Diurnal periodicity in the phytoplankton assemblage of a high mountain lake. *Limnology & Oceanography*, **18**: 15–30.

Umena, Y., Kawakami, K., Shen, J.-R. & Kamiya, N. 2011. Crystal structure of oxygen-evolving photosystem II at a resolution of 1.9 Å. *Nature*, **473**: 55–60.

Van de Poll, W.H., Alderkamp, A.-C., Janknegt, P.J., Roggeveld, J. & Buma, A.G.J. 2006. Photoacclimation modulates excessive photosynthetically active and ultraviolet radiation effects in a temperate and an Antarctic marine diatom. *Limnology & Oceanography*, **51**: 1239–1248.

Van de Poll, W.H., Visser, R.J.W. & Buma, A.G.J. 2007. Acclimation to a dynamic irradiance regime changes excessive irradiance sensitivity of *Emiliania huxleyi* and *Thalassiosira weissflogii*. *Limnology & Oceanography*, **52**: 1430–1438.

Van Donk, E., Faafeng, B.A., De Lange, H.J. & Hessen, D.O. 2001. Differential sensitivity to natural ultraviolet radiation among phytoplankton species in Arctic lakes (Spitsbergen, Norway). *Plant Ecology*, **154**: 247–259.

Van Leeuwe, M.A., Van Sikkelerus, B., Gieskes, W.W.C. & Stefels, J. 2005. Taxon-specific differences in photoacclimation to fluctuating irradiance in an Antarctic diatom and a green flagellate. *Marine Ecology Progress Series*, **288**: 9–19.

Villafañe, V.E., Andrade, M., Lairana, V., Zaratti, F. & Helbling, E.W. 1999. Inhibition of phytoplankton photosynthesis by solar ultraviolet radiation: studies in Lake Titicaca, Bolivia. *Freshwater Biology*, **42**: 215–224.

Villafañe, V.E., Sundbäck, K., Figueroa, F.L. & Helbling, E.W. 2003. Photosynthesis in the aquatic environment as affected by UVR. In: *UV Effects in Aquatic Organisms and Ecosystems* (Eds E.W. Helbling & H. Zagarese), pp. 357–398. Comprehensive Series in Photochemical & Photobiological Sciences, Vol. 1. The Royal Society of Chemistry, Cambridge.

Villafañe, V.E., Buma, A.G.J., Boelen, P. & Helbling, E.W. 2004. Solar UVR-induced DNA damage and inhibition of photosynthesis in phytoplankton from Andean lakes of Argentina. *Archiv für Hydrobiologie*, **161**: 245–266.

Villafañe, V.E., Gao, K., Li, P., Li, G. & Helbling, E.W. 2007. Vertical mixing within the epilimnion modulates UVR-induced photoinhibition in tropical freshwater phytoplankton from southern China. *Freshwater Biology*, **52**: 1260–1270.

Visser, P.M., Poos, J.J., Scheper, B.B., Boelen, P. & Van Duyl, F.C. 2002. Diurnal variation in depth profiles of UV-induced DNA damage and inhibition of bacterioplankton production in tropical coastal waters. *Marine Ecology Progress Series*, **228**: 25–33.

Wang, K.S. & Chai, T. 1994. Reduction in omega-3 fatty acids by UV-B irradiation in microalgae. *Journal of Applied Phycology*, **6**: 415–421.

Watkins, E.M., Schindler, D.W., Turner, M.A. & Findlay, D. 2001. Effects of solar ultraviolet radiation on epilithic metabolism, and nutrient and community composition in a clear-water boreal lake. *Canadian Journal of Fisheries and Aquatic Sciences*, **58**: 2059–2070.

West, L.J.A., Greenberg, B.M. & Smith, R.E.H. 1999. Ultraviolet radiation effects on a microscopic green alga and the protective effects of natural dissolved organic matter. *Photochemistry and Photobiology*, **69**: 536–544.

Wilhelm, S.W. & Smith, R.E.H. 2000. Bacterial carbon production in Lake Erie is influenced by viruses and solar radiation. *Canadian Journal of Fisheries and Aquatic Sciences*, **57**: 317–326.

Wilhelm, S.W., Bullerjahn, G.S., Eldridge, M.L., Rinta-Kanto, J.M., Poorvin, L. & Bourbonniere, R.A. 2006. Seasonal hypoxia and the genetic diversity of prokaryote populations in the central basin of Lake Erie: evidence for abundant cyanobacteria and photosynthesis. *Journal of Great Lakes Research*, **32**: 657–671.

Williamson, C.E., Stemberger, R.S., Morris, D.P., Frost, T.M. & Paulsen, S.G. 1996. Ultraviolet radiation in North American lakes: Attenuation estimates from DOC measurements and implications for plankton communities. *Limnology & Oceanography*, **41**: 1024–1034.

Williamson, C.E., Salm, C., Cooke, S.L. & Saros, J.E. 2010. How do UV radiation, temperature, and zooplankton influence the dynamics of alpine phytoplankton communities? *Hydrobiologia*, **648**: 73–81.

Wulff, A., Mohlin, M. & Sundbäck, K. 2007. Intraspecific variation in the response of the cyanobacterium *Nodularia spumigena* to moderate UV-B radiation. *Harmful Algae*, **6:** 388–399.

Xenopoulos, M.A., Frost, P.C. & Elser, J.J. 2002. Joint effects of UV radiation and phosphorus supply on algal growth rate and elemental composition. *Ecology*, **83**:423–435.

Xenopoulos, M.A. & Frost, P.C. 2003. UV radiation, phosphorus, and their combined effects on the taxonomic composition of phytoplankton in a boreal lake. *Journal of Phycology*, **39**: 291–302.

Xenopoulos, M.A. & Schindler, D.W. 2003. Differential responses to UVR by bacterioplankton and phytoplankton from the surface and the base of the mixed layer. *Freshwater Biology*, **48**: 108–122.

Xenopoulos, M.A., Leavitt, P.R. & Schindler, D.W. 2009. Ecosystem-level regulation of boreal lake phytoplankton by ultraviolet radiation. *Canadian Journal of Fisheries and Aquatic Sciences*, **66**: 2002–2010.

Yan, N.D., Keller, W., Scully, N.M., Lean, D.R.S. & Dillon, P.J. 1996. Increased UV-B penetration in a lake owing to drought-induced acidification. *Nature*, **381**: 141–143.

Zhang, J., Hudson, J., Neal, R., Sereda, J., Clair, T., Turner, M., Jeffries, D., Dillon, P., Molot, L., Somers, K. & Hesslein, R. 2010. Long-term patterns of dissolved organic carbon in lakes across eastern Canada: Evidence of a pronounced climate effect. *Limnology & Oceanography*, **55**: 30–42.

Appendix A:

Complete PSII variable fluorescence data for Lake Ontario

Table A.1. All recorded fluorescence parameters of Lake Ontario phytoplankton at the study site on 15 July 2008.

Time (h)	Depth (m)	$F_V:F_M$	$F_Q':F_M'$	$rETR_{max}$	E_K	α
7:30	0	0.451	0.268	67	277	0.24
	1	0.447	0.296	-	-	-
	2.5	0.487	0.303	-	-	-
	5	0.498	0.308	63	242	0.26
	7.5	0.511	0.286	-	-	-
	10	0.548	0.311	67	293	0.23
9:30	0	0.381	0.223	46	255	0.18
	1	0.304	0.218	-	-	-
	2.5	0.374	0.294	-	-	-
	5	0.452	0.265	55	230	0.24
	7.5	0.471	0.274	-	-	-
	10	0.448	0.257	41	147	0.28
11:30	0	0.313	0.243	54	282	0.19
	1	0.316	0.228	-	-	-
	2.5	0.367	0.243	-	-	-
	5	0.417	0.305	53	251	0.21
	7.5	0.472	0.308	-	-	-
	10	0.449	0.334	76	360	0.21
13:30	0	0.219	0.149	33	328	0.10
	1	0.212	0.136	-	-	-
	2.5	0.293	0.200	-	-	-
	5	0.396	0.228	53	251	0.21
	7.5	0.465	0.281	-	-	-
	10	0.473	0.292	61	234	0.26
15:00	0	0.172	0.117	24	214	0.11
	1	0.174	0.124	-	-	-
	2.5	0.261	0.165	-	-	-
	5	0.336	0.185	38	200	0.19
	7.5	0.447	0.230	-	-	-
	10	0.443	0.231	45	186	0.24
18:00	0	0.205	-	-	-	-
	1	0.256	-	-	-	-
	2.5	0.257	-	-	-	-
	5	0.324	-	-	-	-
	7.5	0.478	-	-	-	-
	10	0.465	-	-	-	-

Table A.2. All recorded fluorescence parameters of Lake Ontario phytoplankton at the study site on 06 August 2008.

Time (h)	Depth (m)	$F_V:F_M$	$F_Q':F_M'$	$rETR_{max}$	E_K	α
7:30	0	0.451	0.268	67	277	0.24
	1	0.447	0.296	-	-	-
	2.5	0.487	0.303	-	-	-
	5	0.498	0.308	63	242	0.26
	7.5	0.511	0.286	-	-	-
	10	0.548	0.311	67	293	0.23
9:30	0	0.381	0.223	46	255	0.18
	1	0.304	0.218	-	-	-
	2.5	0.374	0.294	-	-	-
	5	0.452	0.265	55	230	0.24
	7.5	0.471	0.274	-	-	-
	10	0.448	0.257	41	147	0.28
11:30	0	0.313	0.243	54	282	0.19
	1	0.316	0.228	-	-	-
	2.5	0.367	0.243	-	-	-
	5	0.417	0.305	53	251	0.21
	7.5	0.472	0.308	-	-	-
	10	0.449	0.334	76	360	0.21
13:30	0	0.219	0.149	33	328	0.10
	1	0.212	0.136	-	-	-
	2.5	0.293	0.200	-	-	-
	5	0.396	0.228	53	251	0.21
	7.5	0.465	0.281	-	-	-
	10	0.473	0.292	61	234	0.26
15:00	0	0.172	0.117	24	214	0.11
	1	0.174	0.124	-	-	-
	2.5	0.261	0.165	-	-	-
	5	0.336	0.185	38	200	0.19
	7.5	0.447	0.230	-	-	-
	10	0.443	0.231	45	186	0.24
18:00	0	0.205	-	-	-	-
	1	0.256	-	-	-	-
	2.5	0.257	-	-	-	-
	5	0.324	-	-	-	-
	7.5	0.478	-	-	-	-
	10	0.465	-	-	-	-

Table A.3. All recorded fluorescence parameters of Lake Ontario phytoplankton at the study site on 13 August 2008.

Time (h)	Depth (m)	$F_V:F_M$	$F_Q':F_M'$	$rETR_{max}$	E_K	α
7:30	0	0.509	0.298	60	239	0.25
	1	0.454	0.226	-	-	-
	2.5	0.450	0.311	-	-	-
	5	0.491	0.327	41	143	0.29
	7.5	0.465	0.303	-	-	-
	10	0.426	0.266	47	172	0.27
9:30	0	0.272	0.192	51	460	0.11
	1	0.251	0.133	-	-	-
	2.5	0.350	0.227	-	-	-
	5	0.425	0.275	54	224	0.24
	7.5	0.484	0.309	-	-	-
	10	0.432	0.277	48	155	0.31
11:30	0	0.366	0.272	41	197	0.21
	1	0.393	0.251	-	-	-
	2.5	0.378	0.261	-	-	-
	5	0.395	0.247	41	203	0.20
	7.5	0.437	0.240	-	-	-
	10	0.412	0.267	56	243	0.23
13:30	0	0.220	0.157	19	177	0.11
	1	0.207	0.145	-	-	-
	2.5	0.267	0.198	-	-	-
	5	0.356	0.204	36	181	0.20
	7.5	0.392	0.251	-	-	-
	10	0.457	0.269	75	503	0.15
15:00	0	0.240	0.187	43	360	0.12
	1	0.296	0.220	-	-	-
	2.5	0.305	0.227	-	-	-
	5	0.372	0.257	47	245	0.19
	7.5	0.432	0.268	-	-	-
	10	0.467	0.286	49	212	0.23
18:00	0	0.309	-	-	-	-
	1	0.355	-	-	-	-
	2.5	0.342	-	-	-	-
	5	0.411	-	-	-	-
	7.5	0.425	-	-	-	-
	10	0.433	-	-	-	-

Table A.4. All recorded fluorescence parameters of Lake Ontario phytoplankton at the study site on 27 August 2008.

Time (h)	Depth (m)	$F_V:F_M$	$F_Q':F_M'$	$rETR_{max}$	E_K	α
7:30	0	0.519	0.365	76	317	0.24
	1	0.484	0.344	-	-	-
	2.5	0.479	0.350	-	-	-
	5	0.474	0.329	192	1373	0.14
	7.5	0.477	0.319	-	-	-
	10	0.492	0.311	68	325	0.21
9:30	0	0.332	0.242	58	342	0.17
	1	0.305	0.244	-	-	-
	2.5	0.378	0.262	-	-	-
	5	0.397	0.254	85	424	0.20
	7.5	0.465	0.253	-	-	-
	10	0.469	0.219	60	250	0.24
11:30	0	0.187	0.144	47	336	0.14
	1	0.184	0.162	-	-	-
	2.5	0.247	0.165	-	-	-
	5	0.375	0.239	62	367	0.17
	7.5	0.376	0.204	-	-	-
	10	0.406	0.223	72	398	0.18
13:30	0	0.231	0.156	37	311	0.12
	1	0.203	0.139	-	-	-
	2.5	0.223	0.142	-	-	-
	5	0.332	0.197	57	302	0.19
	7.5	0.363	0.199	-	-	-
	10	0.460	0.264	61	255	0.24
15:00	0	0.266	0.189	40	234	0.17
	1	0.269	0.191	-	-	-
	2.5	0.278	0.189	-	-	-
	5	0.369	0.230	44	177	0.25
	7.5	0.490	0.302	-	-	-
	10	0.439	0.255	66	300	0.22
18:00	0	0.459	-	-	-	-
	1	0.471	-	-	-	-
	2.5	0.459	-	-	-	-
	5	0.493	-	-	-	-
	7.5	0.479	-	-	-	-
	10	0.513	-	-	-	-

Table A.5. All recorded fluorescence parameters of Lake Ontario phytoplankton at the study site on 18 September 2008.

Time (h)	Depth (m)	$F_V:F_M$	$F_Q':F_M'$	$rETR_{max}$	E_K	α
7:30	0	0.502	0.317	70	232	0.30
	1	0.450	0.163	-	-	-
	2.5	0.500	0.298	-	-	-
	5	0.548	0.288	76	283	0.27
	7.5	0.471	0.261	-	-	-
	10	0.467	0.231	45	248	0.18
9:30	0	0.434	0.263	63	275	0.23
	1	0.366	0.282	-	-	-
	2.5	0.445	0.300	-	-	-
	5	0.465	0.290	74	336	0.22
	7.5	0.339	0.224	-	-	-
	10	0.323	0.202	49	258	0.19
11:30	0	0.285	0.236	66	368	0.18
	1	0.258	0.230	-	-	-
	2.5	0.319	0.276	-	-	-
	5	0.424	0.314	90	374	0.24
	7.5	0.434	0.305	-	-	-
	10	0.414	0.295	78	489	0.16
13:30	0	0.227	0.207	61	437	0.14
	1	0.183	0.178	-	-	-
	2.5	0.272	0.209	-	-	-
	5	0.458	0.333	52	346	0.15
	7.5	0.441	0.333	-	-	-
	10	0.474	0.330	75	287	0.26
15:00	0	0.256	0.148	40	331	0.12
	1	0.240	0.164	-	-	-
	2.5	0.200	0.135	-	-	-
	5	0.313	0.181	52	346	0.15
	7.5	0.348	0.222	-	-	-
	10	0.410	0.235	53	221	0.24
18:00	0	0.375	-	-	-	-
	1	0.350	-	-	-	-
	2.5	0.365	-	-	-	-
	5	0.480	-	-	-	-
	7.5	0.525	-	-	-	-
	10	0.548	-	-	-	-

Table A.6. All recorded fluorescence parameters of Lake Ontario phytoplankton at the study site on 1 October 2008.

Time (h)	Depth (m)	$F_V:F_M$	$F_Q':F_M'$	$rETR_{max}$	E_K	α
7:30	0	0.680	0.351	87	265	0.22
	1	0.651	0.354	-	-	-
	2.5	0.685	0.392	-	-	-
	5	0.679	0.371	89	269	0.33
	7.5	0.688	0.371	-	-	-
	10	0.663	0.315	81	253	0.32
9:30	0	0.485	0.257	79	304	0.26
	1	0.467	0.273	-	-	-
	2.5	0.551	0.351	-	-	-
	5	0.574	0.314	87	272	0.32
	7.5	0.611	0.331	-	-	-
	10	0.612	0.307	68	263	0.26
11:30	0	0.356	0.282	82	409	0.20
	1	0.400	0.302	-	-	-
	2.5	0.524	0.376	-	-	-
	5	0.583	0.373	127	471	0.27
	7.5	0.612	0.354	-	-	-
	10	0.602	0.288	81	338	0.24
13:30	0	0.499	0.305	82	358	0.23
	1	0.483	0.330	-	-	-
	2.5	0.596	0.384	-	-	-
	5	0.638	0.400	99	291	0.34
	7.5	0.630	0.313	-	-	-
	10	0.645	0.288	75	233	0.32
15:00	0	0.514	0.318	72	232	0.31
	1	0.500	0.313	-	-	-
	2.5	0.583	0.378	-	-	-
	5	0.622	0.376	102	301	0.34
	7.5	0.637	0.249	-	-	-
	10	0.646	0.268	72	232	0.31
18:00	0	0.667	-	-	-	-
	1	0.700	-	-	-	-
	2.5	0.704	-	-	-	-
	5	0.721	-	-	-	-
	7.5	0.701	-	-	-	-
	10	0.666	-	-	-	-

Appendix B:

Predicted and observed *in situ* F_V:F_M of Lake Ontario phytoplankton

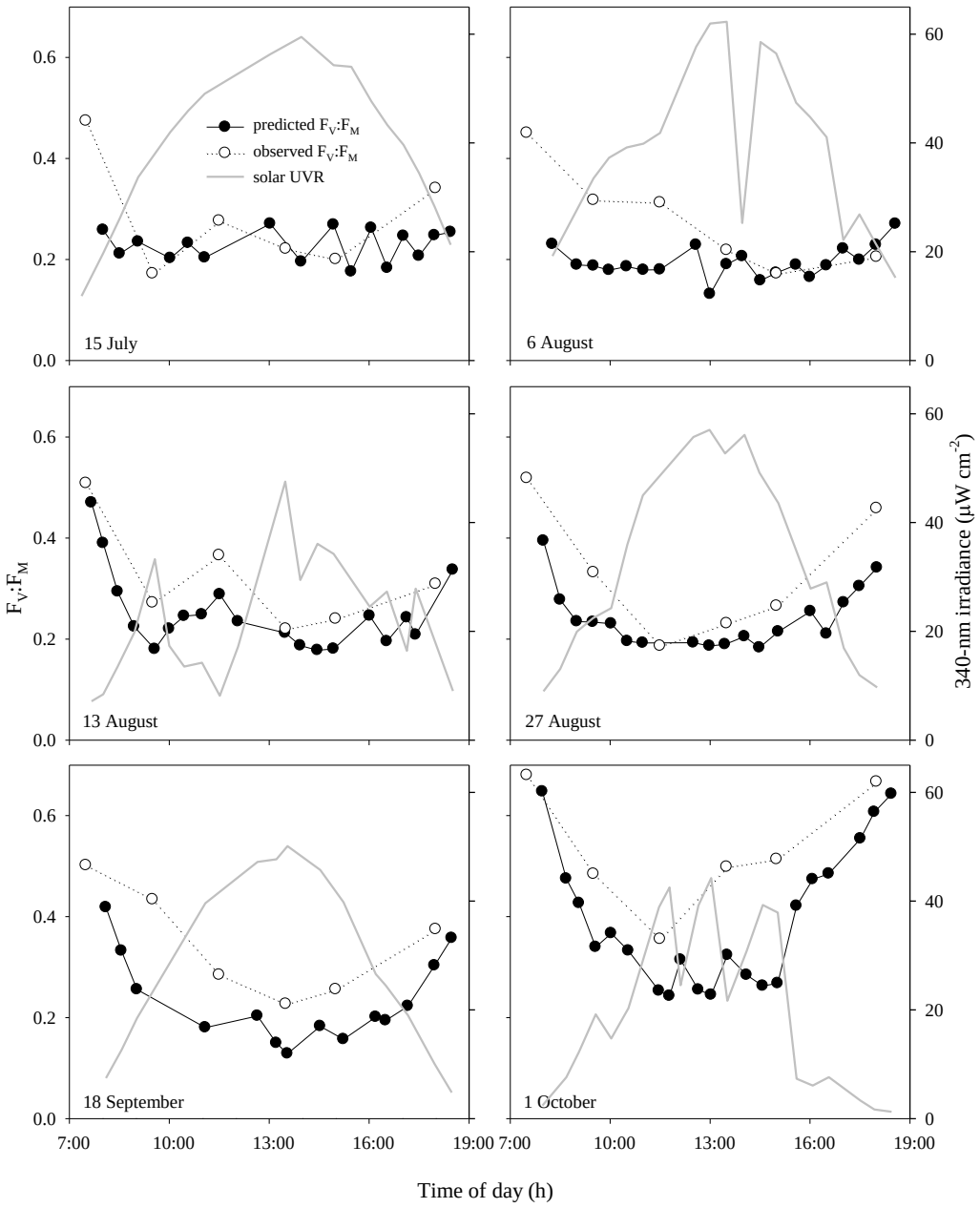

Figure B.1. Diurnal variation in observed and predicted F_V:F_M at the lake surface, as well as incident solar irradiance at the study site on Lake Ontario in 2008.

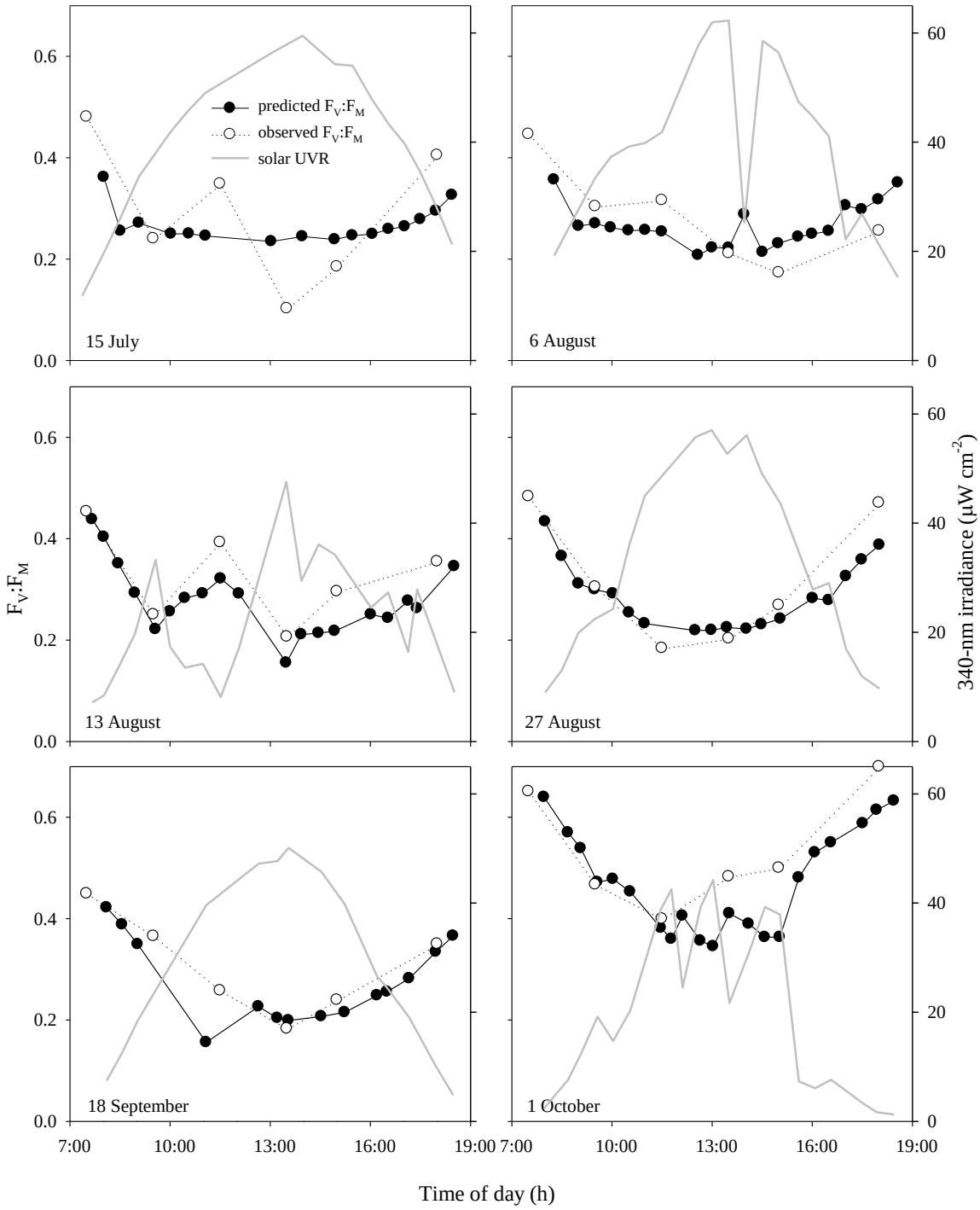

Figure B.2. Diurnal variation in observed and predicted F_V:F_M at a depth of 1 m, as well as incident solar irradiance at the study site on Lake Ontario in 2008.

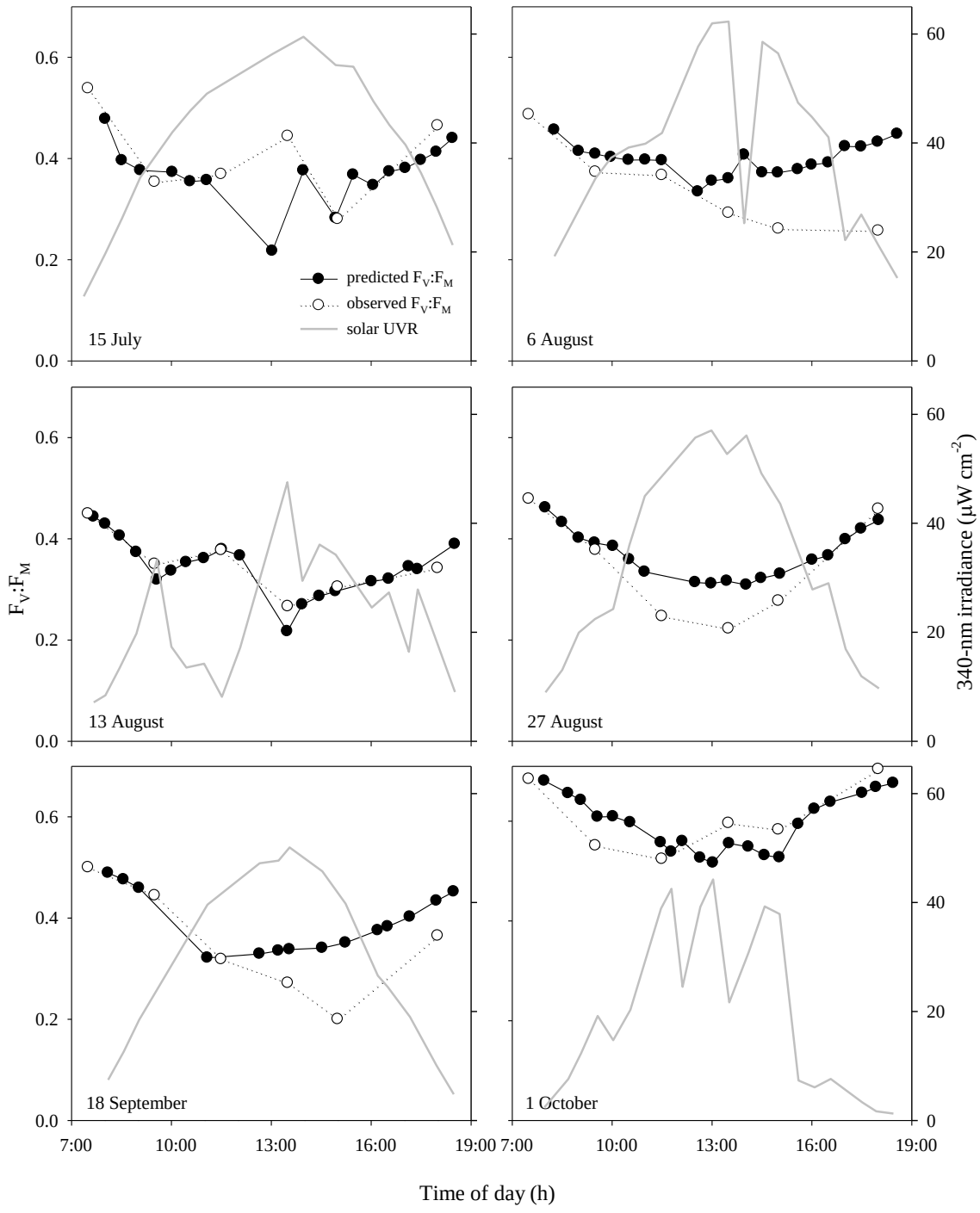

Figure B.3. Diurnal variation in observed and predicted F_V:F_M at a depth of 2.5 m, as well as incident solar irradiance at the study site on Lake Ontario in 2008.

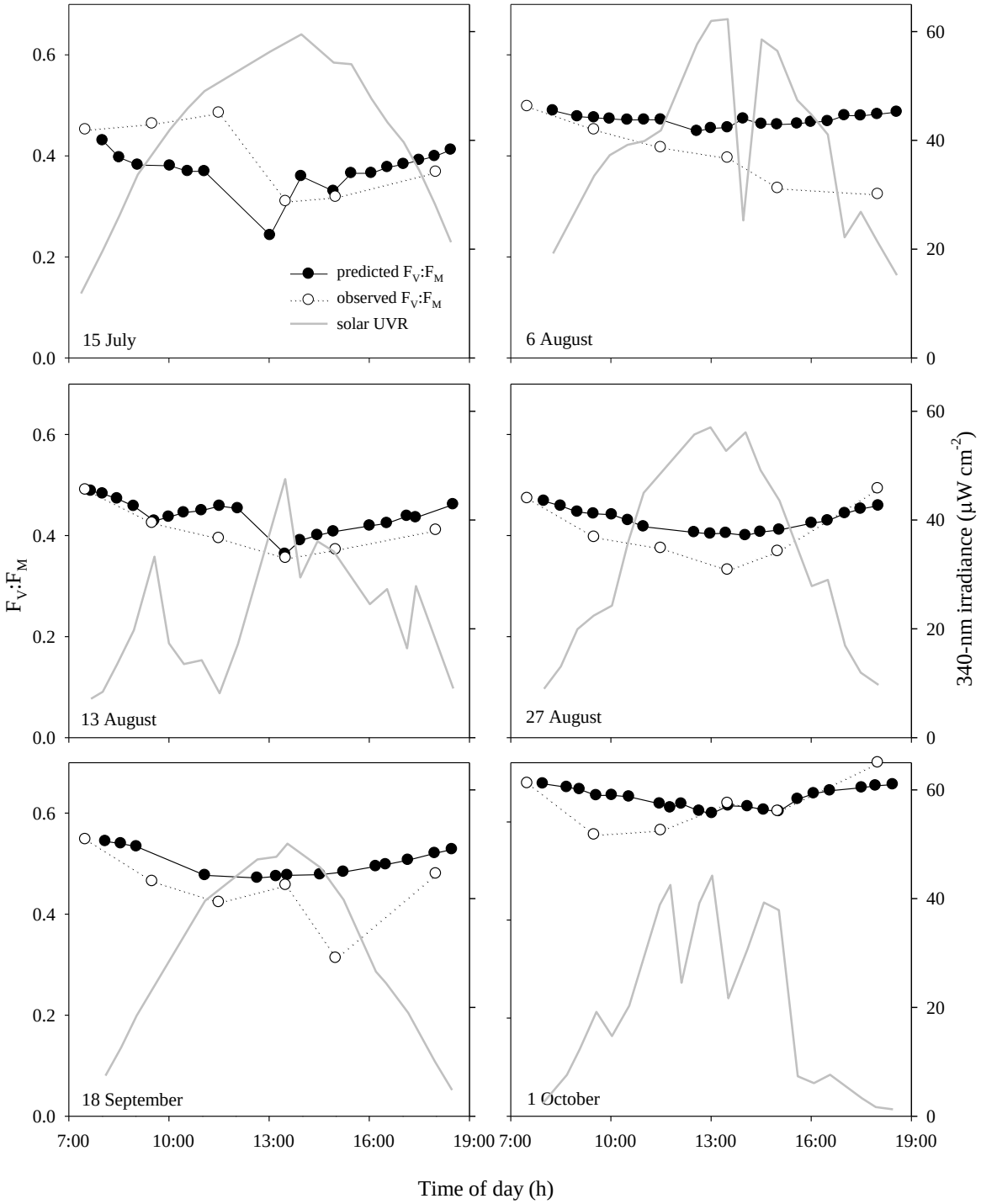

Figure B.4. Diurnal variation in observed and predicted F_V:F_M at a depth of 5 m, as well as incident solar irradiance at the study site on Lake Ontario in 2008.

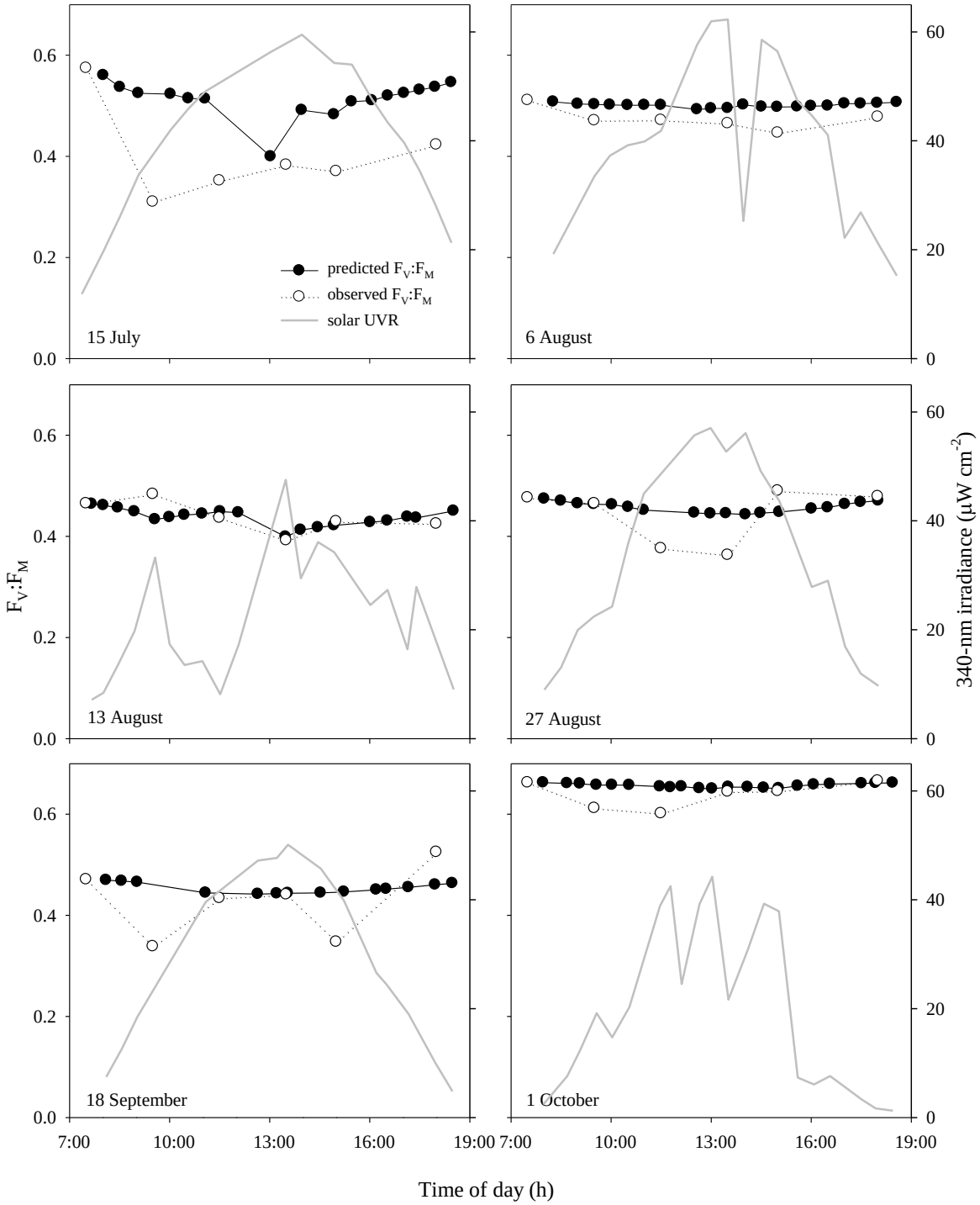

Figure B.5. Diurnal variation in observed and predicted F_V:F_M at a depth of 7.5 m, as well as incident solar irradiance at the study site on Lake Ontario in 2008.

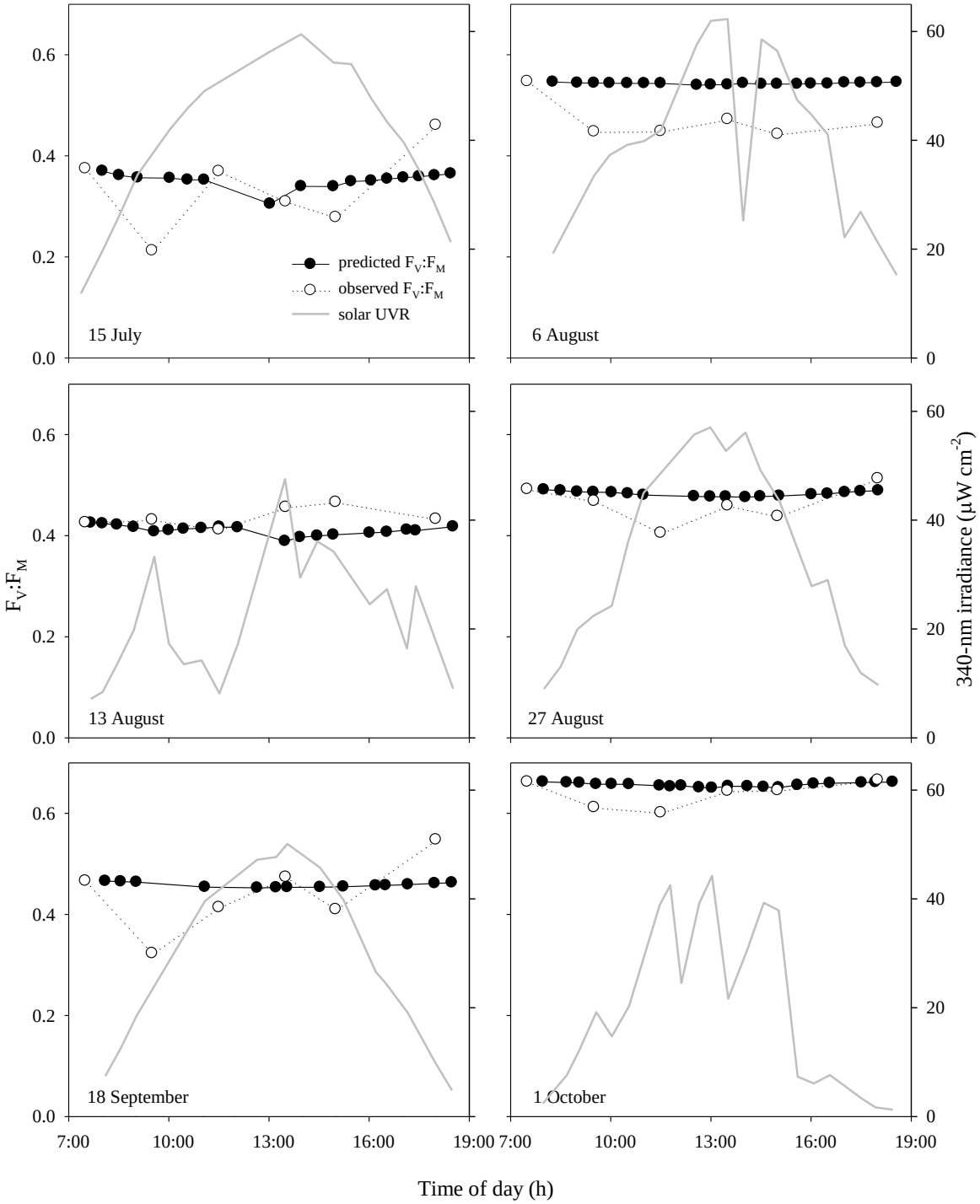

Figure B.6. Diurnal variation in observed and predicted F_V:F_M at a depth of 10 m, as well as incident solar irradiance at the study site on Lake Ontario in 2008.

Appendix C:
Effect of temperature on sensitivity to photoinhibition in winter phytoplankton from Lake Erie

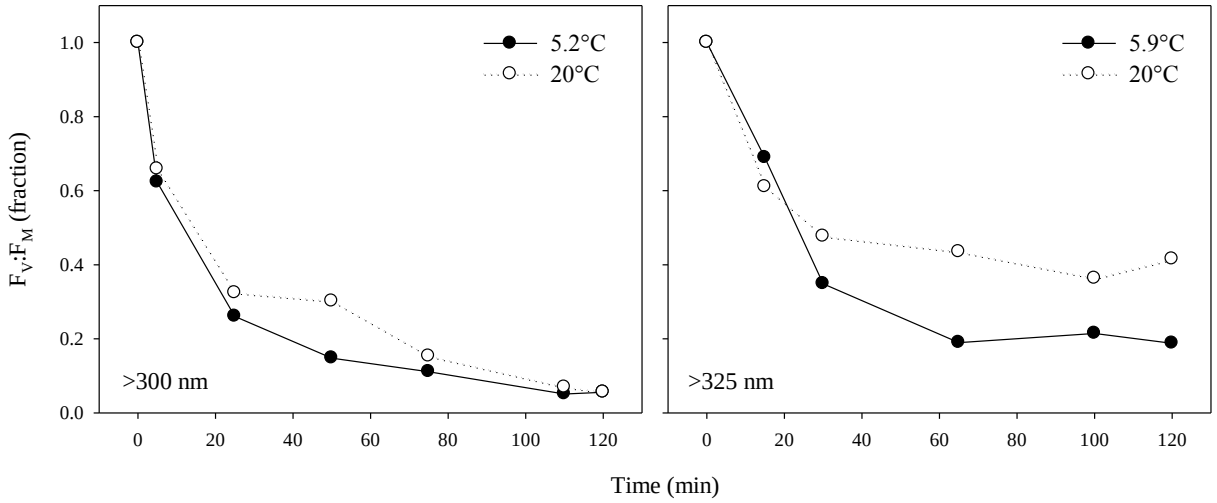

Figure C.1. $F_V:F_M$ of winter phytoplankton from Lake Erie during exposure to >300-nm and >325-nm spectra in the incUVator at different temperatures. The circulating water bath used for temperature control was set at 0.2°C and 20°C for the two experiments; however, the nominal 0.2°C samples had warmed to the temperatures listed on the figure legends by the end of the incubations. Experiments were performed aboard the CCGS Griffon on 18 February 2010 at station 84.